T.R.

GEBZE TECHNICAL UNIVERSITY

GRADUATE SCHOOL OF NATURAL AND APPLIED SCIENCES

AMPLIFIED SEISMIC LOADS IN STEEL FRAMING SYSTEMS

BORA AKŞAR

A THESIS SUBMITTED FOR THE DEGREE OF

DOCTOR OF PHILOSOPHY

DEPARTMENT OF CIVIL ENGINEERING

EARTHQUAKE AND STRUCTURAL ENGINEERING PROGRAM

GEBZE

2017

T.R.

GEBZE TECHNICAL UNIVERSITY

GRADUATE SCHOOL OF NATURAL AND APPLIED SCIENCES

AMPLIFIED SEISMIC LOADS IN STEEL FRAMING SYSTEMS

BORA AKŞAR

A THESIS SUBMITTED FOR THE DEGREE OF

DOCTOR OF PHILOSOPHY

DEPARTMENT OF CIVIL ENGINEERING

EARTHQUAKE AND STRUCTURAL

ENGINEERING PROGRAM

THESIS SUPERVISOR

PROF. DR. BÜLENT AKBAŞ

GEBZE

2017

T.C.
GEBZE TEKNİK ÜNİVERSİTESİ
FEN BİLİMLERİ ENSTİTÜSÜ

ÇELİK YAPI SİSTEMLERİNDE ARTTIRILMIŞ DEPREM ETKİLERİ

BORA AKŞAR

DOKTORA TEZİ
İNŞAAT MÜHENDİSLİĞİ ANABİLİM DALI
DEPREM VE YAPI MÜHENDİSLİĞİ PROGRAMI

DANIŞMANI
PROF. DR. BÜLENT AKBAŞ

GEBZE
2017

GEBZE TEKNİK ÜNİVERSİTESİ	DOKTORA JÜRİ ONAY FORMU

GTÜ Fen Bilimleri Enstitüsü Yönetim Kurulu'nun 05/07/2017 tarih ve 2017/36 sayılı kararıyla oluşturulan jüri tarafından 27/07/2017 tarihinde tez savunma sınavı yapılan 103293000 nolu Bora AKŞAR'ın tez çalışması İnşaat Mühendisliği Ana Bilim Dalı Deprem ve Yapı Mühendisliği Doktora Programında DOKTORA tezi olarak kabul edilmiştir.

JÜRİ

ÜYE (TEZ DANIŞMANI)	: Prof. Dr. Bülent AKBAŞ
ÜYE	: Prof. Dr. Bilge SİYAHİ
ÜYE	: Doç. Dr. M. Eren UÇKAN
ÜYE	: Doç. Dr. Bilge DORAN
ÜYE	: Yrd. Doç. Dr. Ahmet Anıl DİNDAR

ONAY

Gebze Teknik Üniversitesi Fen Bilimleri Enstitüsü Yönetim Kurulu'nun

...../...../..... tarih ve ...../..... sayılı kararı.

İMZA/MÜHÜR

Doç. Dr. Arif Çağdaş AYDINOĞLU
Gebze Teknik Üniversitesi
Fen Bilimleri Enstitüsü Müdürü

SUMMARY

In this thesis, amplified seismic load are investigated for low-, medium- and high-rise steel special moment frames (SMF) and steel special concentrically braced frames (SCBF). Stability of load bearing system especially column should be maintained when structure is in inelastic region, during strong ground motion. For this purpose, approximate lateral strength of structure need to determined. Lateral strength of a structure can be defined as the maximum lateral force that the building can resist during a strong ground motion. The amplification factor (Ω_o) in design codes is used to estimate for the lateral strength of a steel building. Amplification factor, (Ω_o) is obtained by dividing the actual strength of the structure into the design strength and depending on the structural system and varies between 2.0 and 3.0. The required compressive axial strength and tensile strength of columns in the seismic force resisting systems (moment frames, braced frames, shear walls) are determined using the load combinations in the seismic design code including the amplified seismic load [AISC 341-10, 2010]. The specification permits to neglect applied moment in this determination [AISC 341-10, 2010]. The requirements in the specification are mostly based on engineering judgment and a comprehensive analytical investigation is urgently needed to justify these requirements. In this thesis, nonlinear dynamic time history analyses were carried out to investigate the increase in the axial load levels on columns, brace and system overstrength factors for Special Moment Resisting Frames (SMRFs) and steel special concentrically braced frames (SCBF) under strong ground motions.

Key Words: Steel Moment Frame, Steel Concentrically Braced Frame, Amplified Seismic Load, Overstrength Factor, Nonlinear Dynamic Time History Analyses.

ÖZET

Bu çalışmada az, orta ve çok katlı süneklik düzeyi yüksek moment aktaran çelik çerçeveler ile süneklik düzeyi yüksek merkezi çelik çaprazlı çerçevelerde artırılmış deprem etkileri incelenmiştir. Şiddetli deprem yer hareketine maruz kalan bir yapı, doğrusal olmayan evreye girdikten sonra yapının taşıyıcı sisteminin, özellikle de kolonların, stabilitesinin sağlanması gerekmektedir. Bu nedenle yapının yaklaşık yanal dayanımının belirlenmesi gerekmektedir. Yapının şiddetli deprem yer hareketi sırasında maruz kalacağı maksimum yatay kuvvet, yapının yanal dayanımı olarak tanımlanır. Deprem yönetmeliklerinde tanımlanan büyütme katsayısı, (Ω_o) esas olarak bir yapının yanal dayanımının yaklaşık olarak belirlenmesine yarar. (Ω_o) aslında yapının gerçek dayanımın tasarım dayanımına bölünmesi ile elde edilir. (Ω_o) taşıyıcı sistemin türüne bağlı olarak 2.0 ile 3.0 arasında değerler almaktadır. Çelik yapılarda deprem yüklerini aktaran taşıyıcı sistemdeki (moment çerçeveler, çaprazlı çerçeveler, çelik perde duvarlar) kolonların eksenel basınç ve eksenel çekme dayanımlarının arttırılmış deprem etkilerini içeren yük kombinasyonları kullanılarak kontrol edilmesi gerekmektedir [AISC 341-10, 2010]. Bu kontrolü yaparken, eğilme momentlerinin ihmal edilmesine yönetmelik izin vermektedir [AISC 341-10, 2010]. Arttırılmış deprem etkileriyle ilgili hükümler daha çok mühendislik sezgilerine dayanmaktadır, bu hükümlerin kapsamlı bir analitik çalışma ile incelenmesi ve değerlendirilmesi gerekmektedir. Bu tezde, süneklik düzeyi yüksek Moment Çerçeveler (ÖMÇ) ve süneklik düzeyi yüksek Merkezi Çaprazlı Çerçevelerde (MÇÇ) şiddetli yer hareketi altında doğrusal olamayan analizler gerçekleştirilmiş ve sistem büyütme katsayıları ile kolon ve çapraz elemanlardaki eksenel kuvvet seviyesindeki artışlar incelenmiştir.

Anahtar Kelimeler: Çelik Moment Çerçeve, Çelik Merkezi Çaprazlı Çerçeve, Arttırılmış Sismik Yük, Büyütme Katsayısı, Doğrusal Olmayan Dinamik Zaman Geçmişi Analizi.

ACKNOWLEDGEMENTS

I would like to express my gratitude and special tanks to my supervisor Prof. Dr. Bülent AKBAŞ for his precious guidance and support from the very first day that I stepped in to his office as a PhD student.

I would also like to express my appreciation to the jury members; Prof. Dr. Bilge SİYAHİ and Assoc.Prof. Dr. Eren UÇKAN for their valuable time and criticism.

I would like to express my special thanks to Assoc. Prof. Dr. Bilge DORAN, Assoc. Prof. Dr. Ferit ÇAKIR, and Asst. Prof. Dr. Ercan Şerif KAYA who helped me during the part of my thesis.

I wish to thank my colleague, Selçuk Doğru for his support and help at all times. I thanks to my friends to their support.

A special thanks to my beloved wife Duygu AKŞAR for his incredible support at every step of my academic life, his encouragement, patience and help. Also I would like to express my very special thanks to my beloved daughter Öykü Mira AKŞAR.

I would like to express my deepest gratitude to my parents Tamer AKŞAR, Nuray AKŞAR and my brother Volkan AKŞAR for their love and sacrifices.

I would like to thank to my previous managers Erdoğan KARAKUŞ, Kemal KARAKUŞ and Erdal KARAKUŞ for their valuable support and encouragement at the time i was working.

I would like to thank to The Scientific and Technological Research Council of Turkey (TUBITAK) for supporting this research (Grant # 114R044).

This thesis is dedicated to the memory of my beloved father, Tamer AKŞAR, who was a source of inspiration, motivation and inherent guidance. I miss him every day, thank you for everything.

TABLE of CONTENTS

LIST of ABBREVIATIONS and ACRONYMS

Abbreviations and Acronyms		**Explanations**
C_d	:	Deflection amplification factor
C_u	:	Coefficient of upper limit for period
E_E	:	Elastic strain energy
E_D	:	Damping energy
E_I	:	Total input energy
E_H	:	Hysteretic energy
E_K	:	Kinetic energy
m	:	Mass
R	:	Response modification coefficient
sec	:	Second
S_1	:	Spectral acceleration parameter at a period of 1s
S_S	:	Spectral acceleration parameter at short period
T	:	Period
T_a	:	Approximate fundamental period
u	:	Displacement
ASCE	:	American society of civil engineers
AISC	:	American institute of steel construction
MDOF	:	Multi degree of freedom system
SDOF	:	Single degree of freedom system
GM	:	Ground motion
CP	:	Collapse prevention
LS	:	Life safety
SCBF	:	Special concentrically braced frame
SMF	:	Special moment frame
PGA	:	Peak ground acceleration
DBE	:	Design basis earthquake
MCE	:	Maximum considered earthquake
ρ	:	Redundancy factor
Ω_o	:	Overstrength factor

LIST of FIGURES

LIST of TABLES

1. INTRODUCTION

Many modern steel moment resisting frames (SMRF) suffered from unexpected structural damage and seismic behavior during the January 17, 1994, Northridge, USA and January 17, 1995, Kobe, Japan earthquakes. The damage mostly occurred in flange welds, girder flanges, column flanges and webs, shear plate connections of the girder web in the girder-to-column connection [Astaneh-Asl et al., 1998)]. These events triggered comprehensive analytical and theoretical investigations and substantial changes in steel building design. One of the major counter measure methods in design code is to consider amplified earthquake effects on steel building design. Under strong ground motion, SMRF which provides ductility by yielding of beams subjected to amplified seismic loads generally 2 or 3 times greater than anticipated seismic load and this should be considered in design of column and connections. When SMRF is in inelastic region during earthquake, the stability of the the columns should be maintained. Seismic codes require that column stability should be checked under amplified seismic loads [AISC 341-10, 2010].

Seismic code defines response modification factor (R values) deflection amplification factors (C_d values) and system over strength factors (Ω_o values) under seismic design procedure [ASCE 7-10, 2010]. R is a coefficent related to ductility of the structure and equal to cross product of over strength factor (SRF) and ductility reduction factor. Ductility reduction factor is the ratio of the assumed entirely elastic story drift to actual story drift under earthquake ground motion. C_d is defined as the ratio of the inelastic story drift corresponding to design earthquake ground motion divided by the design displacement; i.e. C_d is a fraction of R. Ω_o is the ratio of actual strength (V_{max}) divided by the design strength (V) (Figure 1.1). Conceptually, the columns and connections should be designed for forces corresponding to V, but stability of the columns should be maintained under V_{max}.

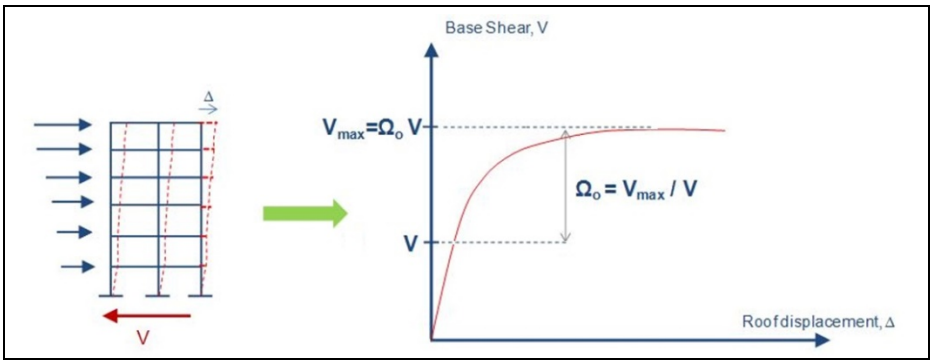

Figure 1.1: Schematic illustration of amplified seismic load, (Ω_o)

In seismic force resisting systems (SFRS) such as moment frames, braced frames and shear walls, the compressive axial strength and tensile strength of columns should provide following requirements [AISC 341-10, 2010]:

- The compressive axial strength and tensile strength of a column will be determined using the load combinations including the amplified seismic load.
- Bending moments in the column can be neglected in the strength check of a column using load combinations including the amplified seismic load.
- The required axial compressive strength and tensile strength of a column not exceed either of the following:
- The maximum load transferred to the column by the system, including the effects of material overstrength and strain hardening in those members where yielding is expected.
- The forces corresponding to the resistance of the foundation to overturning uplift (difficult to obtain).

As described in the second commentary ignoring bending moments in the column isn't very realistic because before the collapse like axial force, bending moment also has an increase in column. Hence validity of that should be examined. Columns in seismic force resisting system which are transferring seismic load should have enough strength against global buckling and tensile rapture. Under strong ground motion columns in SMRF can be exposure large tensile forces [Astaneh-,Asl et al., 1998]. For this reason, all regulations since 1980 require adequate strength in columns under strong ground motions. Limiting the axial forces that could be imposed on columns during the ground motion is the main purpose of this

requirement. Bending moment at columns ends is not taken into consideration by the regulations [AISC 341-10, 2010]. Newell and Uang have shown that during large story drifts, column can resist axial forces up to $0.75F_y$ with high end rotations [Newell and Uang, 2008]. F_y is the specified minimum yield strength. There are two acceptance based on this approach:

- Bending moment has maximum values at the ends of the column
- Reverse curvature occurs as a result of bending moments in column.

Researches have shown that the second commentary is not valid for every condition and nonlinear time history analysis mainly shows conditions which columns end moment's sign remains same and may cause buckling [Shen, at al., 2010]. Another word, column end moments could contribute to column buckling.

For SFRS, the requirement in design regulations does not guarantee to prevent column yielding and not prevent columns end yielding which may be occurred by the combination of axial load and bending moment [AISC 341-10, 2010]. Yielding in columns can occur as a result of high bending moment – average axial force combination (like moment frames) or high axial force – bending moment from end rotation combinations (like braced frame). Column yielding in SFRS is life safety threatening situation and unwanted damage mode.

In previous AISC provisions order to check columns strength with amplified load effect, if the proportion of $Pu/(\varphi cPn)$ ratio (acc. to LRFD) were greater than 0.4, where Pu is the required axial strength of a column using LRFD load combinations, Pn is the nominal axial strength of a column, and φc is 0.90. In the fact, especially for columns having low axial load and large (Ω_o) values this limitation does not led to reliable results [AISC 341-05, 2005]. As a result of that, this limitation value requirement was voided from the latest AISC regulations and strength control under amplified seismic load is required to apply all columns in SFRSs [AISC 341-10, 2010].

Related requirement about amplified seismic load effects on column stability were prepared usually based on engineering pre-cognition in seismic design code [AISC 341-10, 2010]. Regulation should be examined with comprehensive researches and renewed if necessary. Turkish Earthquake Regulations also based on

American regulation [TDY, 2007]. Turkish Earthquake Regulations has following requirements for amplified load effects [TDY, 2007]:

Besides having adequate strength under axial force and bending moments from the combinations of vertical and lateral loads, column in first and second seismic hazard region also should have enough strength capacity under axial tension and compression forces (without considering bending moments) results from amplified load combinations.

Traditional structural design is based on strength. Strength demand of a structure is found by applying determined lateral seismic force with vertical forces. Designing structural elements is based on basis of that strength demand is equal or smaller than strength capacity. Horizontal static seismic force described in earthquake regulations provides minimum lateral strength and the aim is not to stay elastic under design earthquake. According to this approach, under severe earthquake ground motion structure is expected to perform high nonlinear deformations. Collapse depends on ductility of the structure.

The points where amplified seismic load effects are taken in to considerations in high ductile load bearing systems are stated in AISC341-10 as follows [AISC341-10, 2010]:

- Determining compressive axial and tensile strength of columns in load-bearing system which is transferring seismic load (moment frames, braced frames and plate shear systems)
- Determining the strengt of column to column joints,
- Determining column axial load and bending moment during the design of column footing,
- Determining shear force bases on designing joints, etc

Regulations about amplified seismic effects are based on engineering decisions and an extensive analytical investigation is needed to justify these requirements.

1.1. Objective

The purpose of this thesis is to explore the amplified seismic loads in steel special moment frames (SMF) and special concentrically braced frames (SCBF) under strong ground motions. To this end, plastic hinge rotations, P-M interactions for side columns and pushover curves for all frames will be evaluated. Moreover, the increase in axial loads on columns and braces for the maximum lateral load level and the corresponding lateral displacement will be investigated. Also system overstrength factor will also be determined and compared with the values in regulations.

1.2. Scope

To investigate the amplified seismic load in low, medium and high-rise building, 4-, 8-, 12- and 20-story SMF and SCBF are selected and designed in accordance with American provisions.

For SCBF with two different bracing configurations (inverted V and two-story X) are designed. Four different span lengths with SMF are used to specify the effect of span length difference amplified seismic load. An ensemble of ground motions is selected so that the seismic response of each of the four frames would range from moderate to severe and the seismic energy demand would be evaluated based on the response of the frames. Two sets of ground motions corresponding to 10% and 2% probability of exceedance in 50-year time period which correspond to the life safety performance level (LS) and collapse prevention performance level (CP) respectively are used in nonlinear dynamic time history analyses.

2. AMPLIFIED SEISMIC LOADS IN SEISMIC PROVISIONS

For structures in seismic Design Category D, E or F and for Seismic Design Categories A, B or C; when using R > 3, applying requirements in seismic provisions is mandatory [ASCE 7-10, 2010]. Basic LRFD Load Combinations including horizontal and vertical seismic effects in ASCE-7-10 as follows [ASCE-7-10, 2010]:

$$1.2D + 1.0E + 0.5L + 0.2S \tag{2.1}$$

$$0.9D + 1.0E \tag{2.2}$$

Definition of E in basic load combinations for equation 2.1 and 2.2 as follow:

$$E = \rho Q_E \pm 0.2S_{DS}\, D \tag{2.3}$$

In Eq. (1.3) ρQ_E represent horizontal seismic effects and $0.2S_{DS}$ D represent vertical seismic effects in a simple way. In the equation Q_E is the effect of horizontal earthquake-induced forces; S_{DS} is the design spectral acceleration at short periods; D is the dead load effect; L is the live load effect; S is the snow load effect; ρ is the redundancy factor that depends on extent of redundancy in the seismic lateral resisting system. ρ varies from 1.0 to 1.5. Replacing E in equation (2.3) with equations (2.1) and (2.2) results in:

$$(1.2 + 0.2S_{DS})D + 1.0\rho Q_E + 0.5L + 0.2S \tag{2.4}$$

$$(0.9 - 0.2S_{DS})D + 1.0\rho Q_E \tag{2.5}$$

$0.2S_{DS}$ is simply modified dead load in equation 1.4 and 1.5. Amplified earthquake effects are obtained by multiplying the horizontal effects of E with $\boldsymbol{\Omega_0}$. Thus, equation 2.3 takes the following form:

$$E = \Omega_0 Q_E \pm 0.2S_{DS}\, D \tag{2.6}$$

ρ and (Ω_o) are replaced in equation 2.6. The effect of amplified seismic load is obtained by replacement of E in equation 2.1 with E in equation 2.6.

$$(1.2 + 0.2S_{DS})D + 1.0\Omega_0 Q_E + 0.5L + 0.2S \quad (3.7)$$

$$(0.9 - 0.2S_{DS})D + 1.0\Omega_0 Q_E \quad (3.8)$$

For amplified seismic load effects, two load combinations are given in Turkish Earthquake regulations (equations 2.9 and 2.10) [TDY, 2007]. In TDY beside columns in steel structural system satisfying adequate strength under axial force and bending moment from the combinations of earthquake and vertical loads, columns also have adequate strength capacity under axial tension and compression loads resulting from amplified seismic loads given in equation 2.9 or if more critical in equation 2.10 for structures in seismic zones one and two.

$$1.0G + 1.0Q \mp \Omega_0 Q_E \quad (3.9)$$

$$0.9G \mp \Omega_0 Q_E \quad (3.10)$$

Amplified seismic load effects should be taken into consideration in the design of columns in steel structures under axial forces, in the design of column splices, in the design of beam-column connections in high ductile normal frame system and in the design of other connection details. Ω_0 used to determine amplified seismic load effects depend on seismic load resisting system and shown in Table 2.1 and 2.2. (Ω_o) basically is used to determine approximately lateral strength of a structure (Figure 1.1). The maximum lateral force that the structure is subjected to during earthquake ground motion is defined as the lateral strength of the structure. That is, $\Omega_0 Q_E$, is used for estimating lateral strength of a structure.

Table 2.1: Amplified load factor Ω_0 [ASCE 7-10, 2010].

System	Ω
Moment Frames (high, normal and low ductile moment frames)	3
Concentrically Braced Frames (high and normal ductile central braced frames)	2
Eccentrically Braced Frames (EBF)	2
High Ductile Special Plate Shear Walls (SPSW)	2
Buckling Restrained Braced Frames (BRBF) Moment resisting beam-column connections Simple beam-column connections	 2.5 2

Table 2.2: Increase coefficients Ω_0 [TDY, 2007].

Type of Structural Systems	Ω
High Ductile Frames	2.5
Normal Ductile Frames	2
Central Braced Shear Walls (high and normal ductile)	2
Eccentric Braced Shear Walls	2.5

Amplified load factor Ω_0, is given as 3 for moment resisting frames (Table 2.1). This, indicates that , average lateral strength of a moment resisting frame is 3 times more than Q_E; that means, lateral strength of the structure, is quite larger than design lateral force. This could be due to many reasons:

- Use of strength reduction factors in determination of design strength,
- Actual yield strength is larger than the minimum yield strength,
- Selecting larger sections to assure relative displacement requirement especially in moment frames,
- Selecting larger sections to ease design and construction process (use of same beam sections at least in two stories etc.)
- Increase in strength that takes place from formation of first plastic hinge until the formation of plastic mechanism.

It is important to note that whenever the design of a member or connection is required under increased earthquake effects, this also means that plastic analysis is allowed for determining the maximum load acting on the connection or member. In other words, increased earthquake loading is used instead of plastic analysis.

3. LITERATURE SURVEY

Researches have been made to investigate amplified seismic loads in structural systems. One of first studies on amplified seismic load is Freemans. In his study, conducted in 1990, the author reported overstrength factors for 3 three-story steel moment frames, two constructed in seismic zone 4 and one in seismic zone 3 were 1.9, 3.6, and 3.3, respectively.

Osteraas and Krawinkler studied on overstrength and ductility of steel frames designed in compliance with the Uniform Building Code working stress design provisions [Osteraas and Krawinkler, 1990]. Moment frames, perimeter frames and braced frames having various bay sizes and heights were subjected to non-linear static analysis using an invariant triangular load distribution. For moment frames the overstrength factor ranged from 8.0 in the short period range to 2.1 at a period of 4.0 seconds. For concentric braced frames reported overstrength factors ranged from 2.8 to 2.2 at periods of 0.1s to 0.9s respectively.

Rahgozar and Humar obtained overstrength factors ranging from 1.5 to 3.5 for two types of concentrically braced ten-story frames [Rahgozar and Humar, 1998]. Stating as a result of their study the main parameter that controls the reserve strength in those frames was the slenderness ratio of the bracing members. PΔ effect has a negligible effect on the overstrength factor and overstrength increases with an increase in the brace slenderness ratio or a decrease in the design earthquake load.

Kappos examined five R/C buildings, with one to five stories, consisting of beams, columns, and structural walls and as a result overstrength factors 1.5 to 2.7 are obtained [Kappos, 1999].

Balendra and Huang investigated overstrength and ductility of buildings that are designed for gravity loads and wind loads or notional horizontal load [Balendra and Huang, 2003]. In order to do that, steel frames of three, six and ten-story three-bay moment resisting frames (MRFs) concentrically braced frames (CBFs) and semi rigid frames are designed according to BS 5950, which does not have any seismic provisions. A nonlinear push-over analysis involving P-D effect has been performed on these steel frames, considering the effects of various combination of dead load (DL) and imposed load (IL) as 1.0DL + 0.4IL (most common state) 1.0DL1 + 1.0IL (serviceability state) and 1.2DL + 1.2IL (ultimate state). As a result of the study, The

overstrength factors of MRFs decrease from 8 to 3.5 as the number of storys increase from 3 to 10. When the rigid connections are replaced with semirigid connections, the overstrength factors of these three frames decrease around 50%. The overstrength factors for three-, six-, and ten-story low-rise semirigid frames frames are 6, 3, and 1.5, respectively. For inverted-V-braced and split-Xbraced frames the overstrength factors are 5.5, 3, and 2.5 for three-, six- and ten-story frames, respectively.

Lee, Cho and Ko analyzed overstrength factors and plastic rotation demands for 5, 10, 15 story R/C buildings designed in low and high seismicity regions utilizing three dimensional pushover analysis [Lee et al., 2005]. One of their conclusions is that the overstrength factors in low seismicity regions are larger than those of high seismicity regions for structures designed with the same response modification factor. They have reported factors ranging from 2.3 to 8.3

Kim and Choi evaluated overstrength, ductility, and the response modification factors of the 21 special concentric braced steel frames and 9 ordinary concentric braced frames with various stories and span lengths by performing pushover analyses [Kim and Choi, 2005]. The overstrength factors increased as the structure's height decreased and the span length increased. In SCBF, the factors turned out to be 1.9 to 3.2 for a 6m span, 2.4 to 4.1 for an 8m span, and 2.5 to 4.7 for a 10 m span. In OCBFs, factors were found close to 1.5 for all configurations.

Jin and El-Tawil were conducted nonlinear pushover and transient analyses of 4-, 8-, and 16-story frames with reduced beam section (RBS) connections with the objective of developing a better understanding of RBS frame behavior and exercising as well as critiquing the recently published FEMA-350 design specifications [Jin and El-Tawil, 2005]. Consequently, the structural overstrength factor, Ω_0 decreases as building height increases as Ω_0 = 2.5, 1.7, and 1.5 for the 4-, 8-, and 16-story buildings respectively.

Annan, Youssef and Naggar evaluated structural overstrength resulting from redistribution of internal forces in the inelastic range, design assumptions, and strain hardening behavior of steel and displacement ductility in typical braced frames of Modular Steel Buildings (MSBs) that are designed and modeled according to the 2005 edition of the National Building Code of Canada [Annan et al., 2008]. In their study, three heights of a typical modular steel dormitory are considered: two-story, four-story, and six-story with the same overall plan dimensions. They conducted nonlinear static pushover analyses to study the inelastic behavior of these frames. As

a result of their study, overstrength factors for two-, four- and six-story frames range from 1.9 to 2.5 and overstrength in MSBs appear to depend on building height contrary to many seismic design codes prescribing a single value for all buildings with a specific structural system.

Kim and Park investigated the seismic behavior of a framed structure with chevron-type buckling restrained braces and their behavior factors, such as overstrength, ductility, and response modification factors [Kim and Park, 2009]. They designed two types of structures, building frame systems (BFS) and dual systems (DS) with 4, 8, 12, and 16 stories according to the IBC 2003, the AISC LRFD and the AISC Seismic Provisions. To compute behavior factors they conducted Nonlinear static pushover analyses using two different loading patterns and incremental dynamic analysis using 20 earthquake records. According to the analysis results, the computed overstrength factors of the dual systems, which were designed with larger response modification factor, were smaller than those of the building frame systems. For BFS models overstrength factor ranges from 3.8 to 6 whereas for DS models it changes between 3 and 5.5. The overstrength factors turned out to be larger than those given in the AISC Seismic Provision.

Mahmoudi and M. Zaree evaluated the overstrength of the concentrically steel braced frames (CBFs) considering reserved strength, because of members post-buckling [Mahmoudi and M. Zaree, 2009]. A push over analysis was performed on models with single and double bracing bays, different stories and brace configurations (chevron V, invert V and X-bracing). As a result, The obtained post-buckling overstrength factors for CBFs in type V, inverted V and X with single and two bracing bays are 1.11, 1.08 and 1.28, respectively, for concentrically steel braced frames in type V, inverted V and X with single bracing bay are evaluated as 2.90, 3.75 and 3.10, respectively and concentrically steel braced frames in type V, inverted V and X with two bracing bay are evaluated as 3.80, 4.80 and 4.20, respectively.

Arslan and Topkaya investigated the influence of elastic base shear distribution between the steel plate shear wall and the moment resisting frame on the global system response such as the strength reduction, the overstrength, and the displacement amplification factors. A total of 10 walls and 30 wall–frame systems, ranging from 3 to 15 stories, were selected for numerical assessment [Arslan and Topkaya, 2010]. These systems represent cases in which the elastic base shear resisted by the frame has a share of 10, 25, or 50% of the total base shear resisted by

the dual system. One of their conclusions is that the Increase in the frame base shear resistance increases the overstrength possessed by the system. While the strength reduction factor (R) value remains constant, there is an inverse relationship between overstrength and ductility reduction. It was found out that the overstrength of the system increases with the amount of frame load share, whereas the ductility reduction factor decreases.

Tabeshpoura, Golafshanib and Shalmanib proposed completely closed RBS (CC-RBS) as a function of a new ribbed bracing system (RBS) [Tabeshpoura et al., 2011]. To do so, Three, six and ten-story moment frames equipped with CC-RBS were designed according to Iranian seismic code of practice, standard No. 2800 and were evaluated by performing static pushover (SPo) and incremental dynamic analyses (IDA). As a result of their study, The overstrength factors increased as the structure height increased in both IDA and SPO analyses except the overstrength factor of ten story frame obtained from SPO analyses which decreased in compare of six-story frame's. The factors turned out to be 2.12–2.32 in IDA and 2.30–2.38 in SPO analyses, which are generally larger than the IBC 2000 specified value of 2.0. Static pushover analyses lead to larger overstrength factors in all model structures in compare with the overstrength factors obtained in incremental dynamic analyses.

Mellati, Tehrani, Zeinali and Banazadeh were investigated the effects of various parameters such as the type of the moment frame, Seismic Design Category (SDC) and height of the building on overstrength factors of steel Moment Resisting Frames (MRF) [Mellati et al., 2013]. 12 building with 4,8 and 12 stories designed tree-dimensionally based on ASCE/SEI 7-10, AISC-LRFD 360-05 and AISC 341-05 regulations. Nonlinear static analysis were conducted for 24 two dimensional MRFs of these buildings. As a result, overstrength factors are in the range of 2.9 to 6.07 with the average of 4.43. For OMFs and IMFs, this factor usually decreases by increasing the number of stories.

Mehdi and Kargarmoakhar studied Seismic behavior of steel frames utilized by Shape memory alloys (SMA) bracing in their research [Mehdi and Kargarmoakhar, 2013]. The overstrength, ductility, and the response modification factors of the 24 steel braced frames employing SMA braces with various numbers of stories (4-, 6-, 8-, 10-, 12- and 14-stories) and spans for different types of bracing (diagonal, X and Chevron bracing) were evaluated by performing static pushover and linear dynamic and incremental nonlinear dynamic analyses. It was found out that the overstrength

factor is decreased from 6.0 to 2.9 as the number of stories is increased. Increasing the number of spans had insignificant effects on the overstrength factor. Systems with Chevron V bracing showed higher values for overstrength factors in comparison with other systems in their study. The X bracing and diagonal bracing systems have almost similar results.

Abdollahzadeh and Banihashemi evaluated the overstrength, ductility and response modification factors of the 20 dual system with buckling-restrained braced with various stories number and the type of bracing (type V, inverted V, X and diagonal) by performing static pushover, linear dynamic and incremental nonlinear dynamic analysis. Consequently, the obtained overstrength factor for dual system with buckling restrained braces in type V, inverted V, X and diagonal are, respectively, 2.18, 1.9, 2 and 1.8 [Abdollahzadeh and Banihashemi, 2013]. The over strength factor is decreased as the number of stories is increased.

Kuşyılmaz and Topkaya conducted an analytical study on the design overstrength of steel eccentrically braced frames (EBFs) [Kuşyılmaz and Topkaya, 2013]. The study aimed at examining the influence of geometrical factors and seismic hazard on the design overstrength of EBFs. For analysis number of models with stories varied from 3 to 15, link length to bay width ratio varied as 0.1, 0.15, 0.2, 0.25, and 0.3. Bay widths of 8,10, 12, 14 m were considered. As a result, The average and minimum design overstrength of EBFs considered in their study were found to be 2.36 and1.16, respectively. The average and minimum design overstrength of EBFs considered in their study were found to be 2.36 and 1.16, respectively. The design overstrength is secondarily influenced by the building height and seismic hazard level. In general, the design overstrength decreases as the building height or seismic hazard level decreases.

Farokhi and Bazvand investigated the seismic behavior of a conventional steel moment frame with knee braces by using dynamic time history analysis and nonlinear static analysis for three models of 3, 6 and 10 stories with different bay numbers [Farokhi and Bazvand, 2014]. One of their conclusions is that the overstrength factor for KBMFs is obtained between 2 to 3 and is reduced by increasing the number of stories; so that this factor for 10-story frames is equal to 2. While the proposed value in the regulation is an estimation of the overstrength in frames and is equal to 3.

Dickof, Stiemer, Bezabeh and Tesfamariam analytically investigated A timber-steel hybrid system, where cross-laminated timber (CLT) shear panels are used as infill in steel moment resisting frames [Dickof et al., 2014]. Parametric studies are carried out for three-bay hybrid buildings with three-, six-, and nine-story hybrid buildings for varying panel configuration (a given gap, panel thickness, and crushing strength) values. A monotonic pushover analysis was performed to develop a preliminary ductility and overstrength values based on both steel yield of frame and panel crushing force in the links. As a result of their study, the overstrength value associated with the design strength of the bare frame system shows that the contribution of the infill panels is significant, and they should not be counted as a nonstructural component. When looking at the overstrength value related to each system's first yield, a value of 1.25 for all systems appears to be warranted.

Fanaie and Ezzatshoar evaluated overstrength, ductility and response modification factors of steel frames with gate bracing [Fanaie and Ezzatshoar, 2014]. For this purpose, three frames of different stories considered on soil type II have been subjected to 10 well known global earthquakes and analyzed through static pushover analysis, linear dynamic analysis and nonlinear incremental dynamic analysis. Overall, the average overstrength factor was to be found as 1.43.

Elkady and Lignos investigated the effect of the gravity framing system on the overstrength and collapse risk of steel frame buildings with perimeter special moment frames (SMF) designed in North America [Elkady and Lignos, 2014]. To do so nonlinear static analysis (noted as pushover) and incremental dynamic analysis (IDA) were conducted on SMF with five different high (2-, 4-, 8-, 12- and 20-Story). As a result of their study, steel frame buildings with perimeter SMF only achieve a static overstrength factor larger than the code-specified overstrength (Ω_o) = 3.0 when both the gravity framing and the composite slab effects were considered in the analytical model. For dynamic overstrength factor, Ω_d>3.0 was achieved, regardless if the gravity framing and the composite slab effects are considered as part of the analytical model of the building representation and an average Ω_d=4.0 can be achieved regardless of the number of stories of the steel building under consideration.

Shen, Akbas, Seker, Doran, Wen and Uckan evaluated the seismic axial loads for columns in seismic force resisting systems (SMRFs) under strong ground motions [Shen et al., 2015]. For this purpose, linear elastic analyses and nonlinear dynamic

time history analyses were conducted for three SMRFs with 4-, 9-, and 20-stories. As a result of their study, the average amplification factor for column in compression in low- and medium-rise frames ranges from 1.5 to 2.5 and the (Ω_o) factor increases in upper stories.

Fanaie and Shamlou studied the seismic behavior of mixed structures which have reinforced concrete frames and shear walls in their lower storeys and steel frames with bracing in their upper storeys [Fanaie and Shamlou, 2015]. For this purpose, seventeen structures in three groups of 5, 9 and 15 storey structures with different numbers of concrete and steel storeys were designed. They conducted static pushover analysis, linear dynamic analysis and incremental dynamic analysis (IDA) using 15 earthquake records to evaluate seismic parameters such as period, overstrength factor, response modification factor and ductility factor. They conducted more than 4600 nonlinear dynamic analysis and made regression analysis for achieving proper formula. Overall, the overstrength factor (the final base shear to the base shear corresponding to the first yielding) for all models ranged from 1.20 to 1.80 as an one result of their study.

Massumia and Ramin investigated the effect of redundancy on a fixed plan for seismic behavior factor components and the nonlinear behavior of RC frames [Massumia and Ramin, 2016]. The 3D RC moment resistant frames with equal lateral resistance were designed to examine the role of redundancy in earthquake-resistant design and to distinguish it from total overstrength capacity. For this purpose, eight 3D RC special moment resisting frames with the same story areas and different numbers of storys (6 and 9) and spans (3-, 4-, 5- and 6-bays) were designed according to the Iranian seismic design code [Standard 2800, 2005]. The total overstrength factor wasn't affected from the number of bays where as it degreased with the increase in height. Overstrength factor to be found for 6- and 9-story model were 2.6 and 2.4 respectively.

Gencturk, Kaymaz and Hosseini evaluated seismic design parameters for two different special moment frames: (1) frames entirely composed of reinforced ECC (R/ECC) and (2) reinforced concrete (RC) frames in which RC is replaced with R/ECC at the plastic hinge regions using FEMA P695 methodology [Gencturk et al., 2016]. Authors used a subset of 14 archetype buildings from 18 RC SMF archetype buildings which were FEMA P695 uses as one of the example applications. As a result, Individual archetype MX and R/ECC frame configurations were found to have

25–70% higher overstrength, compared to RC frames. Therefore, a system overstrength, o value of 6.0 is recommended for MX and R/ECC SMF so long as these frame types are designed using the existing regulations for RC.

Denavit, Hajjar, Perea and Leon studied to determine the seismic performance factors (i.e., R, Cd, and Ω_o) for composite special moment frame (C-SMF) following recommendations in FEMA P69 [Denavit et al., 2016]. A suite of 36 archetype frames was selected and designed according to current design specifications. Authors performed nonlinear static pushover analyses and dynamic response history analyses on the frames to characterize the behavior and generate statistical data to be used in evaluation of the seismic performance factors. Overall, the average overstrength for the performance groups ranges from 5.29 for PG-2 (high gravity load, SDC: Dmax, and long period) to 9.90 for PG-4 (high gravity load, SDC: Dmin, and long period).

Kim, Jun and Kang investigated seismic performance of reinforced concrete staggered wall system structures and their behavior factors such as overstrength factors, ductility factors, and the response modification factors [Kim et al., 2016]. To this end, 5, 9, 15, and 25-story staggered wall system (SWS) structures were designed and were analyzed by nonlinear static and dynamic analyses to obtain their nonlinear force–displacement relationships. The overstrength factors of the structures designed with medium-level seismic load turned out to be smaller than those of the structures designed with low-level seismic load. The structures with 9 m-long staggered walls showed higher overstrength than the structures with 6 m long walls. The overstrength factor degreased from 6.5 to 1.5 as the number of the stories increases 5 to 25.

4. THEORETHICAL BACKGROUND

In this thesis, nonlinear dynamic time history analyses are conducted by PERFORM-3D-V5 a nonlinear analysis and performance assessment for 3D structures which uses an event-to-event solution strategy, where the structure properties are re-formed each time there is a nonlinear event. Event is the change in stiffness of each element and for every stiffness change in each element, structures stiffness also change. Between each event, stiffness of the structure and elements stay constant. Solving series of linear problems from one event to another is the main methodology of analysis. The event to event strategy is more reliable than other strategies. It is simple and also gets traces of the complete force deformation and load displacement paths and simulates what happens in the actual structures.

Like linear analysis, nonlinear analysis seeks for finding the state of equilibrium of a structure/element/component corresponding to the applied nodes. Equation of equilibrium can be written as in equation 4.1. Where P^t is external forces applied at a point at time t and F^t is internal forces developed at that point.

$$P^t - F^t = 0 \tag{4.1}$$

In dynamic analysis, equation 4.1 should include all nonlinearities as well as inertia and damping forces. To solve a nonlinear problem, nodal internal forces and displacements at certain load levels or at certain times are required.

In event to event strategy, all elements have multi linear force-deformation relationship (Figure 4.1) and small displacements are assumed.

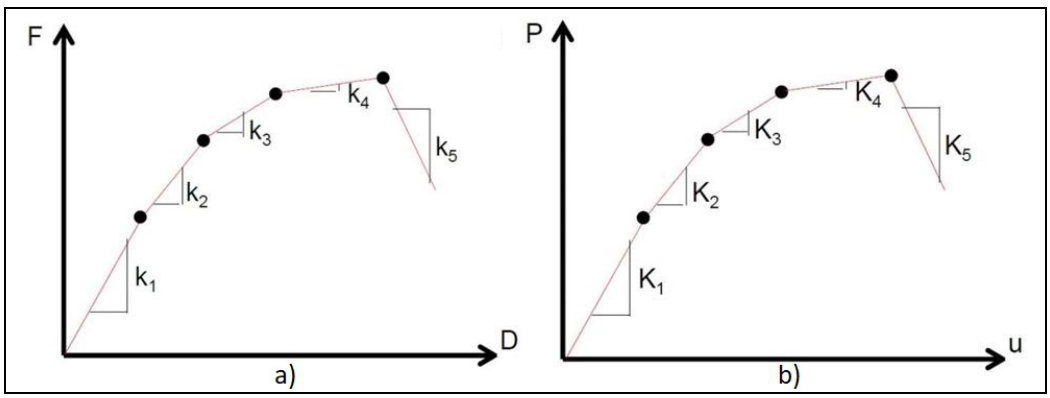

Figure 4.1: a) Multi linear element/component, b) structure model.

Typical element model given in Figure 4.2.

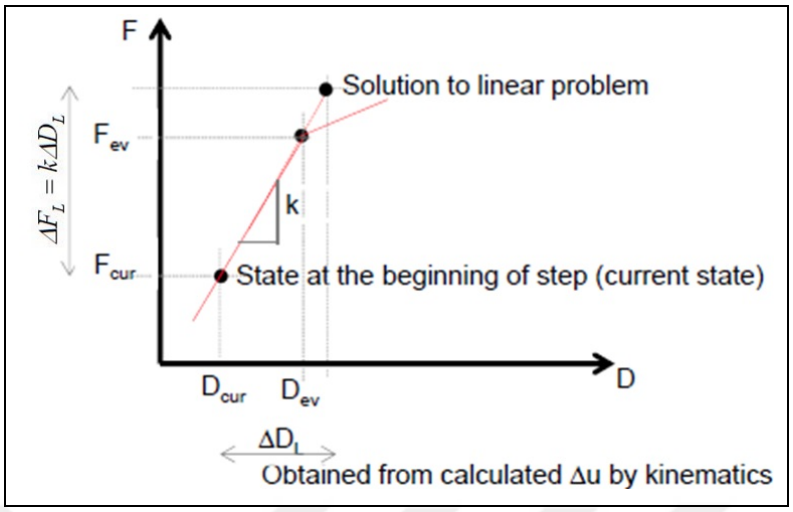

Figure 4.2: Typical element in a structural model.

Event factor can be calculated using equation 5.2 and equation 5.3.

$$f = \frac{D_{ev} - D_{cur}}{\Delta D_L} \tag{4.2}$$

$$f = \frac{F_{ev} - F_{cur}}{\Delta F_L} \tag{4.3}$$

The governing event factor is the smallest event factor calculated considering all elements. Two algorithms can be used in event to event solution strategy. One of them is load increments, given in Figure 4.3

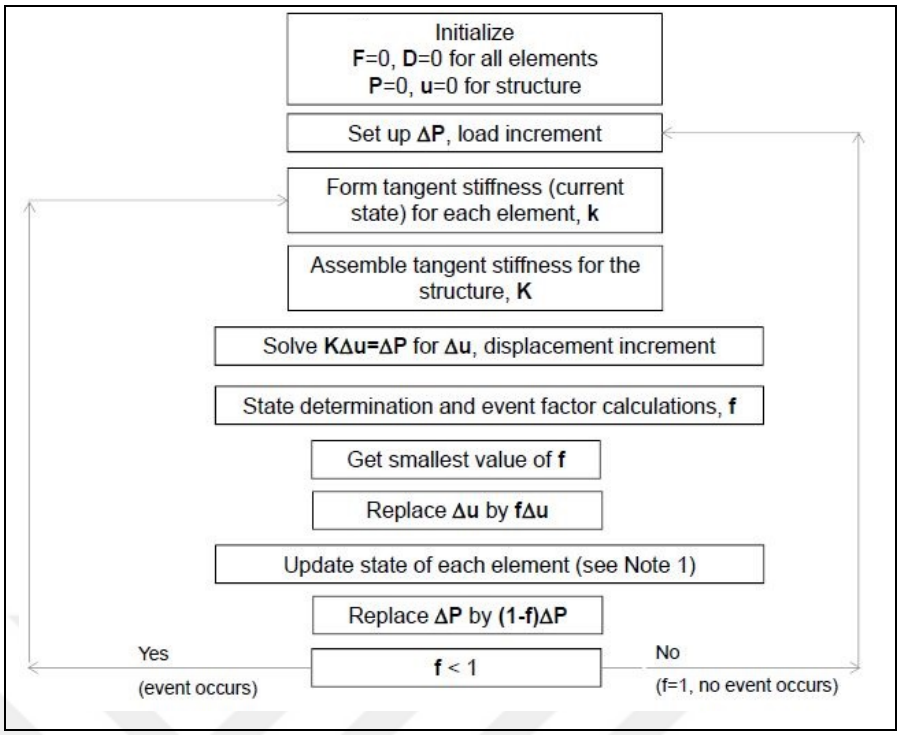

Figure 4.3: Detailed algorithm of load increments.

The other algorithm is total load. Details of the algorithm given in Figure 4.4.

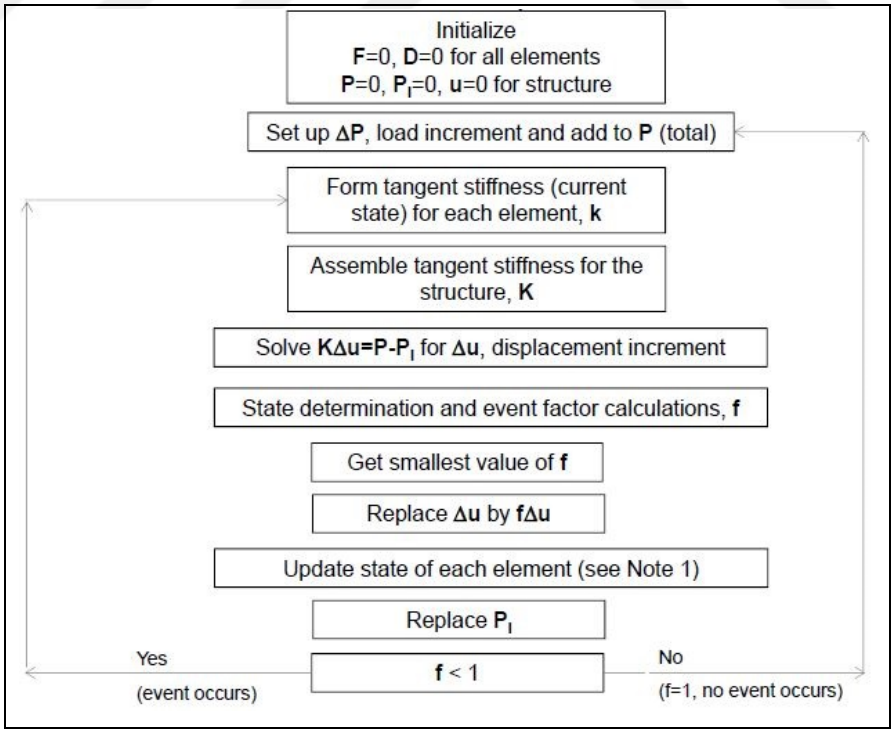

Figure 4.4: Detailed algorithm of total load.

Load can be used when expected displacement is large and structural increments behavior is complex. Convergence within each load increment is quick. However, number of steps decides the computing time. Sometimes total load can be applied and iteration can be used if unbalanced load appears.

It is important that the updated state of the critical element (the one with smallest event factor, (f) be just beyond the event. Because of round-of error the error, state based on fΔP could be just before the event (consider also the case with f=0). This can be taken into account either:

- by adding a small number to the calculated f, or
- by calculating the event factor for a point just beyond the event (equation 4.3)

$$f = \frac{D_{ev} - \Delta D_{tot} + D_{cur}}{\Delta D_L} \tag{4.3}$$

5. NUMERICAL STUDY FOR MOMENT FRAMES

5.1. Design of Special Moment Frames (SMF)

The 4-, 8-, 12- and 20-story steel special moment frames (SMF) with different span lengths are designed based on requirements of American provisions. Four special cases are used in order to include the effects of different span length configurations on amplified seismic load. Details of the case are shown in Table 5.1; Case A) constant span length of 9.0 m (five equal spans); Case B) unequal span length of 6.0m at two edge spans, two 12.0 m spans between the two edge spans and a 9.0 m span in the middle.; Case C) constant span length of 7.5 m (six equal spans); Case D) constant span length of 5.625 m (eight equal spans). Plan dimensions and span lengths are given in Table 5.1.

Table 5.1: Plan dimensions and span lengths of the SMF.

Frame Types	Case	Plan Dimension	Span Length
Moment Frames	Case A	45.0 m x 45.0 m	5@9.00 m
Moment Frames	Case B	45.0 m x 45.0 m	6.0 m - 12.0 m - 9.0 m- 12.0 m - 6.0 m
Moment Frames	Case C	45.0 m x 45.0 m	6@7.50 m
Moment Frames	Case D	45.0 m x 45.0 m	8@5.625 m

Also, typical story plan views of the selected span configurations are given in Figure 5.1.

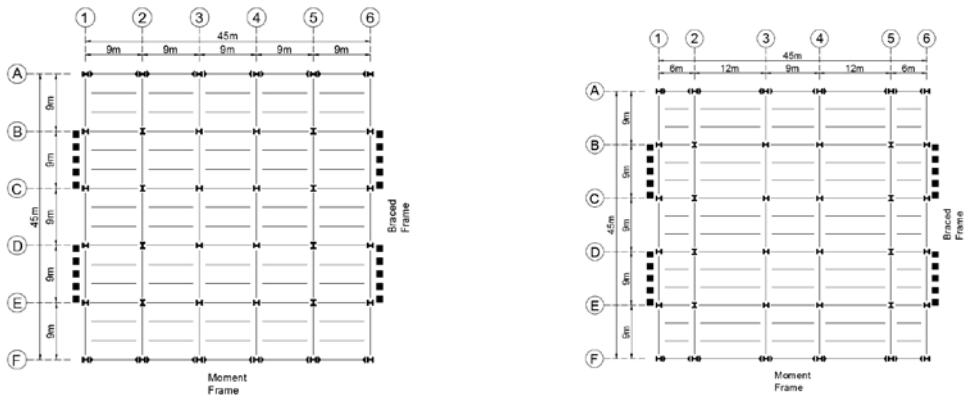

Case A (5@9.00 m) Case B (6.0-12.0-9.0-12.0-6.0 m)

Figure 5.1: Plan of the 4-, 8-, 12- and 20- story SMF buildings.

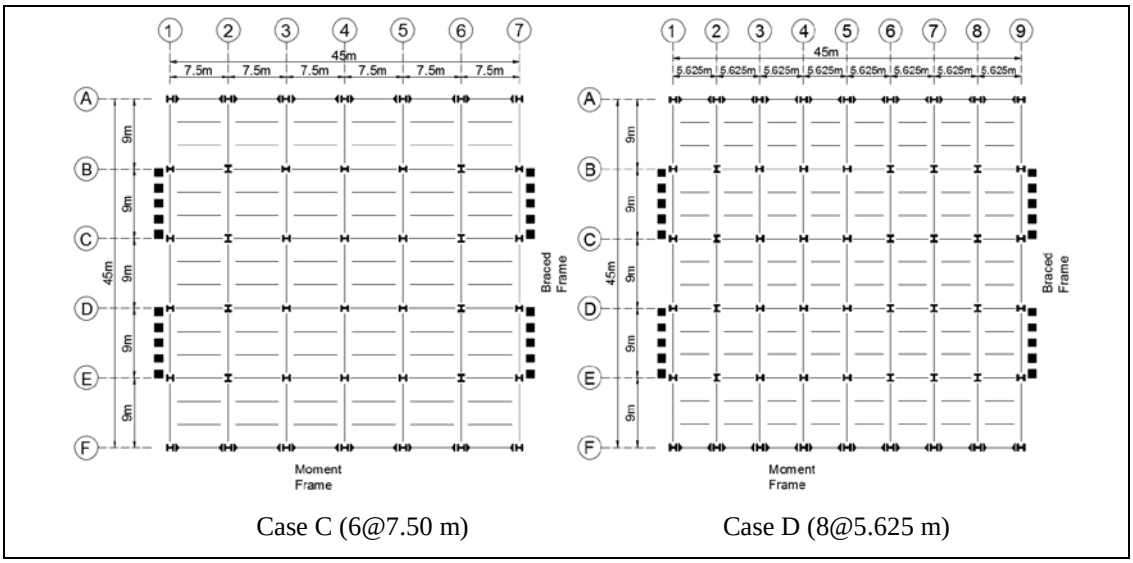

Case C (6@7.50 m) Case D (8@5.625 m)

Figure 5.1: Continuation of the figure.

The plan dimensions of buildings are 45 m x 45 m. The story plans of the buildings are symmetrical. The typical story height for the frames is 4.0 m except for the 8-, 12-, and 20-story frames where the first story height is 5.0 m as shown in Figure 5.2. For the 8-, 12-, and 20-story building, concrete foundation walls and surrounding soil are assumed to prevent any significant horizontal displacement of the structure at the ground level, i.e. the seismic base is assumed to be at the ground level. The columns of the buildings are assumed to be simply connected to the foundation.

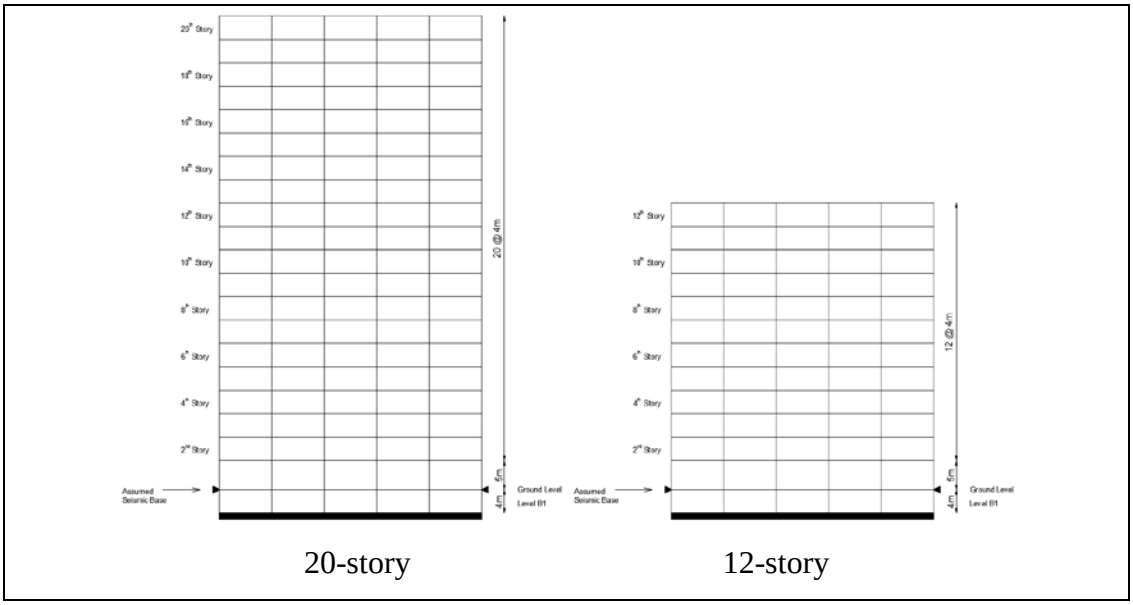

20-story 12-story

Figure 5.2: Elevations of the SMF buildings.

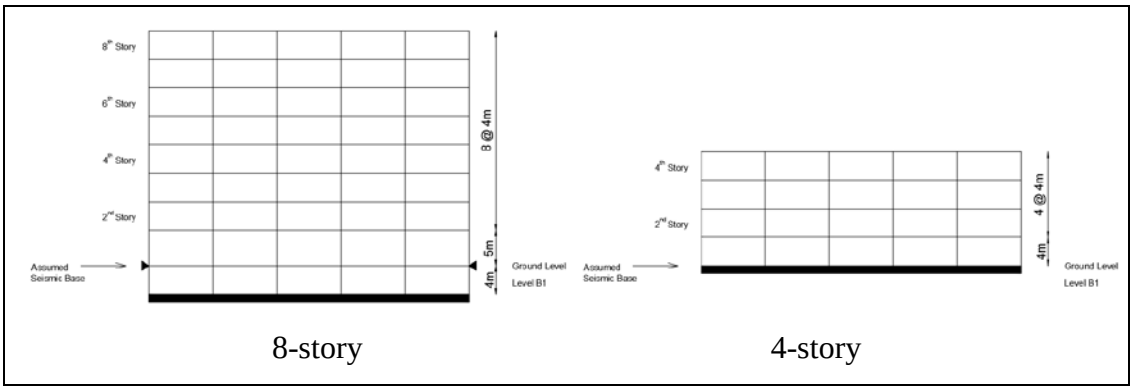

8-story 4-story

Figure 5.2: Continuation of the figure.

The linear analysis of buildings is applied by using Load and Resistance Factor Design (LRFD) methodology in accordance with American provision [AISC 360-10, 2010]. Dead loads including self-weight of the members and live load used in the study are 5.0 kN/m^2 and 2.4 kN/m^2 except at the roof level, where they are taken as 4.0 kN/m^2 and 1.4 kN/ m^2, respectively. European wide flange profiles with steel grades S355 are preferred for design. The member sizes of the frames are given in Appendix B.

The buildings are designed for a site where MCE spectral response acceleration parameters at short period, S_S is 2.0g and at a period of 1s, S_1 is 1.0g. Design earthquake spectral response acceleration parameters are taken as $S_{DS} = 1.333$ (g) at short period, $S_{D1} = 0.666$ (g) at a period of 1s. Long-period transition period, T_L is assumed to be 12.0 s. Response Spectrum Analysis are used in seismic design. Seismic design category *D* is taken for all structures in design. The response spectrum curves corresponding to design level and maximum considered earthquake level (MCE) are developed as specified in provision and shown in Figure 5.3. Shear wave velocity (V_s) of site class is assumed to vary between 300-770 m/s.

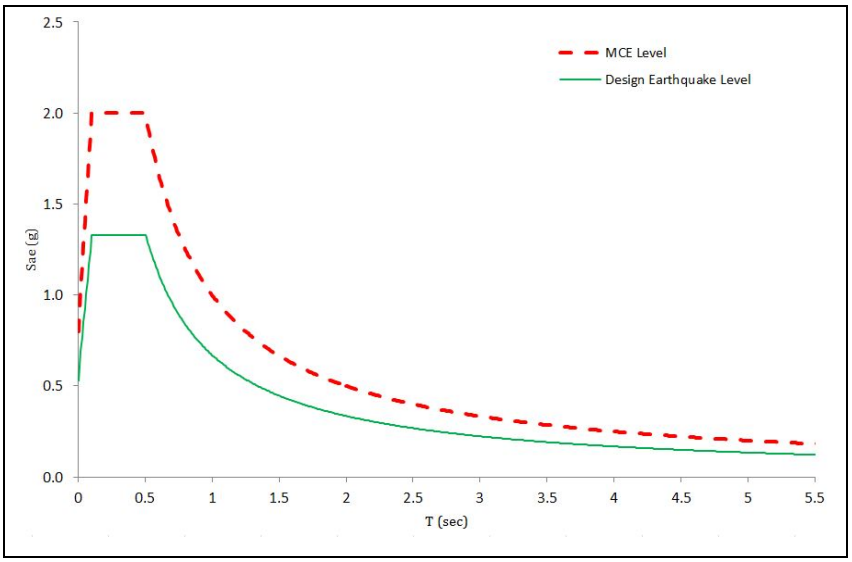

Figure 5.3: Response Spectra for DBE and MCE levels for SMF.

In cases where the combined response for the modal base shear (V_t) is less than 85% of the calculated base shear (V) using the equivalent lateral force procedure, the forces are increased by using coefficient ($0.85V/V_t$) in accordance with ASCE 7-10 [ASCE 7-10, 2010].

The calculated fundamental period of the structure (T) are checked with the approximate fundamental period (T_a) multiplied with coefficient of upper limit (C_u). Where the calculated fundamental period (T) exceeds C_uT_a, C_uT_a is used instead of T in accordance with ASCE 7-10 [ASCE 7-10, 2010]. Based on the same requirement, $C_u = 1.4$ for $S_{D1} = 0.666\ g > 0.4\ g$. The calculated fundamental periods of vibration, the total mass for the frames are given in Table 5.2.

Table 5.2: Calculated fundamental periods and total mass for the SMF.

Story	Case	T (sec)	T_a (sec)	C_u	C_uT_a (sec)	T_{used} (sec)	Total Mass (kN.sec^2/m)	V (kN)	V_t (kN)
4	A	1.363	0.665	1.4	0.931	0.931	2173	1906	1628
	B	1.297	0.665	1.4	0.931	0.931	2173	1906	1625
	C	1.256	0.665	1.4	0.931	0.931	2173	1906	1640
	D	1.293	0.665	1.4	0.931	0.931	2173	1906	1622
8	A	2.245	1.187	1.4	1.662	1.662	4478	2749	2343
	B	2.076	1.187	1.4	1.662	1.662	4478	2749	2442
	C	2.193	1.187	1.4	1.662	1.662	4478	2749	2438
	D	2.098	1.187	1.4	1.662	1.662	4478	2749	2468
12	A	2.616	1.628	1.4	2.279	2.279	6875	4214	3582
	B	2.589	1.628	1.4	2.279	2.279	6875	4214	3657
	C	2.459	1.628	1.4	2.279	2.279	6875	4214	3984
	D	2.562	1.628	1.4	2.279	2.279	6875	4214	3888
20	A	3.349	2.435	1.4	3.409	3.349	11420	7002	6030
	B	3.335	2.435	1.4	3.409	3.349	11420	7002	6083
	C	3.342	2.435	1.4	3.409	3.349	11420	7002	6238
	D	3.516	2.435	1.4	3.409	3.349	11420	7002	5965

The approximate fundamental period (T_a) is calculated as follows:

$$T_a = C_t h_n^x \tag{5.1}$$

Where h_n is the structural height and the coefficients C_t*=0.0724* and *x=0.8 for SMF*. The story system of the buildings is assumed to provide diaphragm action and to be rigid in the horizontal plane. In seismic design of SMF, the appropriate response modification coefficient (*R=8*) overstrength factor (($\boldsymbol{\Omega_o}$)*=3*) and the deflection amplification factor (C_d*=5.5*) are used in determining the base shear, element design forces, and design story drift where redundancy factor ρ is taken as

1.3. Story drift ratio limitation is taken as 2% of story height as specified in ASCE7-10 [ASCE 7-10, 2010]. Story drift ratios of SMF are illustrated as in Figure 5.4.

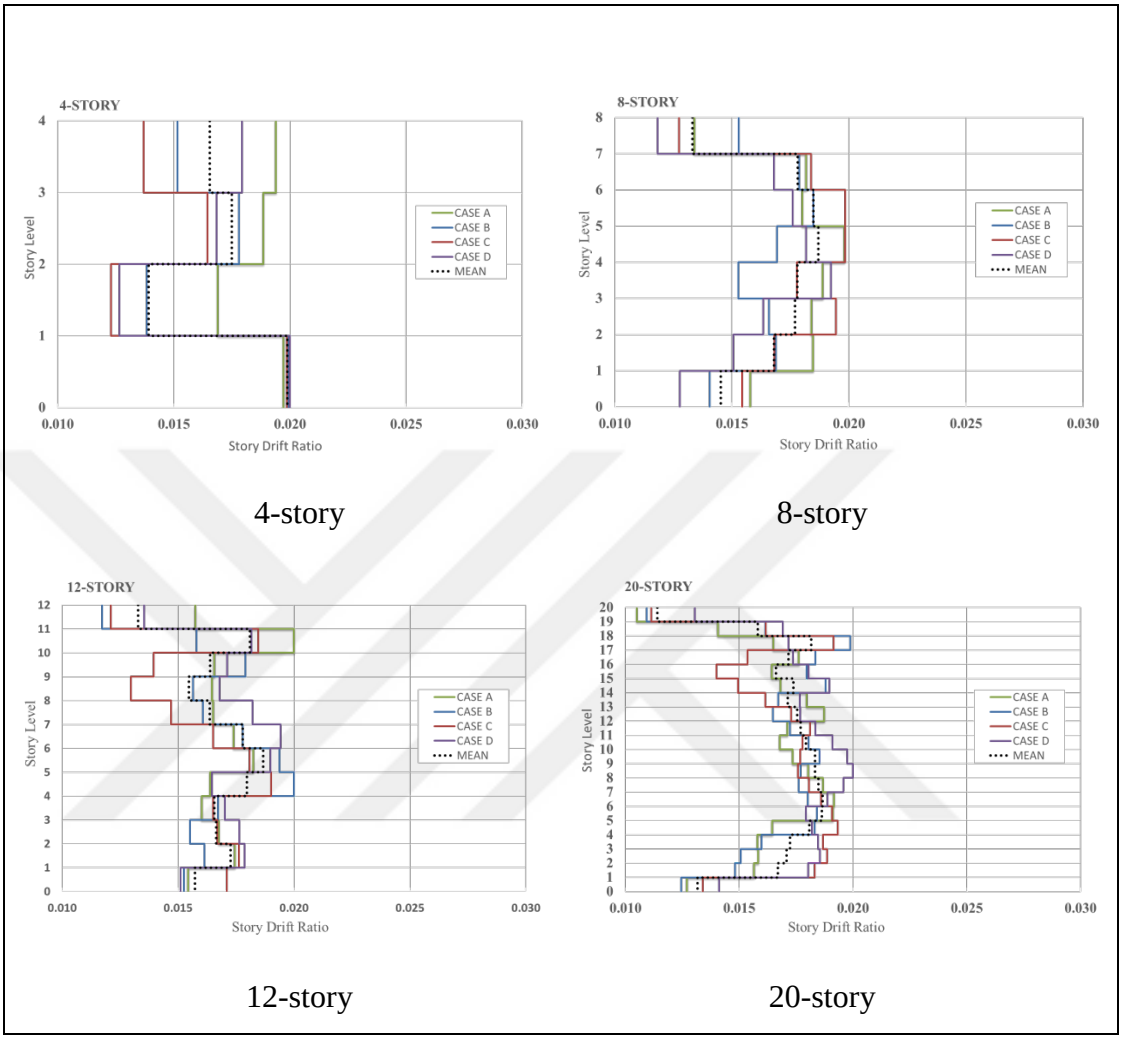

Figure 5.4: Story drift ratio of SMF.

Moment connections are formed with reduced beam sections (RBS) in accordance with AISC 358-10 [AISC 358-10, 2010]. The shear force at the center of the RBS is calculated from a free body diagram of the span between the centers of the RBS. The moment at the center of RBS, M_{pr} is calculated based on the load combination as follows:

$$1.2D + 0.5L + 0.2S \tag{5.2}$$

Based on calculation of elastic drift shall consider the effect of RBS. In lieu of more detailed calculations, effective elastic drifts can be calculated by multiplying elastic drifts by 1.1 in accordance with AISC 358-10 [AISC 358-10, 2010].

The columns and beams satisfy the requirements for highly ductile members according to AISC 341-10 [AISC 341-10, 2010]. Strong-column-weak-beam requirement are checked by following equation:

$$\frac{\sum M_{pc}^{*}}{\sum M_{pb}^{*}} > 1.0 \tag{5.3}$$

Where $\sum M_{pc}^{*}$ is the sum of the projections of the nominal flexural strengths of the columns and $\sum M_{pb}^{*}$ is the sum of the projections of the expected flexural strengths of the beams.

For P-delta effects on story shears and moments are checked using Equation 5.4. Where the stability coefficient (θ) is equal to or less than 0.10, the resulting member forces and moments are not required to be considered. Frame systems are satisfied Equation 5.4.

$$\theta = \frac{P_x \Delta I_e}{V_x h_{sx} C_d} < 0.1 \tag{5.4}$$

where P_x is the total vertical design load, Δ is the design story drift, I_e is the importance factor (1.0 for seismic loads) V_x is the seismic shear force, h_{sx} is the story height.

5.2. Modeling Moment Frames (SMF) for Nonlinear Analyses

The 4-, 8-, 12- and 20-story steel special moment frames were modeled with PERFORM 3D; a nonlinear analysis and performance assessment software to conduct non-linear analyses. The frames were modeled as beam and column elements. As reduced beam section (RBS) concept is used in the design of frames, inelastic behavior is limited to specific locations (plastic hinge) in the beam. Beam elements were modeled as beam compound and Rigid-Plastic hinge concept was used in modeling. In this concept, a moment plastic hinge is literally a hinge, closely analogous to a rusty hinge that rotates only after enough moment has been applied to overcome the friction between the hinge pin and the casing. Figure 5.5 shows a hinge and a possible moment-rotation relationship. The hinge is initially rigid, and begins to rotate at the yield moment.

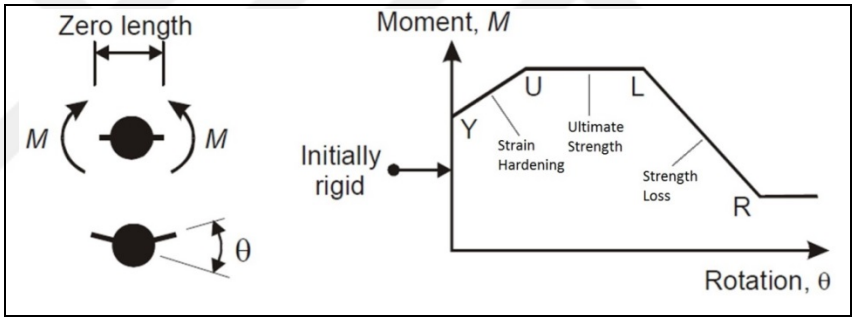

Figure 5.5: Plastic Hinge.

The key points in the relationship in Figure 5.5 are as fallows.

- Y Point. This is the first yield point.
- U Point. This is the ultimate strength point, where the maximum strength is reached.
- L Point. This is the ductile limit point, where significant strength loss begins.
- R Point. This is the residual strength point, where the minimum residual strength is reached.
- X Point. This is usually at a deformation that is so large that there is no point in continuing the analysis.

Beam compound component with RBS section was modelled in PERFORM 3D as shown in Figure 5.6. Half of the column length from its axis modelled as stiff end zone, length between column face and the centre of reduced section length is elastic section. Plastic hinge is in the centre of the reduced section length and between two plastic hinge located in both side of the beam is elastic section.

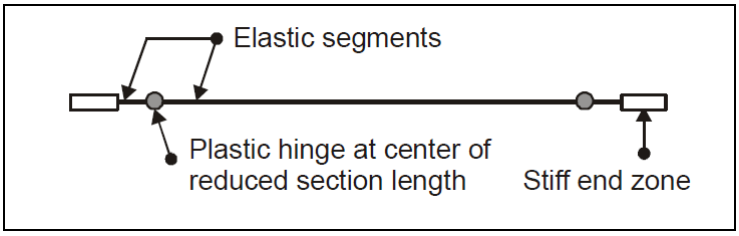

Figure 5.6: Model for Reduced Beam Section.

An example beam compound model used in PERFORM 3D for nonlinear dynamic analyses shown in Figure 5.7. The example model belongs to HE650M beam section on the first story. Moment hinges properties are arranged in “Inelastic Tab” shown in Figure 5.8.

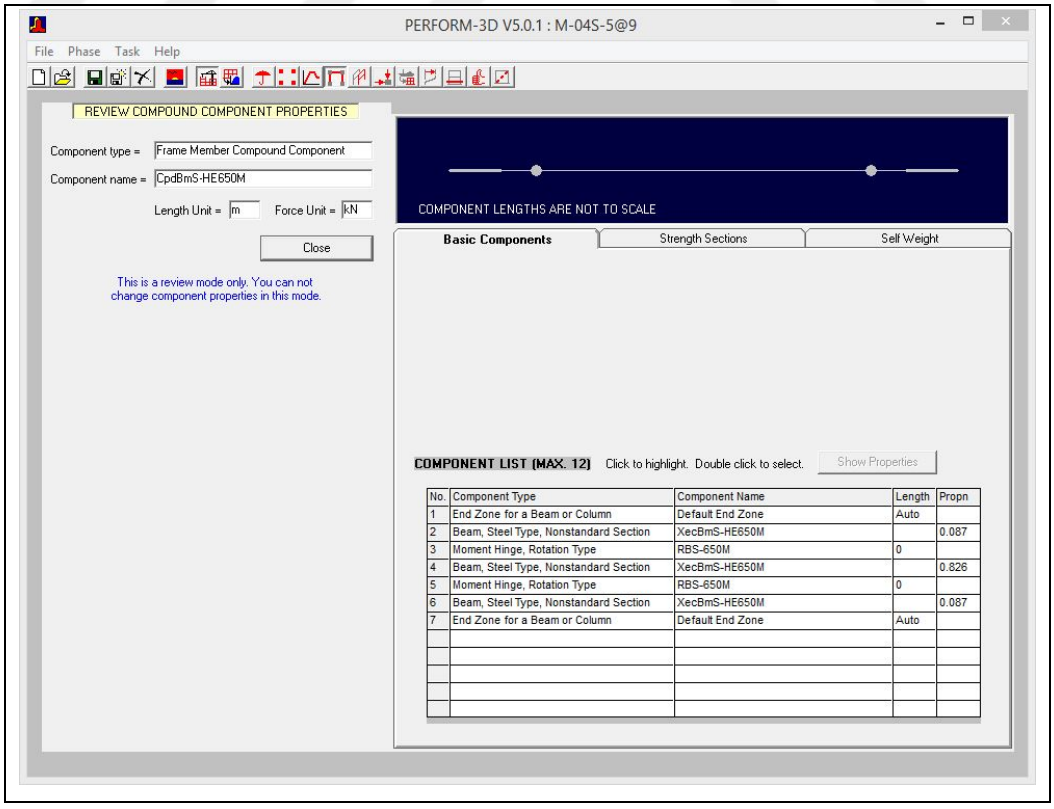

Figure 5.7: RBS Beam compound for HE650M.

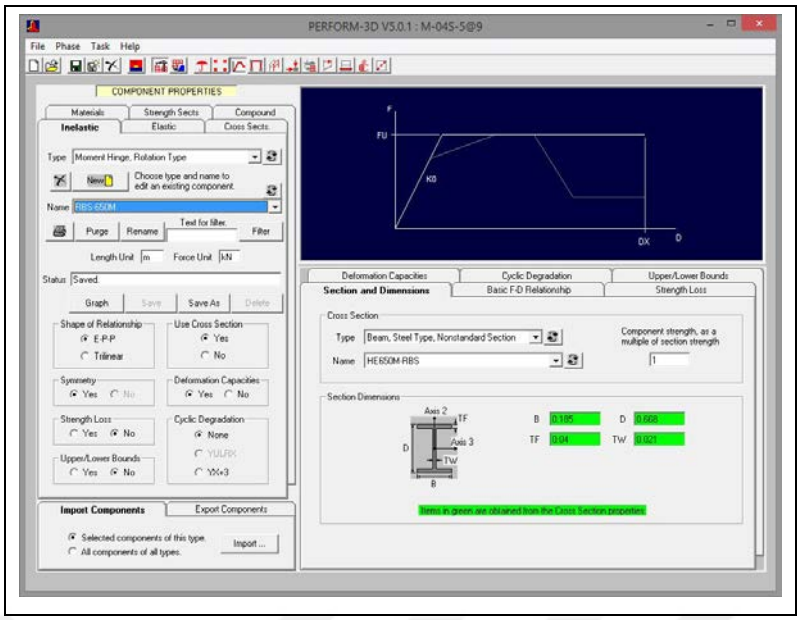

Figure 5.8: Moment Hinge, Rotation Type Menu for HE650M.

Section properties can be defined automatically by using programs own section database as “Beam, Standard Steel Section” or by users as “Beam, Non-Standard Steel Section”. As it’s seen in Figure 5.9, section properties such as young modulus, poisson ratio and yield stress are arranged in this menu. Users can also define inelastic properties in cross section tab (Figure 5.10) so all necessary data to form plastic hinge is given to the program.

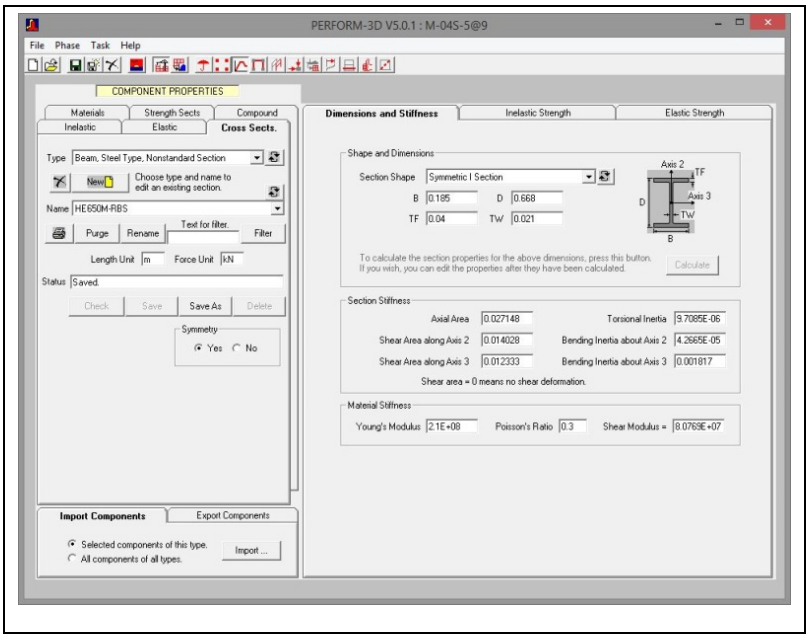

Figure 5.9: Cross section menu for HE650M.

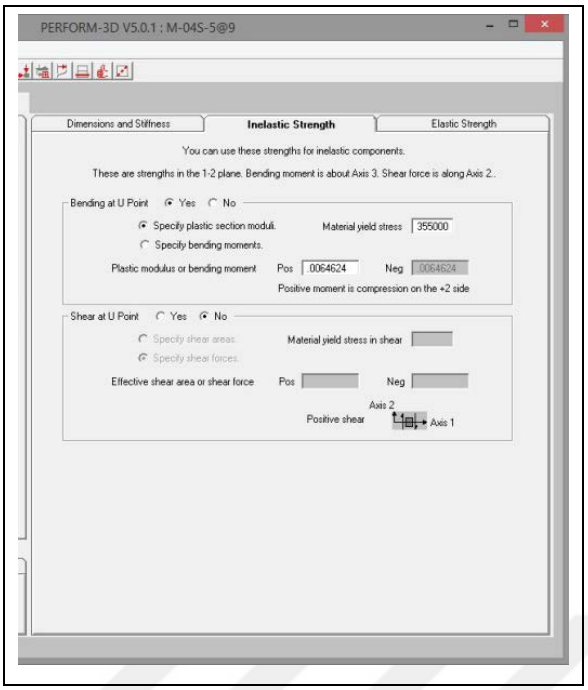

Figure 5.10: Inelastic strength tab in cross section menu for HE650M.

Column elements were modeled using Fema365 regulations and chord rotation model was used. The chord rotation model is the simplest model, with the most Limitations. The basic model is shown in Figure 5.11.

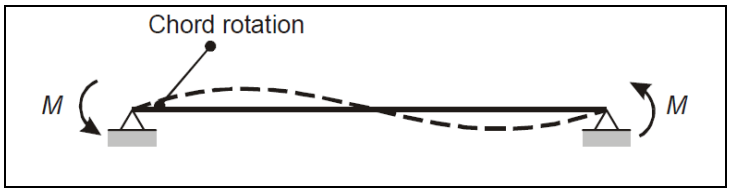

Figure 5.11: Chord rotation model.

The nonlinear relationship between the end moment and end rotation are obtained from Fema-365. The end rotation is the rotation from the chord, which eliminates rigid body rotations.

The interaction between the axial force and bending moment was also considered in columns. P-Δ effects were always included in the time-history analyses. For nonlinear analyses, Columns were modeled as column compound given in Figure 5.12 and elastic-perfectly-plastic (E-P-P) hysteresis loop properties ware used to define the behavior of the members. Figure 5.13. shows the hysteresis loop for E-P-P behavior.

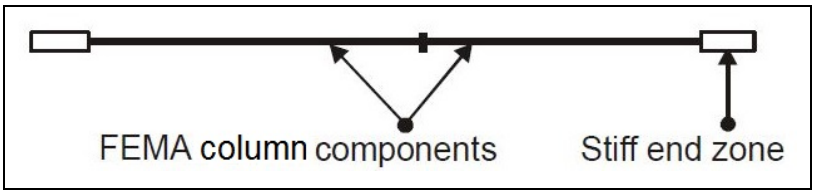

Figure 5.12: Column component.

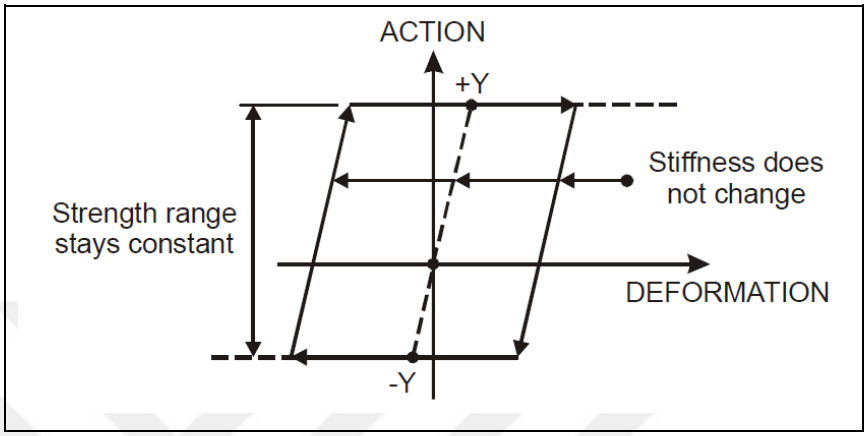

Figure 5.13: Non-Degrading Loop for E-P-P Behavior.

An example “Fema Column Compound” model used in PERFORM 3D for nonlinear dynamic analyses shown in Figure 5.14. The example model belongs to HE600B column section. In the modeling, region from column axis to column face is a rigid part and from column face to half length of the column is assigned as “Inelastic Fema Column, Steel Type”. “Fema Column, Steel Type” menu can be seen in figure 5.15.

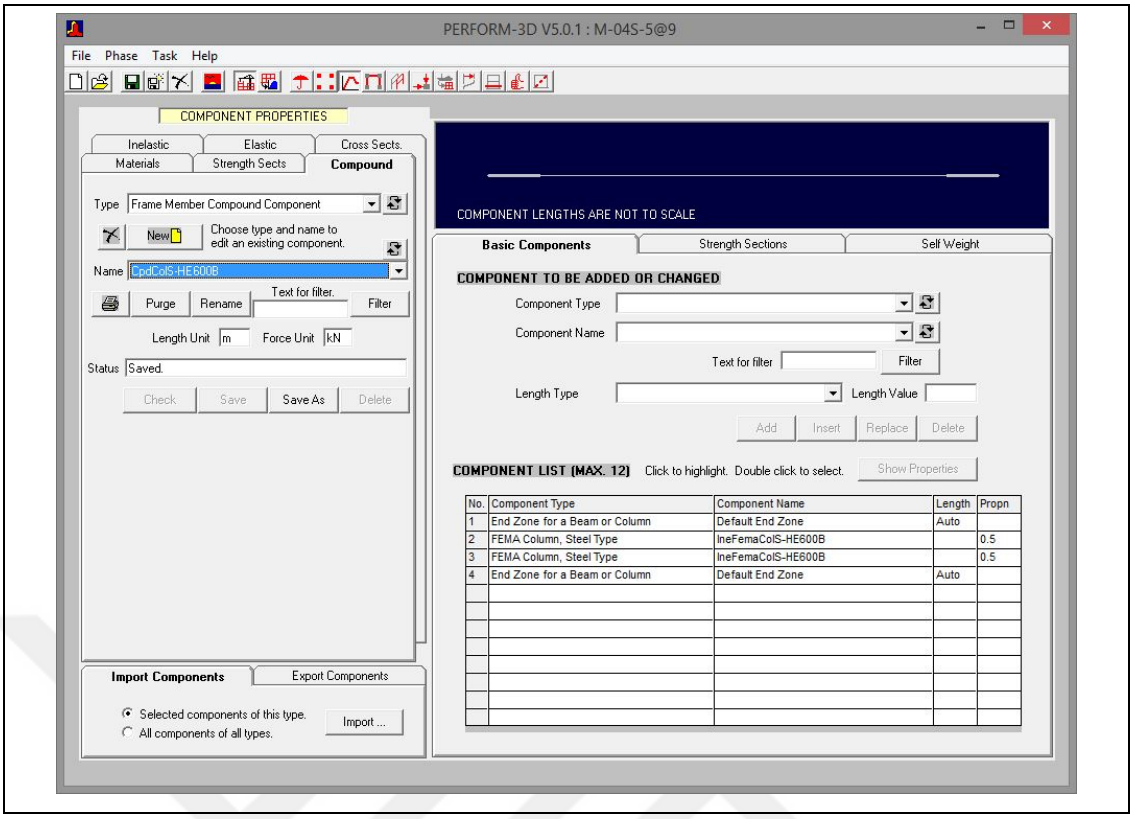

Figure 5.14: Column compound model for HE600B section.

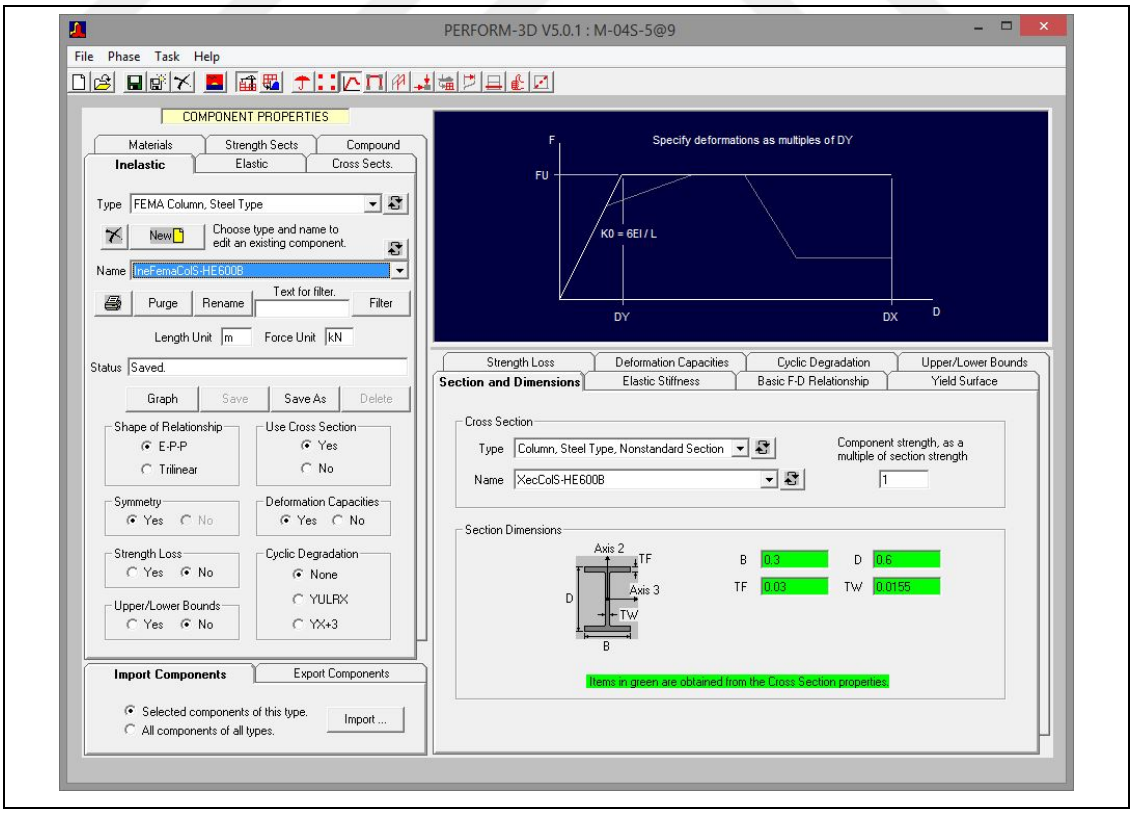

Figure 5.15: Fema Column, Steel Type menu for HE600B section.

Figure 5.16 shows the yield surface for a steel section. Where P_{YC}= Axial compression load in yield, P_{YT}= Axial tension load in yield, M_{3Y}= 3-3 Axis yield moment, M_{2Y}=2-2 axis yield moment.

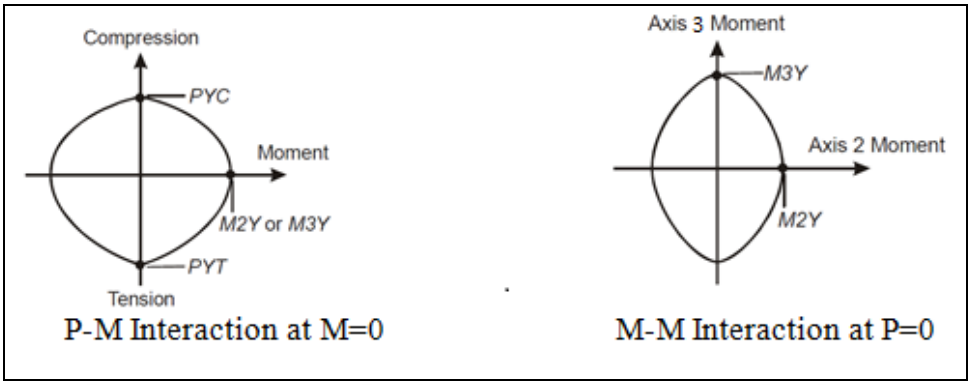

Figure 5.16: Yield Surface at M=0 and P=0.

P-M-M yield surface of the columns are calculated with Equation 5.5;

$$f_{PM} = \left(\frac{P}{P_{Y0}}\right)^{\alpha} + \left(\frac{M}{M_{Y0}}\right)^{\beta} \tag{5.5}$$

In Equation 5.5, f_{PM}, yield function value = 1.0 for yield, P = axial force, M =bending moment, P_{Y0} = yield force at M = 0, and M_{Y0} = yield moment at P = 0.

Section properties can be defined automatically by using programs own section database as “column, Standard Steel Section” or by users as “Column, Non-Standard Steel Section”. As it’s seen in Figure 5.17, section properties such as young modulus, poisson ratio and yield stress are arranged in this menu. Users can also define yield surface from inelastic strength tab (Figure 5.18) so all necessary data to form Fema hinge is given to the program.

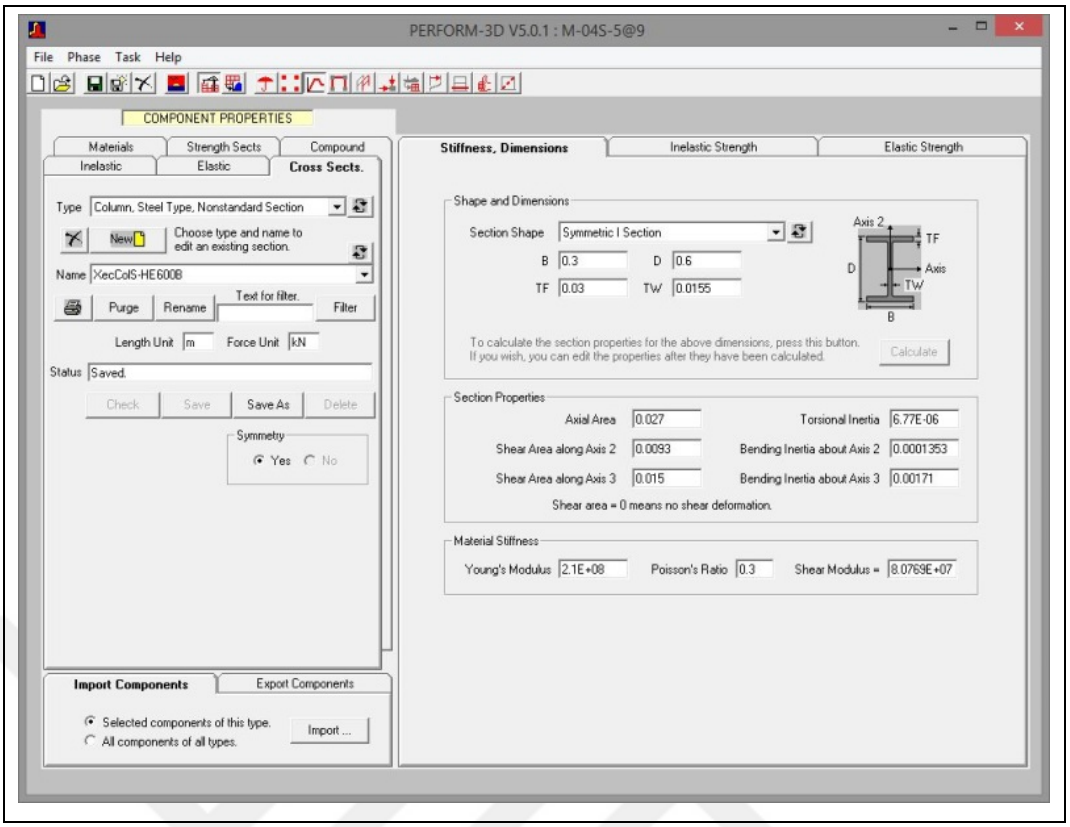

Figure 5.17: Nonstandard column section menu for HE600B section.

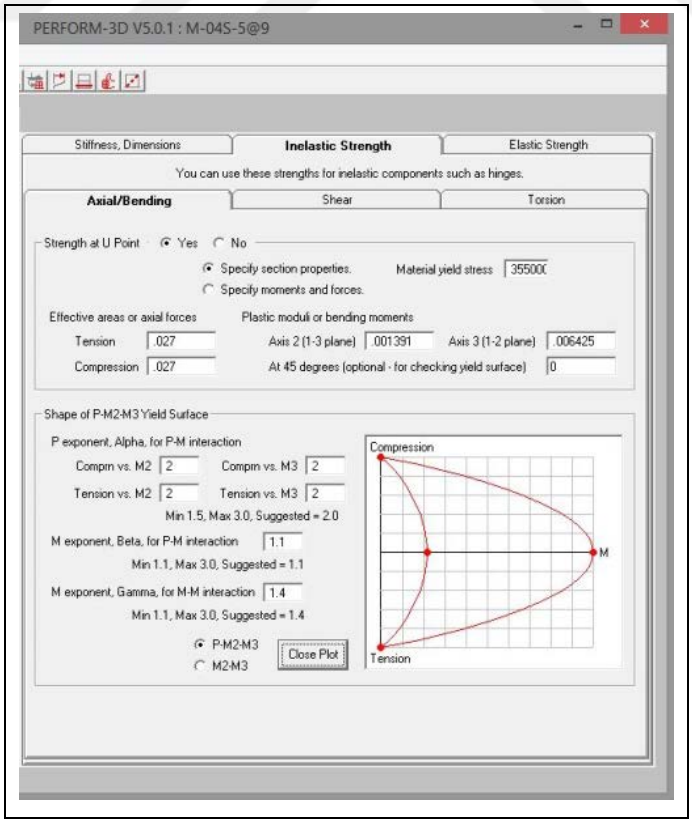

Figure 5.18: Yield surface arrangement in Perform 3D.

4-, 8-, 12- and 20-story special moment frames modeled in PERFORM 3D V5 in order to use in nonlinear dynamic time history and pushover analyses is given in figure 5.19.

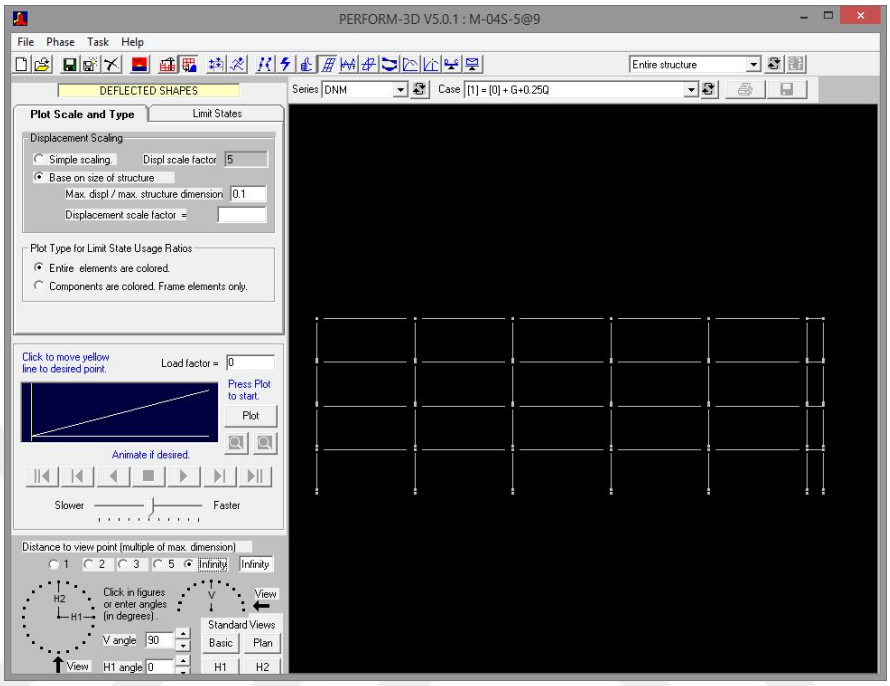

4 Story frame model

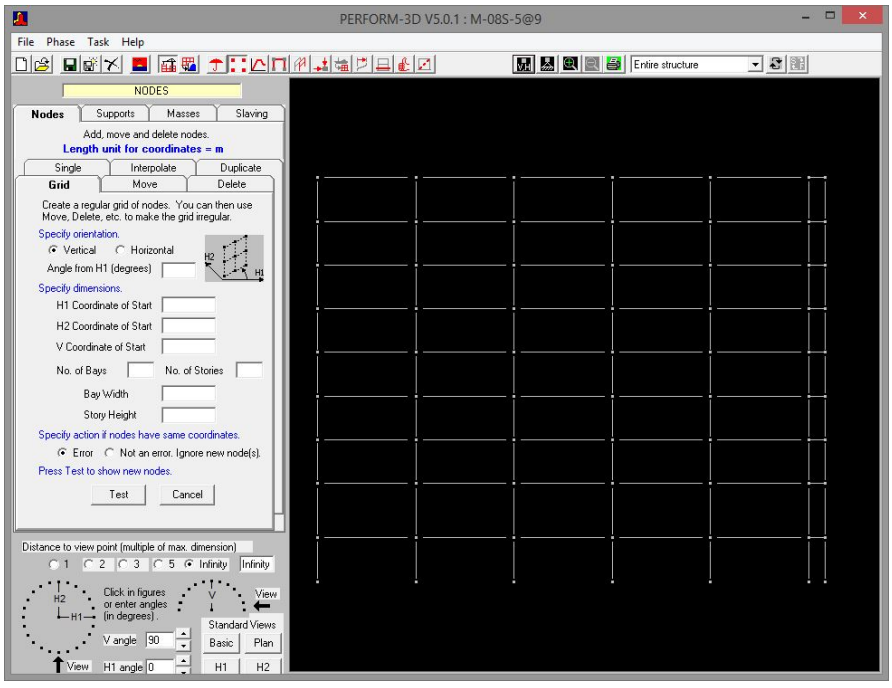

8 Story frame model

Figure 5.19: Perform 3D v5 frame models for 4-, 8-, 12- and 20- story frames.

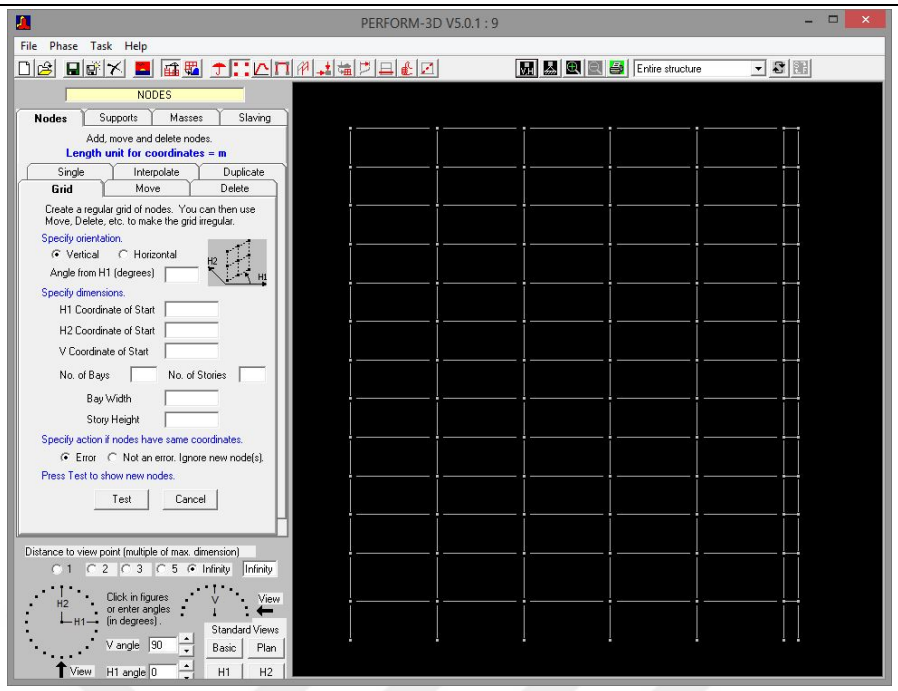

8 Story frame model

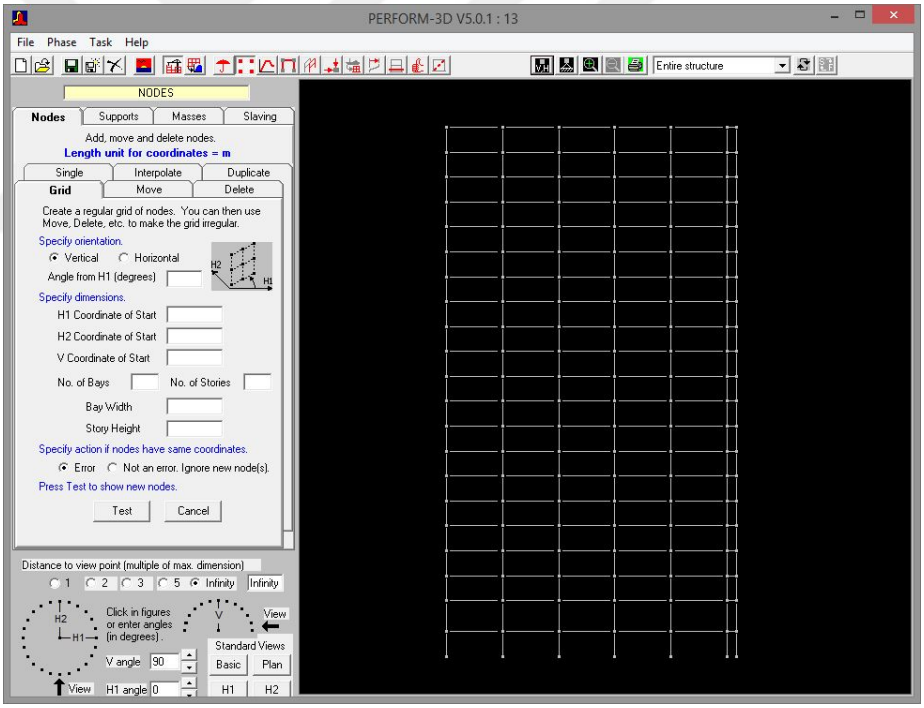

20 Story frame model

Figure 5.19: Continuation of the figure.

5.3. Analytical Study on Moment Frames (SMF)

Two sets of strong ground motion having a 2% and 10% probability of exceedance in 50 year were selected from Pacific Earthquake and Research Centre (PEER) strong ground motion data base for this study. Each set have seven ground motions. Site class selected for analyses have a shear wave velocity (V_s) between 300 m/s and 770 m/s. Response spectra curve was developed based on American regulations and all ground motions selected for this study were scaled with it. The spectrum parameters for the maximum-considered earthquake (MCE) level have a sort period spectral acceleration, S_S = 2.0g and one second spectral acceleration, S_1 = 1.0g. As for design spectrum the parameters are, S_{DS} =1.333 (g) S_{D1}= 0.666 (g). For both spectrums long-period transition period T_L is 12.0 seconds. The characteristic properties of selected strong ground motions are given in Table 6.3.

Table 5.3: Strong ground motion Characteristics selected from PEER database.

	NGA#	Record	Scale Factor	Duration (sec)	PGA (g)
GM 1 (%10)	265	Victoria	1.4530	24.54	0.9377
GM 2 (%10)	289	Irpinia	2.095	35.22	0.2649
GM 3 (%10)	587	New Zealand	1.5605	49.38	0.3757
GM 4 (%10)	881	Landers	1.8989	56.07	0.4235
GM 5 (%10)	1119	Kobe	0.6005	40.99	0.4187
GM 6 (%10)	4132	Park Field	2.0880	21.20	0.7667
GM 7 (%10)	8166	Düzce	1.7683	35.02	0.7007
GM 8 (%2)	265	Victoria	2.1795	24.54	1.4070
GM 9 (%2)	289	Irpinia	3.143	35.22	0.3974
GM 10 (%2)	587	New Zealand	2.3408	49.38	0.5636
GM 11 (%2)	881	Landers	2.8483	56.07	0.6353
GM 12 (%2)	1119	Kobe	3.1325	40.99	0.6281
GM 13 (%2)	4132	Park Field	2.6524	21.20	1.1500
GM 14 (%2)	8166	Düzce	0.9007	35.02	1.0510

Strong ground motions having a 10% probability of exceedance in 50 year were named from GM1 to GM7 that cause moderate structural damage and strong ground motions corresponding to 2% probability of exceedance in 50 year were named from GM 8 to GM14 that cause heavy structural damage. Acceleration time histories of the selected ground are given in Figure 5.20. and 5.21.

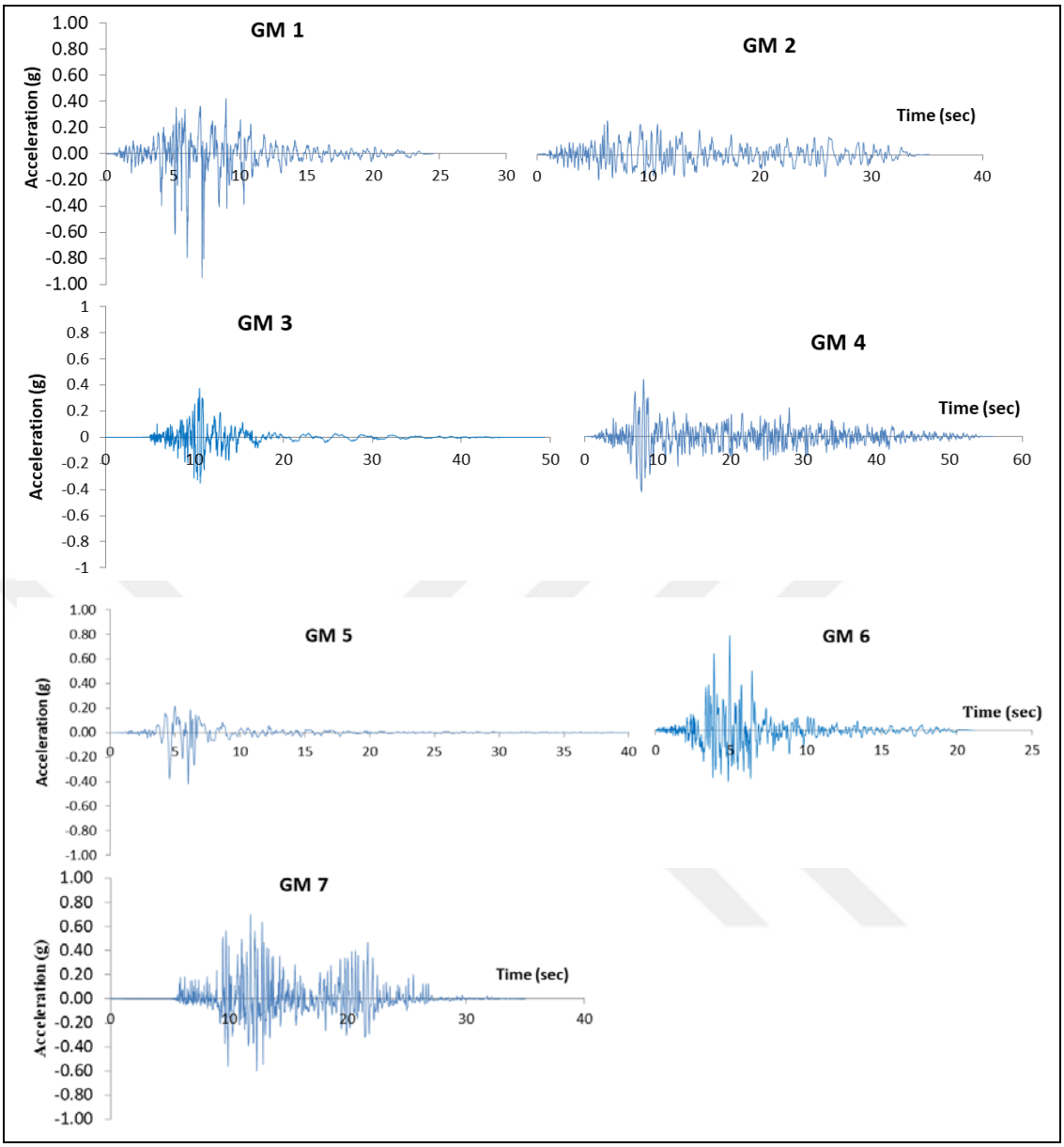

Figure 5.20: Acceleration time histories of the selected ground motions corresponding to 10% probability of exceedance in 50 year.

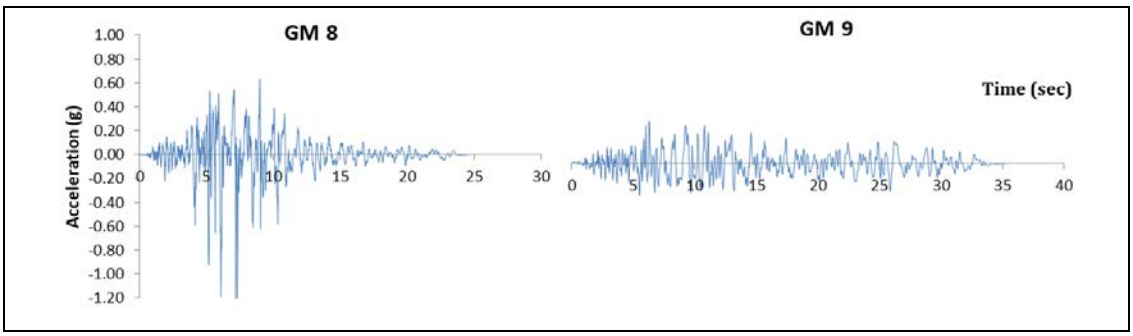

Figure 5.21: Acceleration time histories of the selected ground motions corresponding to 2% probability of exceedance in 50 year.

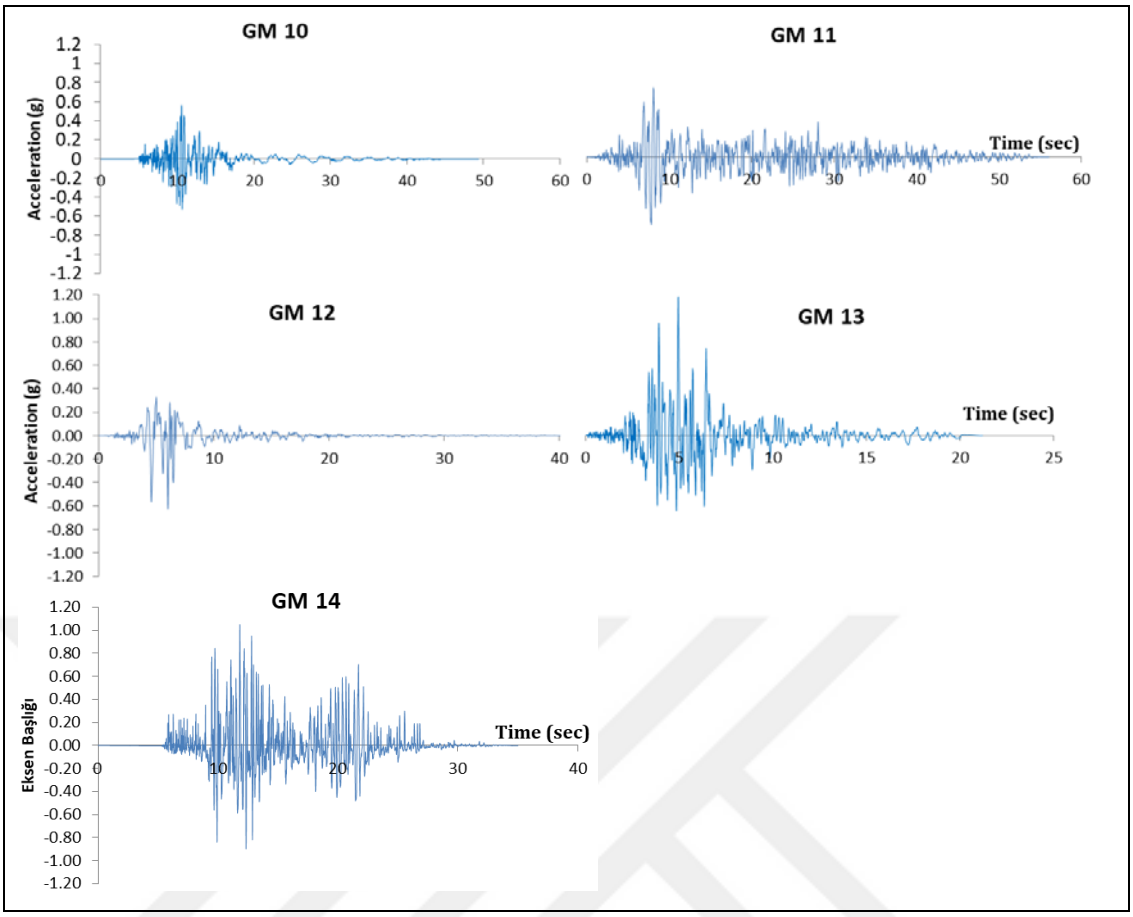

Figure 5.21: Continuation of the figure.

Response spectra of the selected strong ground motions having a 10% probability of exceedance in 50 year are given in Figure 5.22 and response spectra of the selected strong ground motions having a 2% probability of exceedance in 50 year are given in Figure 5.23.

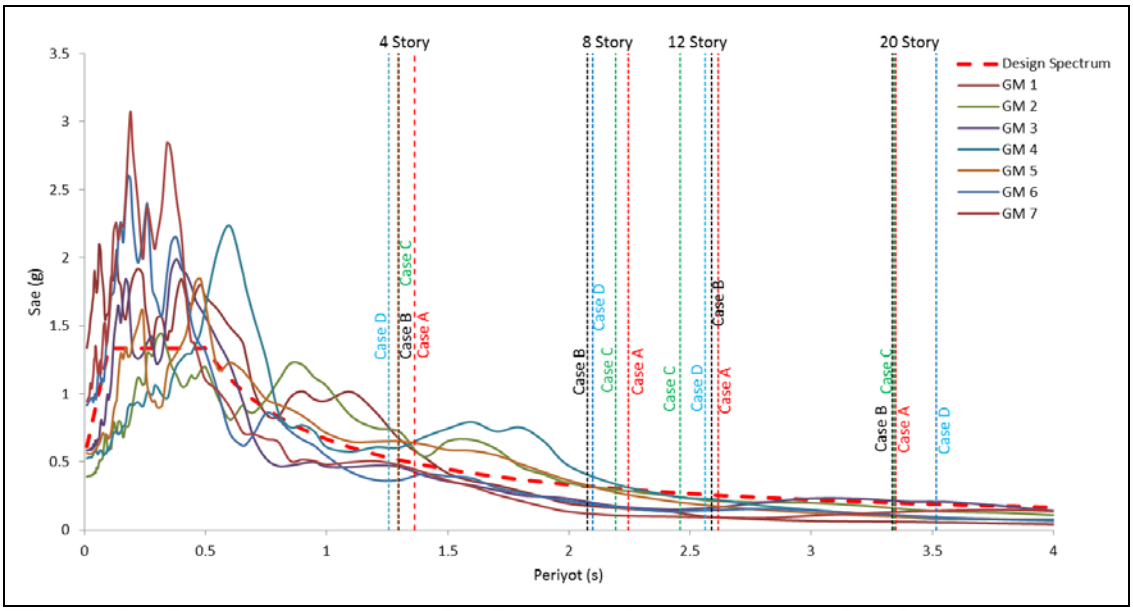

Figure 5.22: Response Spectra of the ground motions (GM1 to GM7) selected from PEER database for design earthquake level corresponding to 10% probability of exceedance in 50 year.

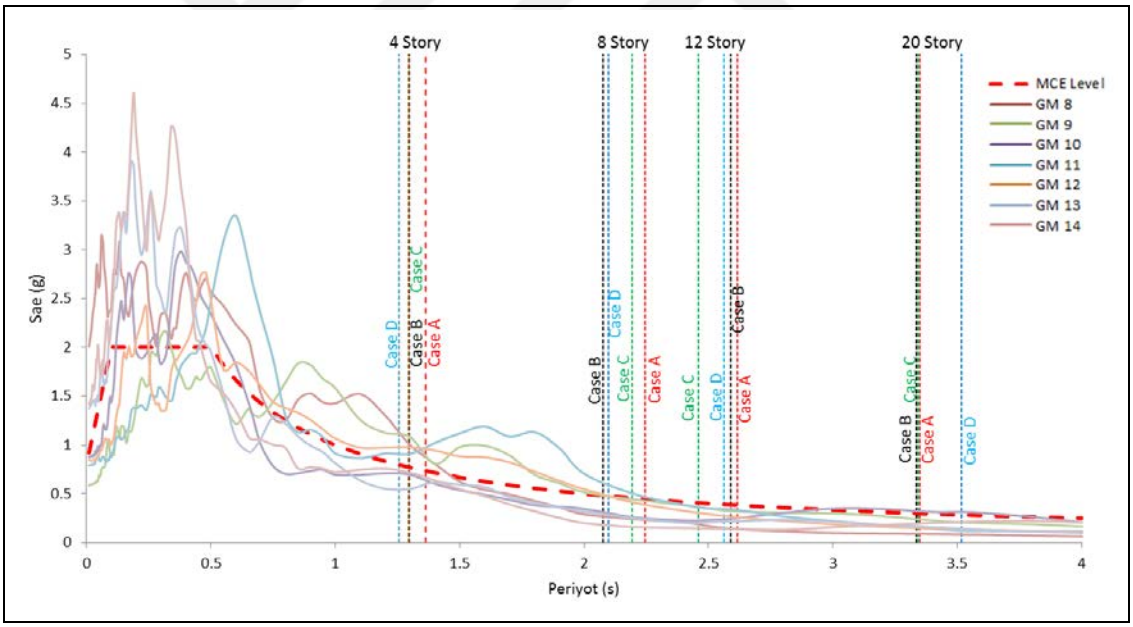

Figure 5.23: Response Spectra of the ground motions (GM8 to GM14) selected from PEER database for design earthquake level corresponding to 2% probability of exceedance in 50 year.

5.4 Analyses Result for Moment Frames (SMF)

Nonlinear dynamic time history analyses were conducted in order to investigate amplified seismic load effects on the 4-, 8-, 12- and 20-story frames. The frames were subjected to two groups of ground motions (a total of 14 ground motions) corresponding to 10% and 2% probability of exceedance in 50 year.

The maximum average drift ratios in each story for 10% and 2% probability of exceedance in 50 year are given in Figure 5.24. For 4-story frames, maximum drift occurs in 4th story while for 8-, 12- and 20-story frames maximum drift occurs 7th, 11th and 18th story respectively. Under strong ground motions corresponding to 10% probability of exceedance in 50 year, maximum average drift ratios do not exceed 2% for all frames and while it's up to 2.78% for strong ground motions corresponding to 2% probability of exceedance in 50 year. Case B has the lowest values for drift ratios.

The maximum drift ratio for each frame under selected ground motions are given in Fig 5.25. The maximum drift ratio varied between 1.55% and 4.26% for 4-story frames. For 8-story frames it varies between 0.87% and 3.78%, for 12-story frames it varies from 0.98% to 3.79% and for 20-story frames drift ratio ranges from 0.95% to 2.74%. For 8-, 12- and 20- story frames.

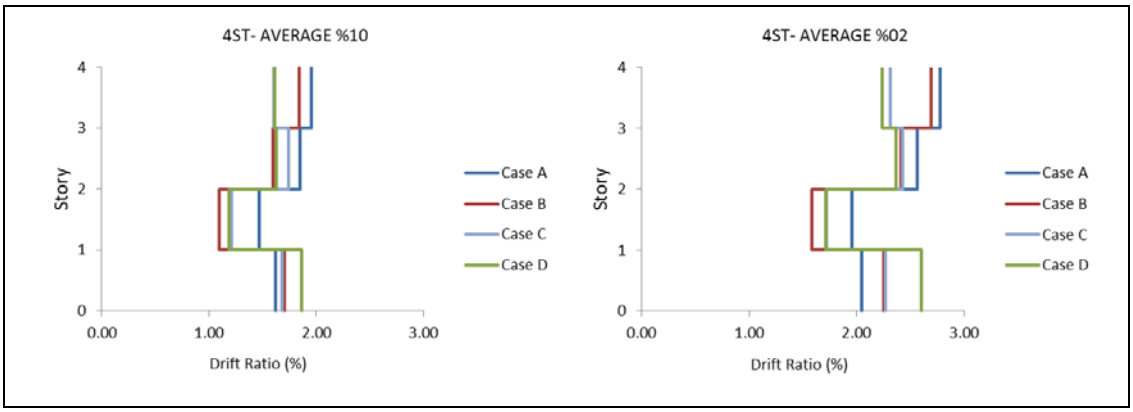

Figure 5.24: Average of maximum drift ratio in each story corresponding to 2% and 10% probability of exceedance in 50 year.

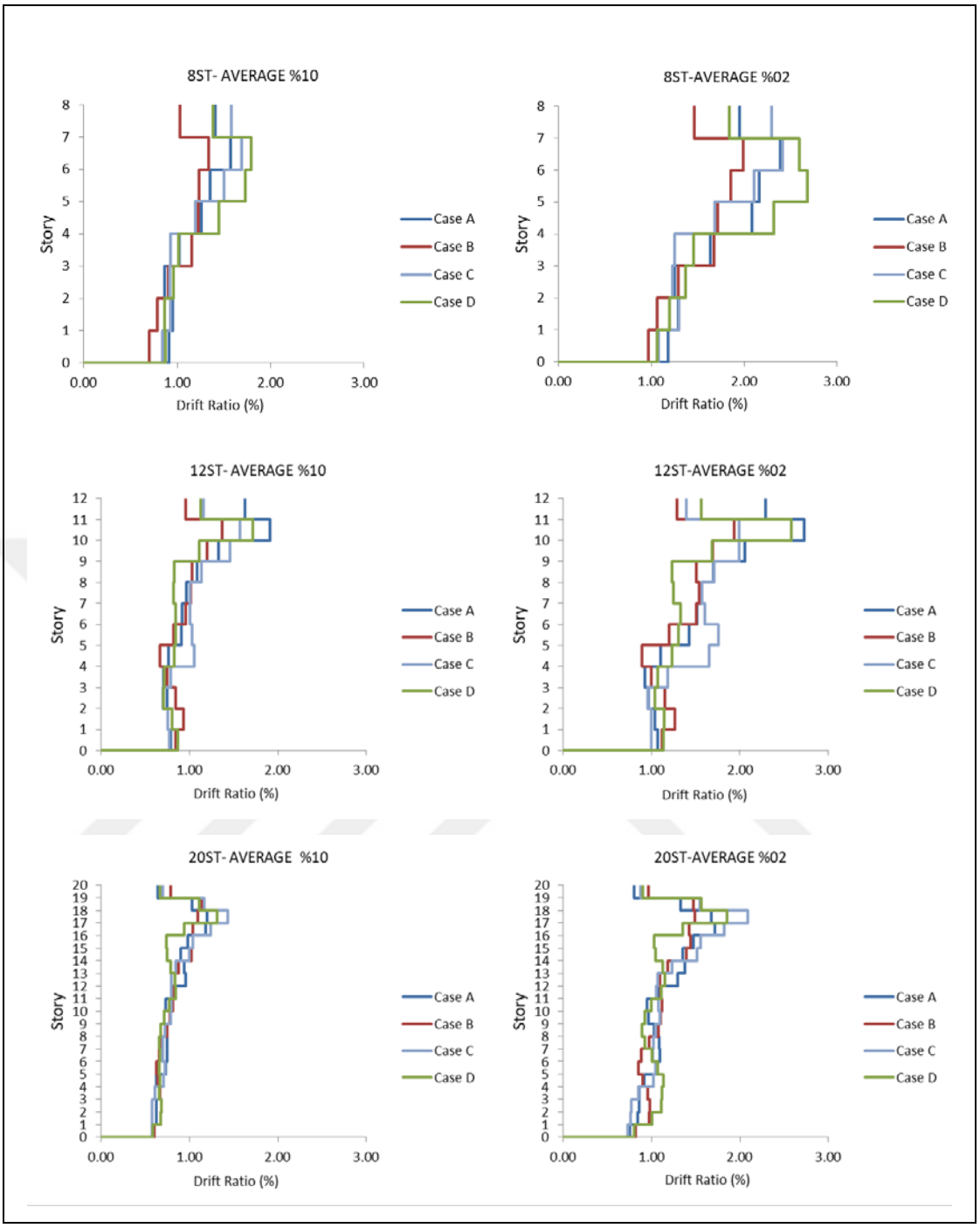

Figure 5.24: Continuation of the figure.

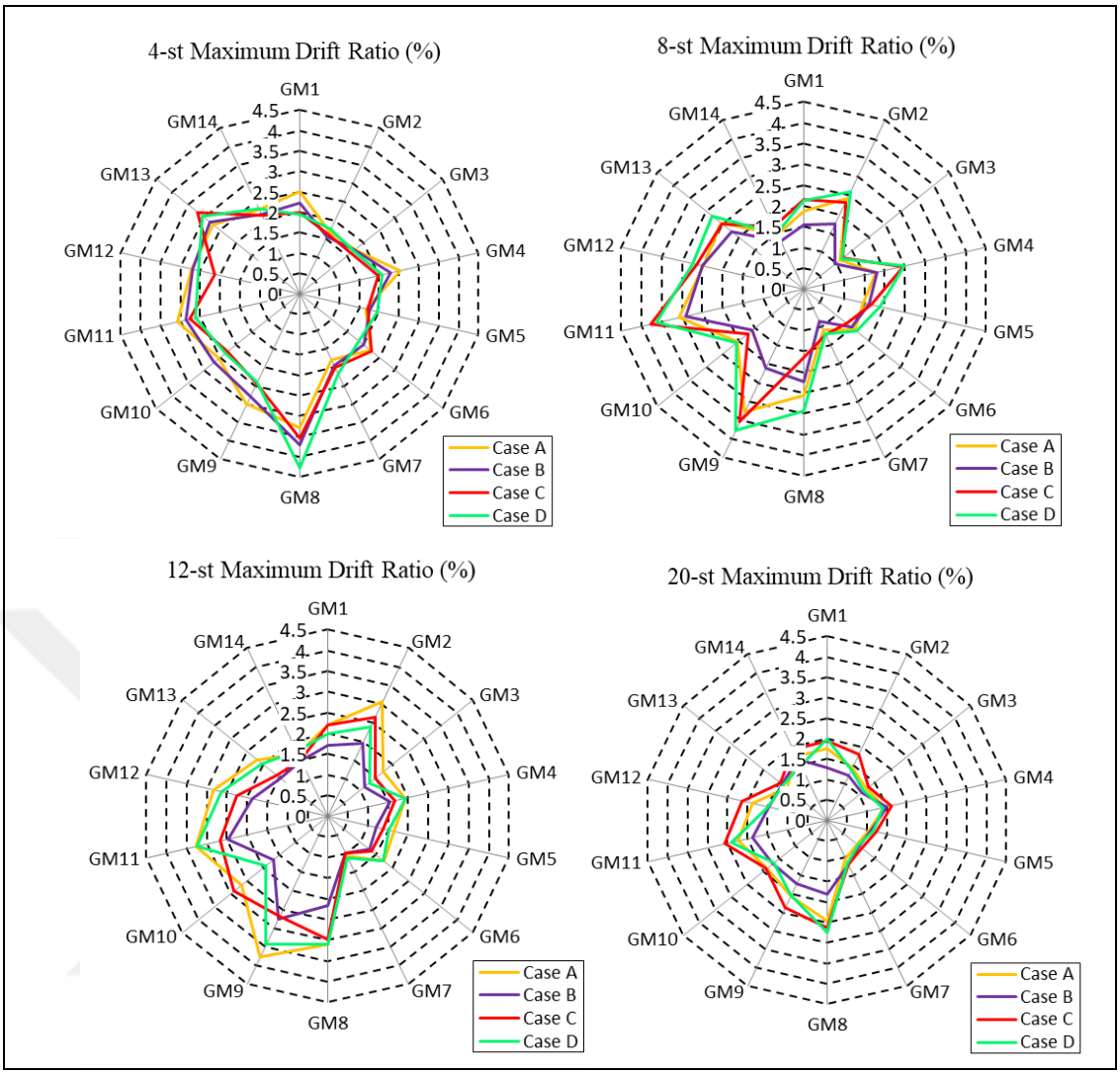

Figure 5.25: Drift Maximum drift ratio in each frame corresponding to 2% and 10% probability of exceedance in 50 year.

The maximum amplification factors of axial compression in each story columns for 10% and 2% probability of exceedance in 50 year are given through Figure 5.26. to 5.29. Maximum increase in amplification factor occurs on side columns in each story. For 4-story frames maximum increase occurs in first story for Case A, while higher values obtain in 4th story for Case B, c and D. For 8-story frames higher increase occurs in 8th story for all cases. For 12- story and 20-story frames higher increase occurs on middle or upper stories depending on strong ground motion.

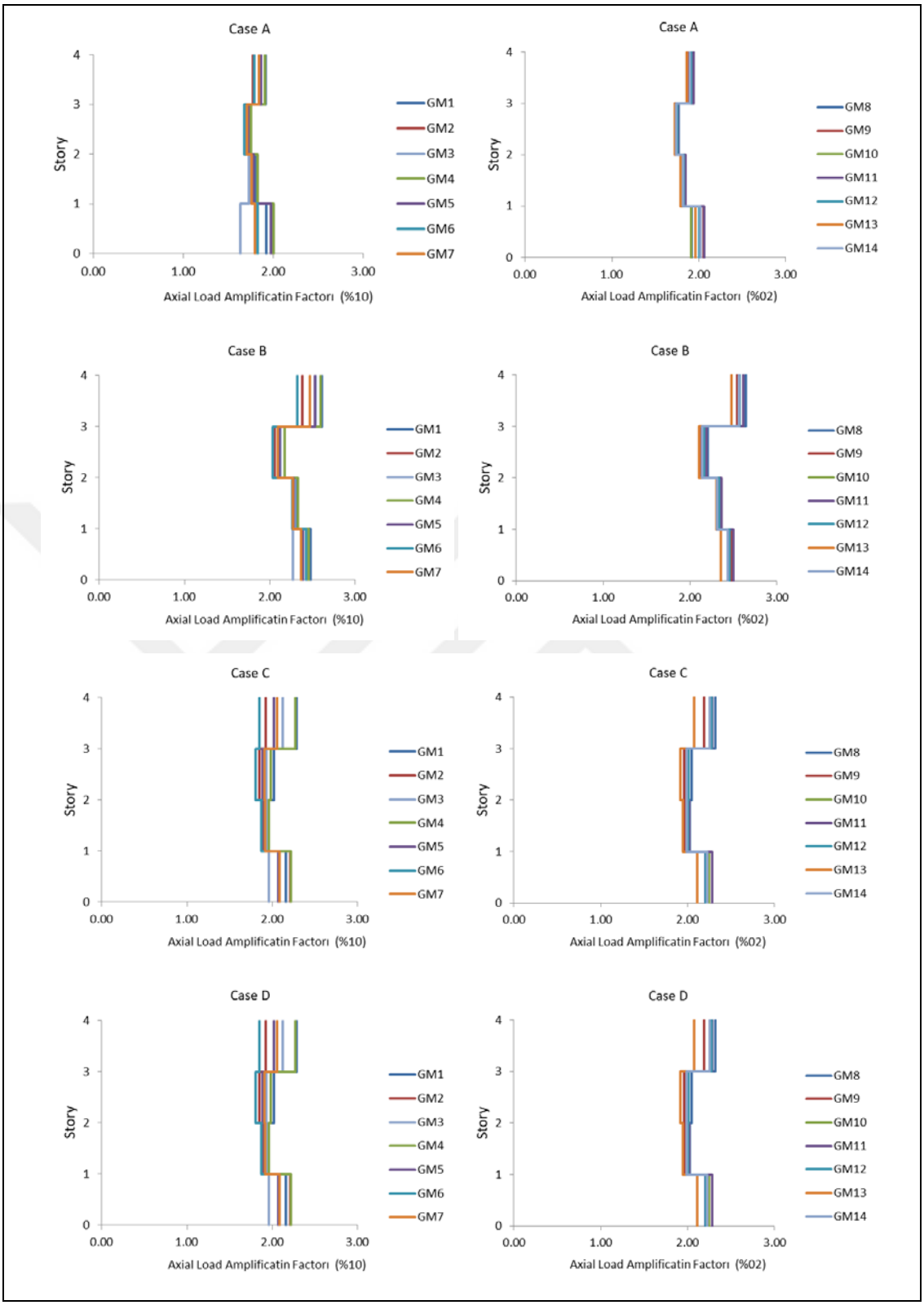

Figure 5.26: Maximum amplification factor for 4- story frames corresponding to 2% and 10% probability of exceedance in 50 year.

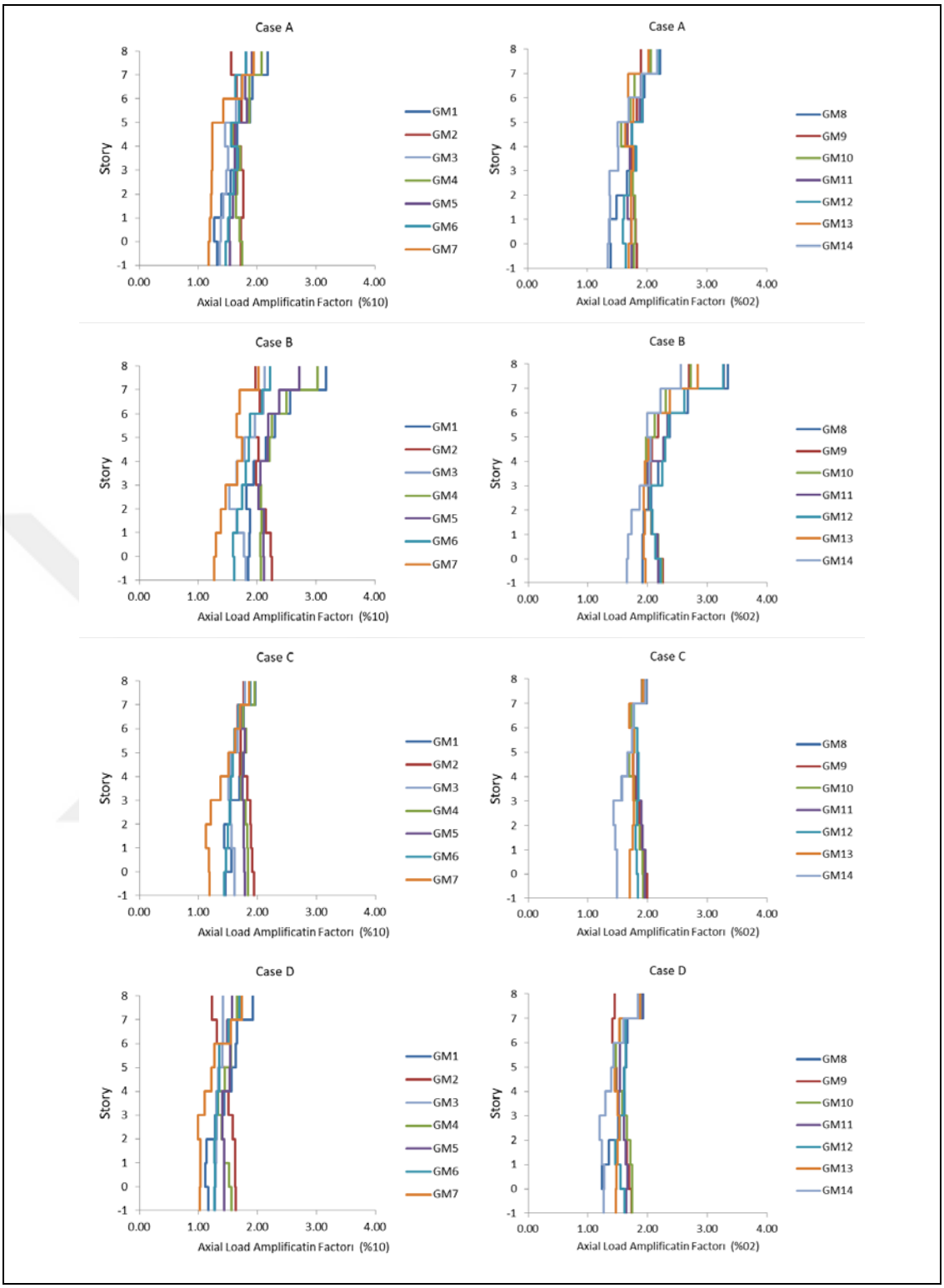

Figure 5.27: Maximum amplification factor for 8- story frames corresponding to 2% and 10% probability of exceedance in 50 year.

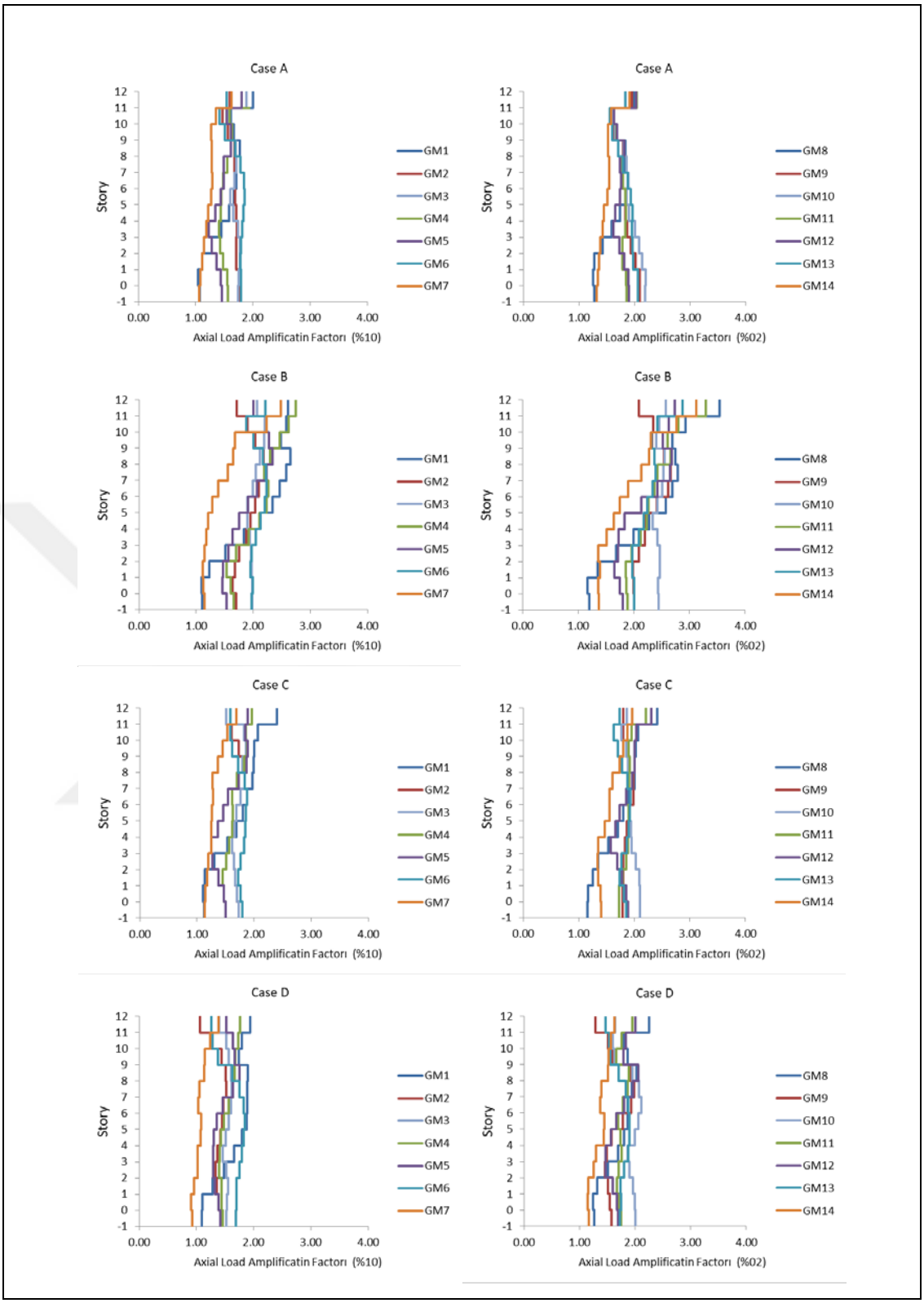

Figure 5.28: Maximum amplification factor for 12- story frames corresponding to 2% and 10% probability of exceedance in 50 year.

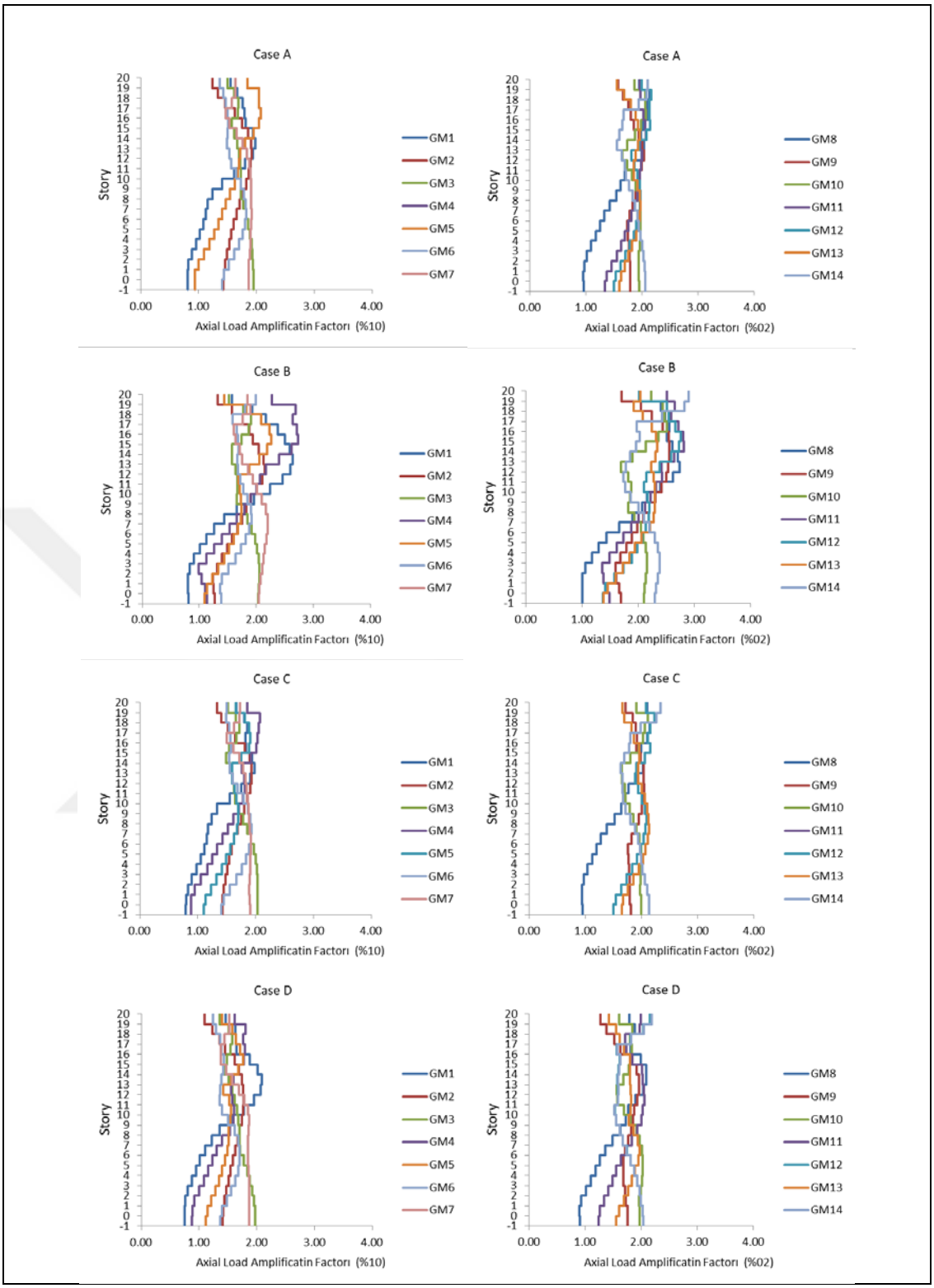

Figure 5.29: Maximum amplification factor for 20- story frames corresponding to 2% and 10% probability of exceedance in 50 year.

The average of the maximum amplification factors of axial compression in each story columns for 10% and 2% probability of exceedance in 50 year are given in Figure 5.30. and the maximum amplification factor of axial compression for each

frame under selected ground motions are given in Figure 5.31. The maximum axial load amplification factors vary from 1.82 to2.65 and 1.42 to 3.35 for 4-and 8-story frames respectively while for 12- and 20-story frames values change from 1.39 to 2.97 and 1.70 to 2.89 respectively.

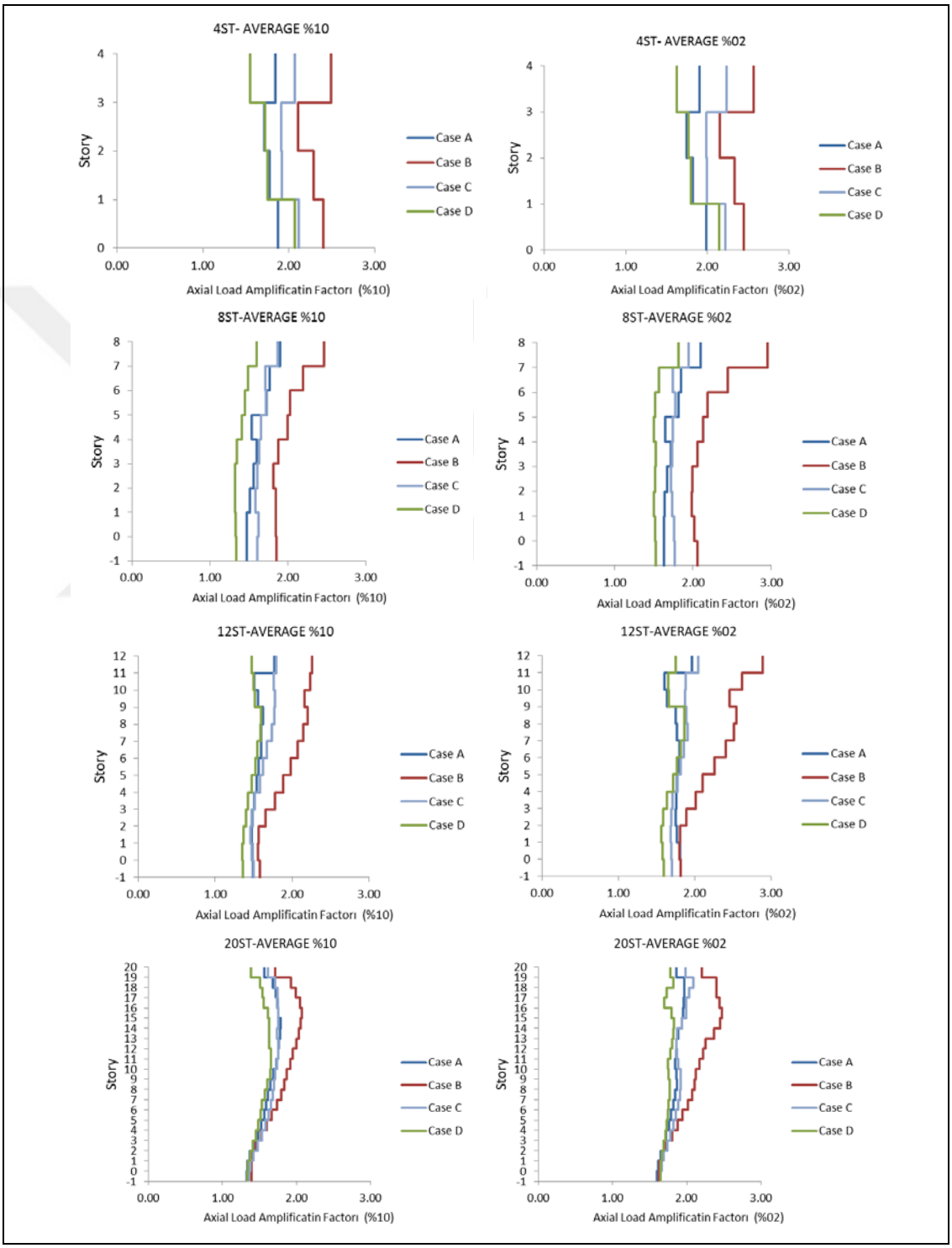

Figure 5.30: Maximum average amplification factor in each story frames corresponding to 2% and 10% probability of exceedance in 50 year.

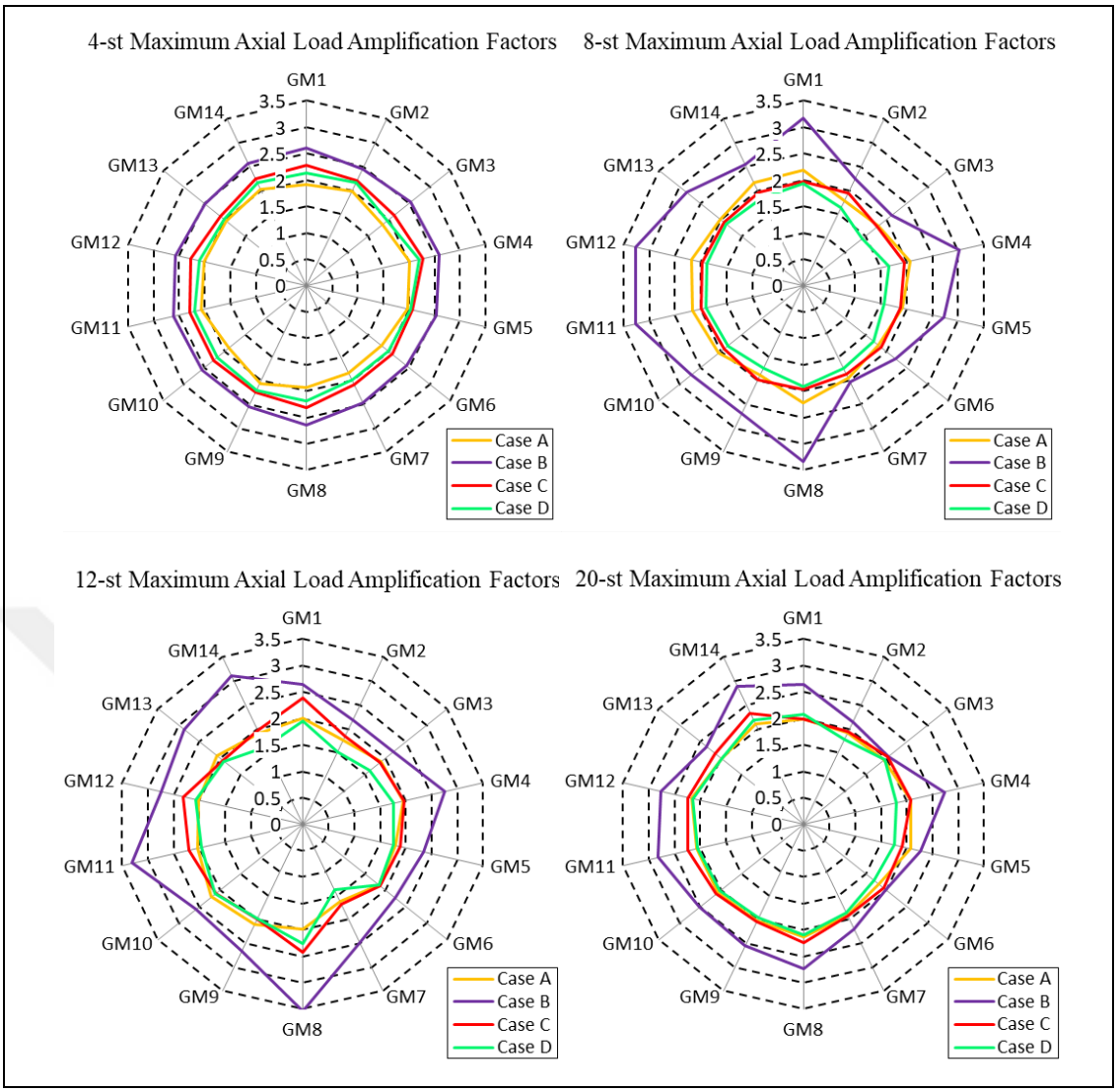

Figure 5.31: Maximum amplification factor in each story frames corresponding to 2% and 10% probability of exceedance in 50 year.

The maximum axial load and moment combination with respect to nominal axial load and nominal moment capacity at the top and bottom of the same column in first story side column under subjected ground motions are given in Figure 5.32. Axial load level for 4-story frames varies between 4% and 17% while it remains between 2%-28% in 8-story frames. For 12-story frames it varies from 0.08% to 52%. and for 20-story frames it is between 6%-75%. Maximum axial load level obtains from Case-B for 4- and 8- story frames while Case-D gives maximum axial load levels for 12- and 20-story frames.

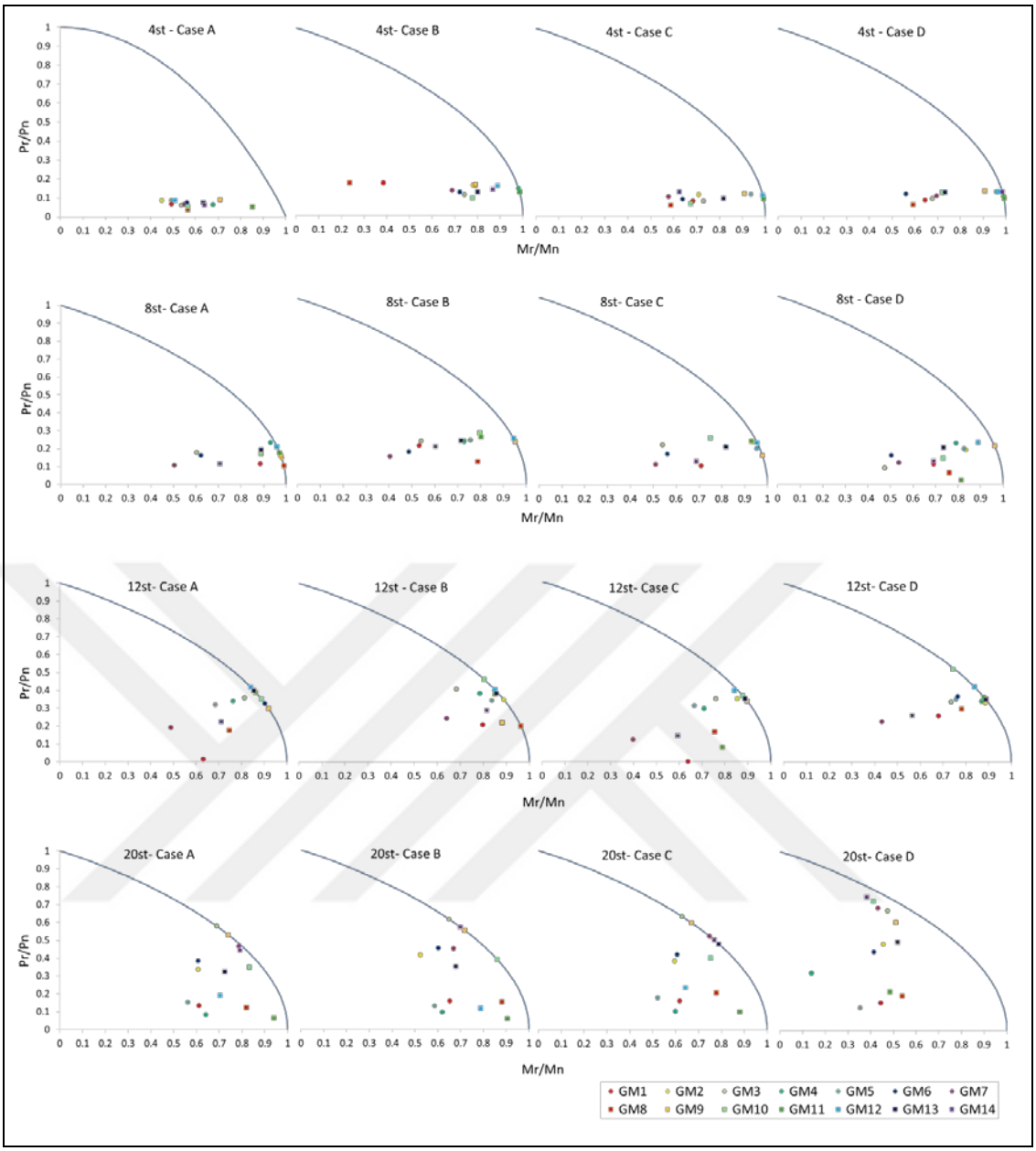

Figure 5.32: The maximum axial load and moment combination variations for each ground motions correspond to 2% and 10% probability of exceedance in 50 year.

Plastic hinge rotations corresponding to the most severe ground motions for each story level are given in Figures 5.33 to 5.36. For all cases in the 4-story frames higher plastic hinge rotations observed under GM8 ground motion and Case B had the highest rotation with a value above 3%. For 8-story frames, GM11 gives higher plastic hinge rotations and Case C had the highest plastic hinge rotations values in all cases. GM9 ground motion has the higher plastic hinge rotations For 12-story frames, and Case D had the highest plastic hinge rotations in all cases. For 20-story

frames, Case D had the higher plastic hinge rotations under GM8. For all cases and story levels, plastic hinge rotations didn't exceed 4% under selected ground motions.

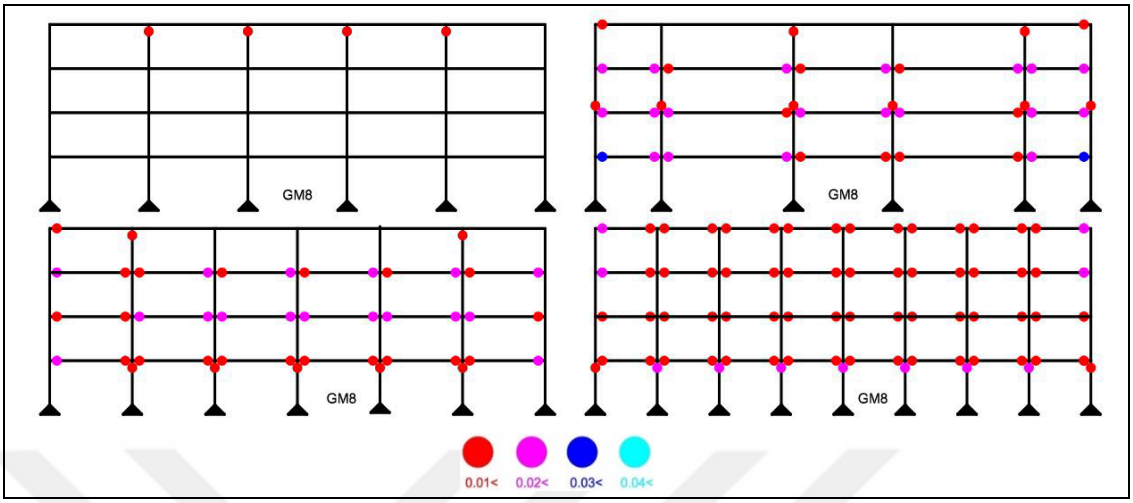

Figure 5.33: Highest plastic hinge rotations for 4 story frames.

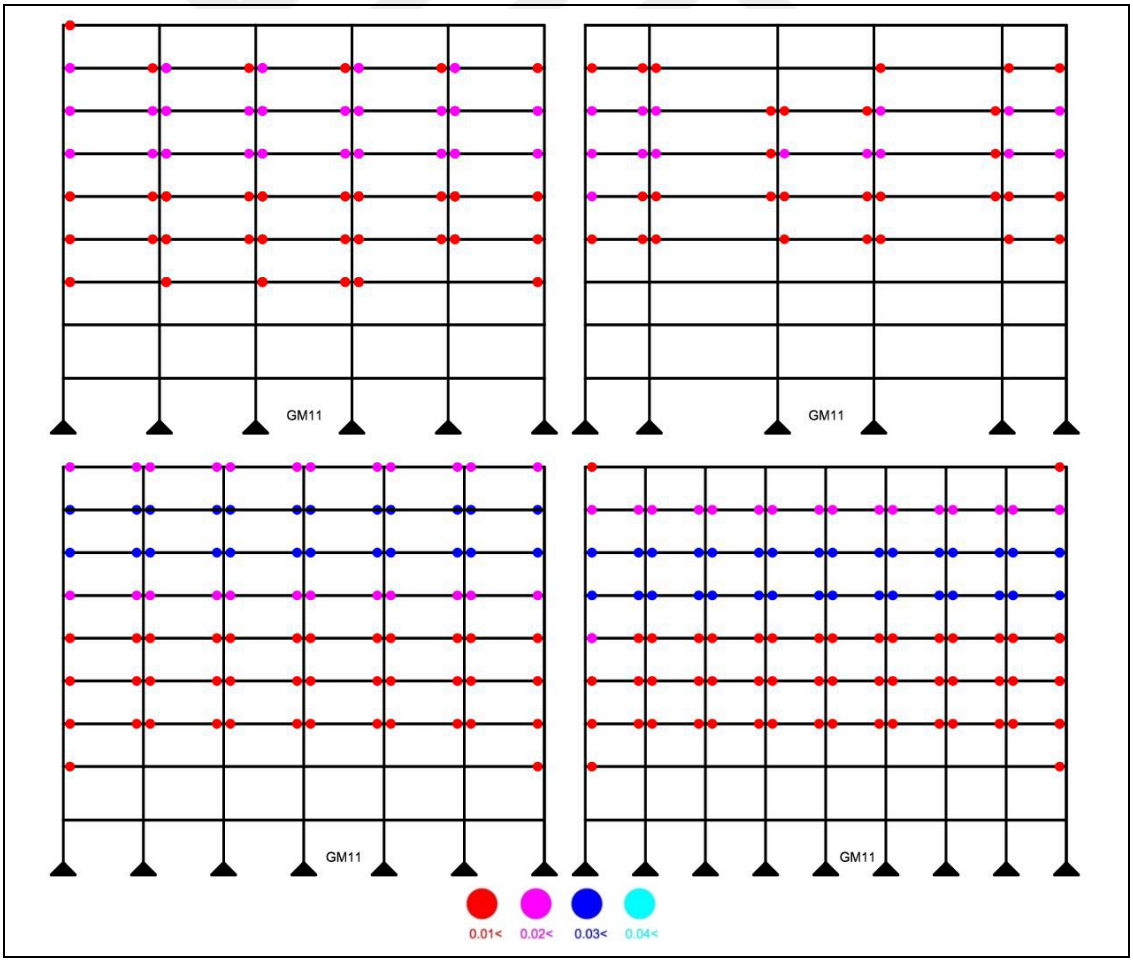

Figure 5.34: Highest plastic hinge rotations for 8 story frames.

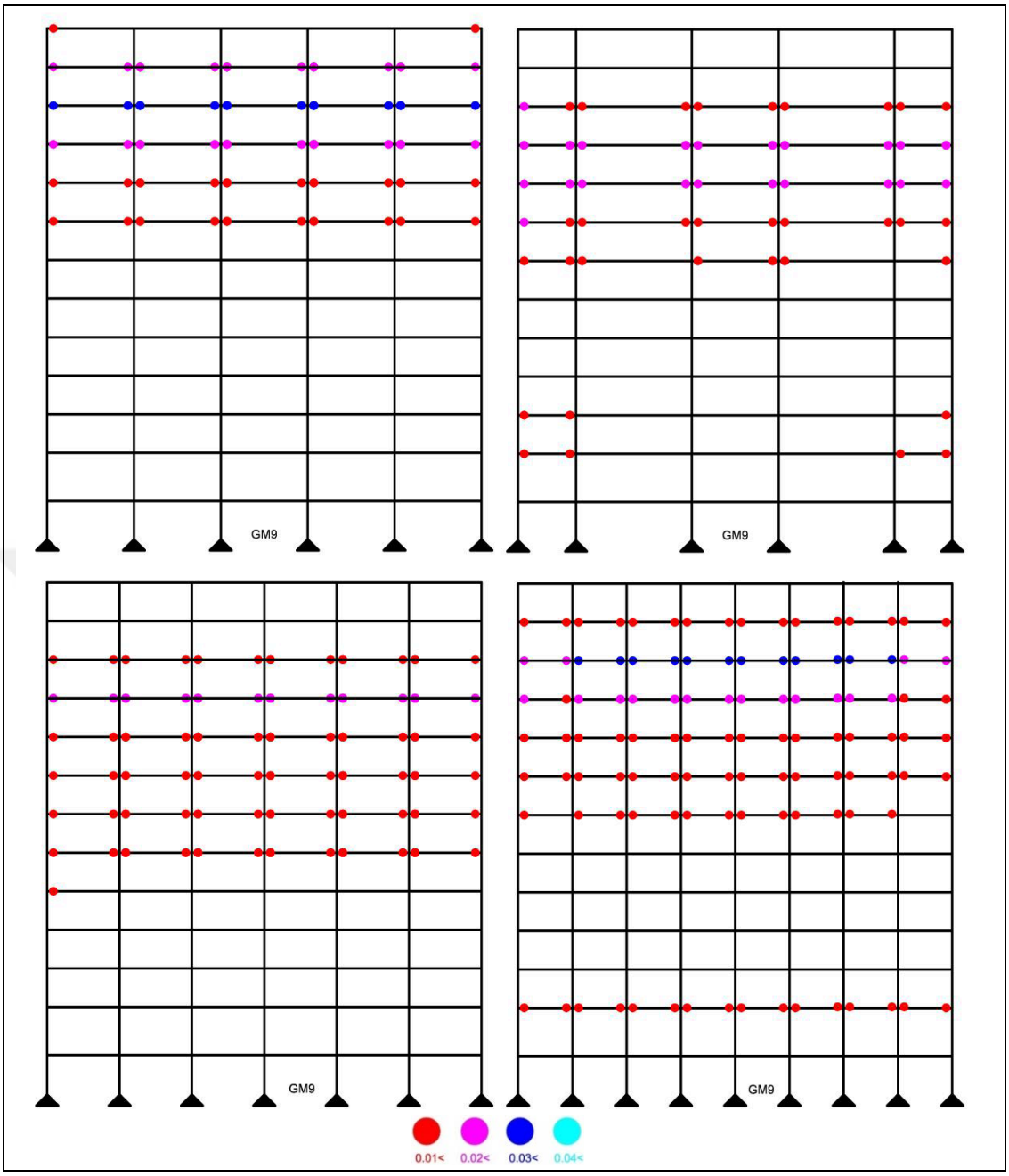

Figure 5.35: Highest plastic hinge rotations for 12 story frames.

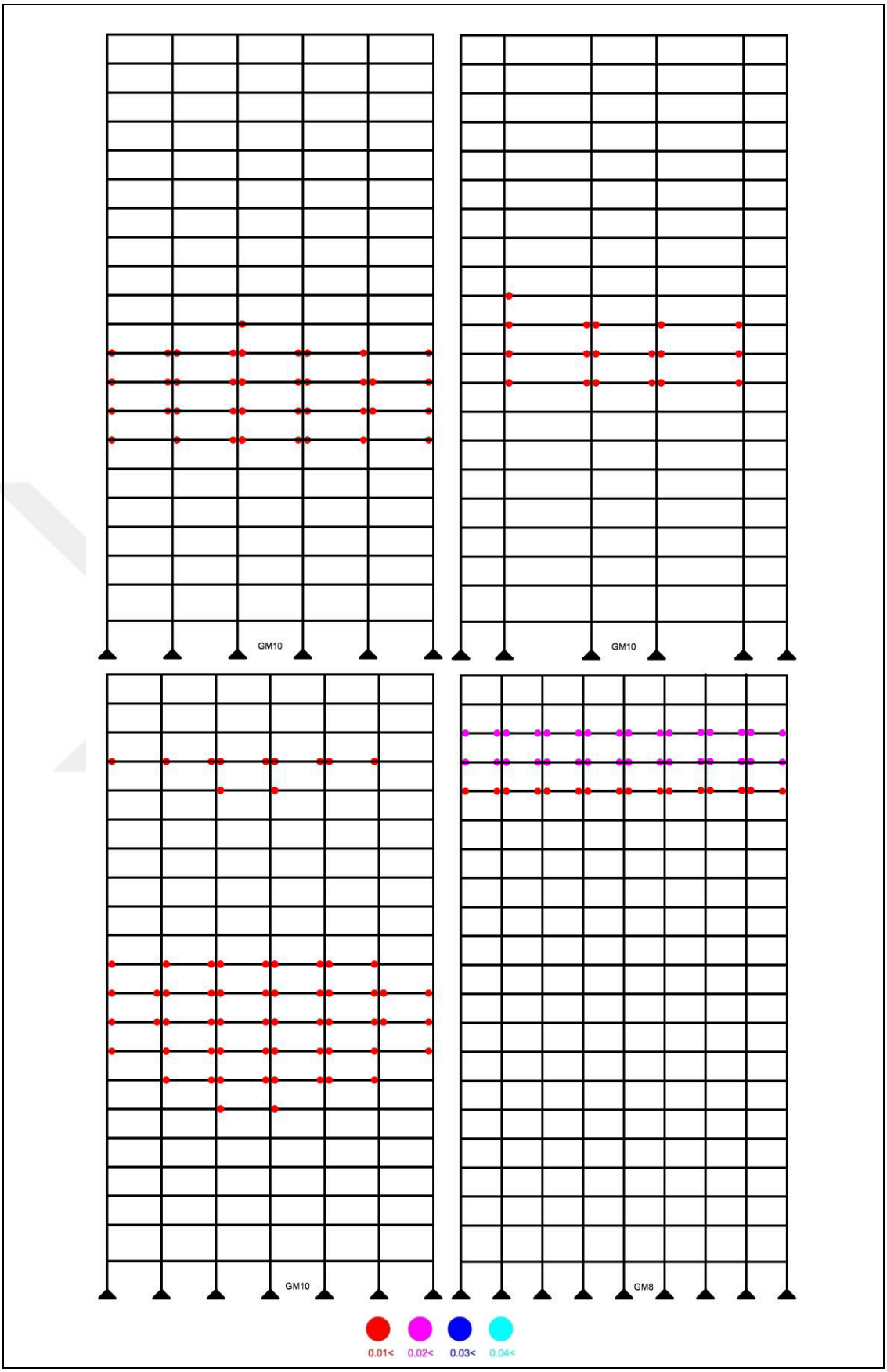

Figure 5.36: Highest plastic hinge rotations for 20 story frames.

Overstrength factors Ω_0 are calculated under GM1 to Gm14 for 4-, 8-, 12- and 20- story frames for all case are given in Figure 5.37. For 4- story frames over strength factors are between 3.22- 4.53. Values vary from 1.75 to 4.00 for 8- story frames while in 12- and 20- story frames, over strength values ranged from 1.40 to 2.91 and 0.92 to 2.12 respectively. System overstrength factor degreases with the increase in story height.

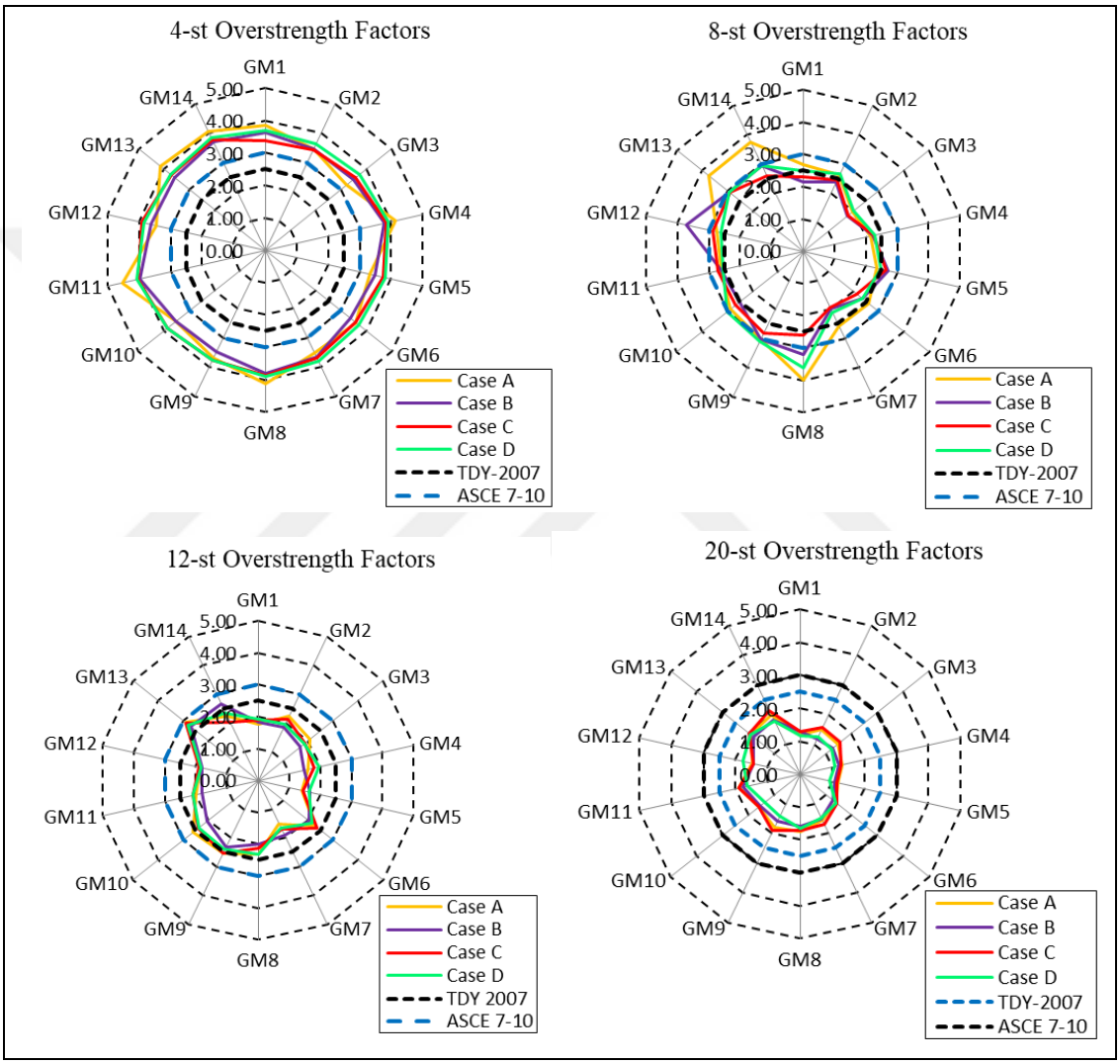

Figure 5.37: Overstrength factors under selected ground motions.

System overstrength factor are given with their average, minimum and maximum values are given in Table 5.4. For comparison, overstrength factor given in Turkish and American regulations also be in Table 5.4.

Table 5.4: Overstrength factors values under selected ground motions.

	4 Story				8 Story				12 Story				20 Story			
	Case A	Case B	Case C	Case D	Case A	Case B	Case C	Case D	Case A	Case B	Case C	Case D	Case A	Case B	Case C	Case D
GM1	3.86	3.63	3.39	3.70	2.68	2.14	2.31	2.50	1.78	1.83	1.89	1.91	1.19	1.29	1.29	1.16
GM2	3.48	3.46	3.44	3.63	2.62	2.37	2.44	2.66	2.22	1.87	2.12	1.96	1.49	1.19	1.57	1.25
GM3	3.22	3.48	3.59	3.75	1.95	1.75	1.78	2.01	2.09	1.69	1.86	1.84	1.47	1.27	1.54	1.22
GM4	4.12	3.78	3.86	3.91	2.16	2.23	2.25	2.30	1.60	1.48	1.79	1.96	1.30	1.22	1.28	1.10
GM5	3.32	3.49	3.73	3.80	2.34	2.72	2.65	2.50	1.40	1.66	1.44	1.63	1.17	1.09	1.15	0.92
GM6	3.59	3.38	3.56	3.72	2.59	2.35	2.14	2.37	2.30	2.05	2.38	2.15	1.38	1.27	1.44	1.41
GM7	3.53	3.65	3.70	3.80	2.57	1.97	1.95	2.11	1.51	1.91	1.69	1.66	1.57	1.50	1.70	1.47
AVG	3.59	3.56	3.61	3.76	2.41	2.22	2.22	2.35	1.84	1.78	1.88	1.87	1.37	1.26	1.43	1.22
MAX	4.12	3.78	3.86	3.91	2.68	2.72	2.65	2.66	2.30	2.05	2.38	2.15	1.57	1.50	1.70	1.47
MİN	3.22	3.38	3.39	3.63	1.95	1.75	1.78	2.01	1.40	1.48	1.44	1.63	1.17	1.09	1.15	0.92
GM8	4.13	3.80	3.85	3.90	4.00	3.21	2.60	3.62	2.32	2.00	2.14	2.32	1.73	1.60	1.73	1.66
GM9	3.69	3.50	3.76	3.77	3.03	3.04	2.81	3.08	2.53	2.31	2.55	2.41	1.80	1.59	1.91	1.42
GM10	3.52	3.52	3.85	3.88	2.87	2.51	2.67	3.02	2.60	2.05	2.40	2.38	1.59	1.55	1.59	1.37
GM11	4.53	3.97	4.03	4.07	2.60	2.61	2.72	2.55	2.00	1.81	2.08	2.09	1.91	1.77	1.89	1.63
GM12	3.44	3.63	3.90	3.86	2.74	3.70	2.88	2.63	1.86	1.80	1.89	1.84	1.48	1.43	1.43	1.78
GM13	4.15	3.59	3.72	3.74	3.75	2.95	2.90	2.95	2.91	2.71	2.88	2.79	1.93	1.80	1.96	1.93
GM14	4.05	3.71	3.78	3.85	3.76	2.94	2.59	2.95	2.25	2.67	2.01	2.35	1.98	1.83	2.12	1.79
AVG	3.93	3.67	3.84	3.87	3.25	2.99	2.74	2.97	2.35	2.19	2.28	2.31	1.77	1.65	1.80	1.66
MAX	4.53	3.97	4.03	4.07	4.00	3.70	2.90	3.62	2.91	2.71	2.88	2.79	1.98	1.83	2.12	1.93
MİN	3.44	3.50	3.72	3.74	2.60	2.51	2.59	2.55	1.86	1.80	1.89	1.84	1.48	1.43	1.43	1.37
TDY-2007	2.50	2.50	2.50	2.50	2.50	2.50	2.50	2.50	2.50	2.50	2.50	2.50	2.50	2.50	2.50	2.50
ASCE 7-10	3.00	3.00	3.00	3.00	3.00	3.00	3.00	3.00	3.00	3.00	3.00	3.00	3.00	3.00	3.00	3.00

6. NUMERICAL STUDY FOR BRACED FRAMES

6.1. Design of Special Concentrically Braced Frames (SCBF)

Inverted V and two-story X- type steel special concentrically braced frames with 4- ,8-, 12- and 20-stories, representing typical low -, medium- and high-rise steel buildings are designed based on the requirements in American provisions. Two special cases are used in order to include the effects of bracing configurations on energy demands. Details of the case are shown in Table 6.1; Case E) Inverted V-type bracing, constant span length of 9.0 m (five equal spans); Case F) Two-story X -type bracing, constant span length of 9.0 m (five equal spans). The structural system for each building consists of seismically resistant perimeter inverted V-type and two-story X- type braced frames whereas the interior frames are designed for gravity loads only. Also, typical story plan views of the selected span configurations are given in Figure 6.1.

Table 6.1: Plan dimensions and span lengths of the SCBF.

Frame Types	Case	Plan Dimension	Span Length
Inverted V- braced frame	Case E	45.0 m x 45.0 m	5@9.00 m
Two-story X -brace frame	Case F	45.0 m x 45.0 m	5@9.00 m

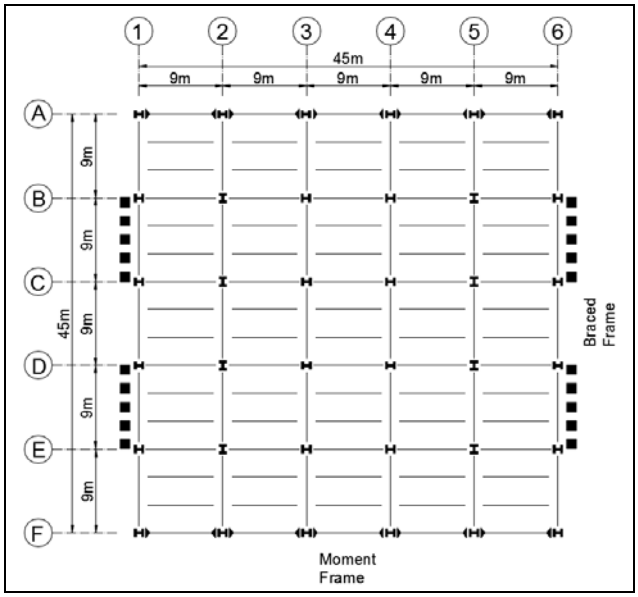

Figure 6.1: Plan of the 4-, 8-, 12- and 20- story SCBF buildings.

The plan dimensions of buildings are 45 m x 45 m. The story plans of the buildings are symmetrical. The typical story height for the frames is 4.0 m except for the 8-, 12-, and 20-story frames where the first story height is 5.0 m as shown in Figure 7.2. For the 8-, 12-, and 20-story building, concrete foundation walls and surrounding soil are assumed to prevent any significant horizontal displacement of the structure at the ground level, i.e. the seismic base is assumed to be at the ground level. The columns of the buildings are assumed to be simply connected to the foundation. The braces are also simply connected to the beams and beam-column connections.

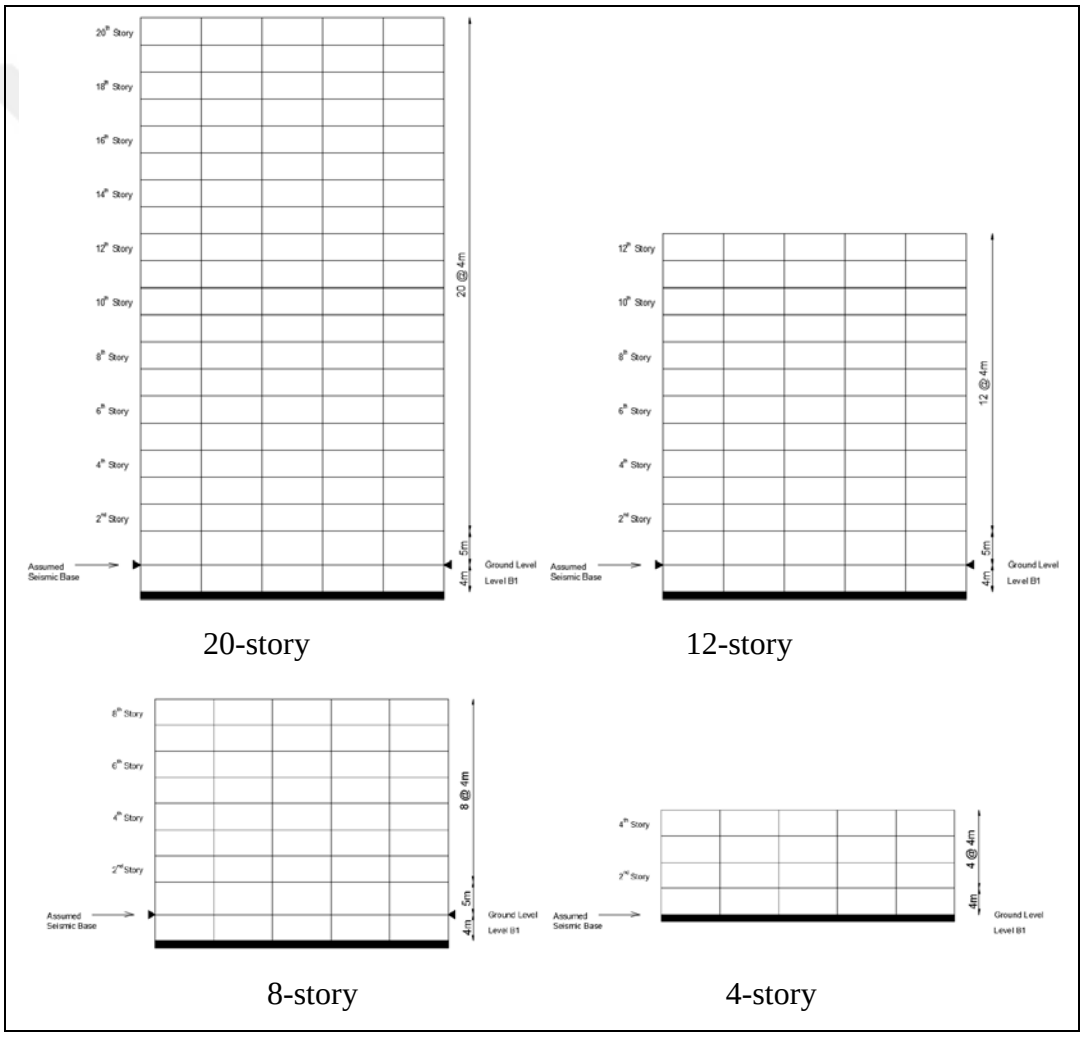

Figure 6.2: Elevations of the SCBF buildings.

The linear analysis of buildings is applied by using Load and Resistance Factor Design (LRFD) methodology in accordance with provision. Dead loads including

self-weight of the members and live load used in the study are 5.0 kN/m^2 and 2.4 kN/m^2 except at the roof level, where they are taken as 4.0 kN/m^2 and 1.4 kN/ m^2, respectively. European wide flange profiles with steel grades S355 are preferred for design. Hollow structural sections are used for braces with steel grade of S275. The member sizes of the frames are given in Appendix C.

The buildings are designed for a site where MCE spectral response acceleration parameters at short period, S_S is 2.0g and at a period of 1s, S_1 is 1.0g. Design earthquake spectral response acceleration parameters are taken as S_{DS} *=1.333* (g) at short period, S_{D1}*= 0.666* (g) at a period of 1s. Long-period transition period, T_L is assumed to be 12.0 s. Response Spectrum Analysis are used in seismic design. Seismic design category *D* is taken for all structures in design. The response spectrum curves corresponding to design level and maximum considered earthquake level (MCE) are developed as specified in provision and shown in Figure 6.3. Shear wave velocity (V_s) of site class is assumed to vary between 300-770 m/s.

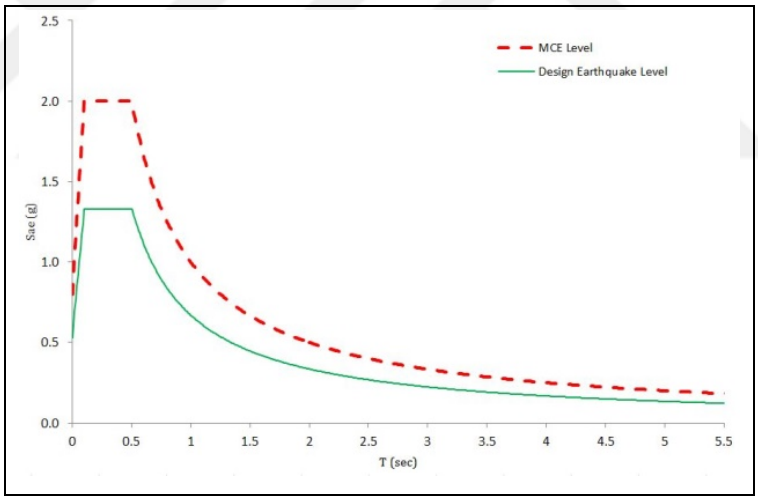

Figure 6.3: Response Spectra for DBE and MCE levels for SCBF.

In cases where the combined response for the modal base shear (V_t) is less than 85% of the calculated base shear (V) using the equivalent lateral force procedure, the forces are increased by using coefficient ($0.85V/V_t$) in accordance with ASCE 7-10 [ASCE 7-10, 2010].

The calculated fundamental period of the structure (T) are checked with the approximate fundamental period (T_a) multiplied with coefficient of upper limit (C_u).

Where the calculated fundamental period (T) exceeds C_uT_a, C_uT_a is used instead of T in accordance with ASCE 7-10 [ASCE 7-10, 2010]. Based on the same requirement, $C_u = 1.4$ for $S_{D1} = 0.666\ g > 0.4\ g$. The calculated fundamental periods of vibration, the total mass for the frames are given in Table 6.2.

Table 6.2: Calculated fundamental periods and total mass for the SCBF.

Story	Case	T (sec)	T_a (sec)	C_u	C_uT_a (sec)	T_{used} (sec)	Total Mass (kN.sec^2/m)	V (kN)	V_t (kN)
4	E	0.563	0.390	1.4	0.546	0.546	2173	1906	1628
	F	0.593	0.390	1.4	0.546	0.546	2173	1906	1622
8	E	1.520	0.656	1.4	0.918	0.918	4478	2749	2343
	F	1.580	0.656	1.4	0.918	0.918	4478	2749	2468
12	E	2.380	0.958	1.4	1.341	1.341	6875	4214	3582
	F	2.450	0.958	1.4	1.341	1.341	6875	4214	3888
20	E	2.700	1.366	1.4	1.912	1.912	11420	7002	6030
	F	2.730	1.366	1.4	1.912	1.912	11420	7002	5965

The approximate fundamental period (T_a) is calculated as follows:

$$T_a = C_t h_n^x \tag{6.1}$$

Where h_n is the structural height and the coefficients $C_t=0.0488$ and $x=0.75$ *for SMF*. The story system of the buildings is assumed to provide diaphragm action and to be rigid in the horizontal plane. In seismic design of SMF, the appropriate response modification coefficient ($R=6$) overstrength factor ($\Omega_o=2$) and the deflection amplification factor ($C_d=5$) are used in determining the base shear, element design forces, and design story drift where redundancy factor ρ is taken as 1.3. Story drift ratio limitation is taken as 2% of story height as specified in ASCE7-10 [ASCE 7-10, 2010]. Story drift ratios of SCBF are illustrated as in Figure 6.4.

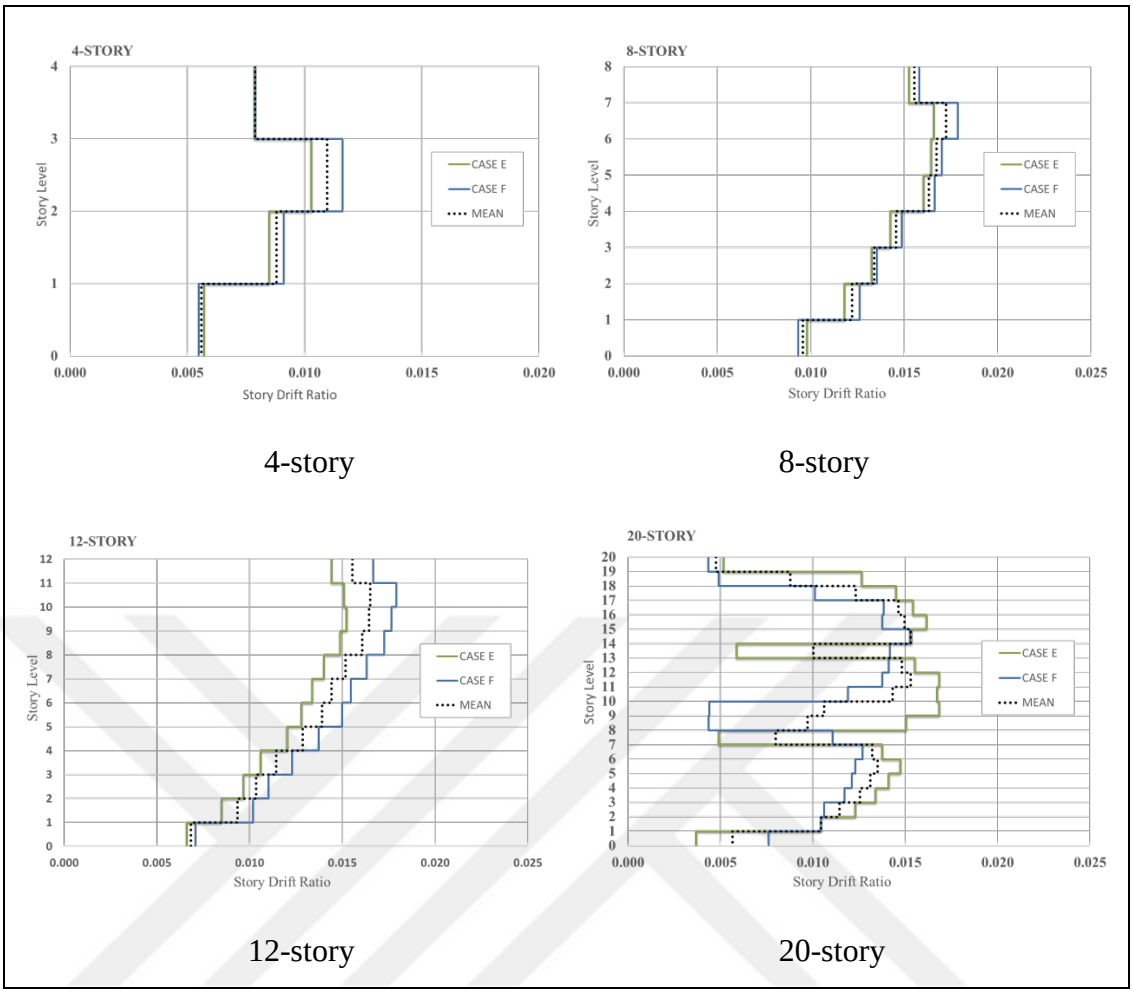

Figure 6.4: Story drift ratio of SCBF.

The columns and braces are classified as highly ductile members, and beams satisfy the requirements for moderately ductile members according to AISC 341-10. For highly ductile members, the width-to-thickness ratios of compression elements satisfy the limiting width-to-thickness ratios. Beams are designated based on analysis in which all braces in tension are assumed to resist forces corresponding to their expected strength ($R_yF_yA_g$, where R_y is the ratio of the expected yield stress to the specified minimum yield stress, F_y is the minimum yield stress and A_g is the gross area) and all braces in compression are assumed to resist their expected post-buckling strength ($0.3F_{cr}A_g$, where F_{cr} is the critical stress).

For P-delta effects on story shears and moments are checked using Equation 6. 2. Where the stability coefficient (θ) is equal to or less than 0.10, the resulting member forces and moments are not required to be considered. Frame systems are satisfied Equation 7.2.

$$\theta = \frac{P_x \Delta I_e}{V_x h_{sx} C_d} < 0.1 \qquad (6.2)$$

where P_x is the total vertical design load, Δ is the design story drift, I_e is the importance factor (1.0 for seismic loads) V_x is the seismic shear force, h_{sx} is the story height.

6.2. Modeling Special Concentrically Braced Frames (SCBF) for Nonlinear Analyses

The steel special braced frames were modeled with PERFORM 3D v5; a nonlinear analysis and performance assessment software to conduct non-linear analyses. The frames were modeled as beam, column and brace elements. Column and beams are modeled with possible plastic regions at their both ends. Axial load-moment interaction (P-M-M) are taken in to account for column element. Braced are modeled as nonlinear steel bar that consider buckling.

In PERFORM 3D; braces are modeled as "Inelastic Steel Bar". Material type and section area are needed for this modeling. "Inelastic Steel Bar" menu is given in Figure 6.5.

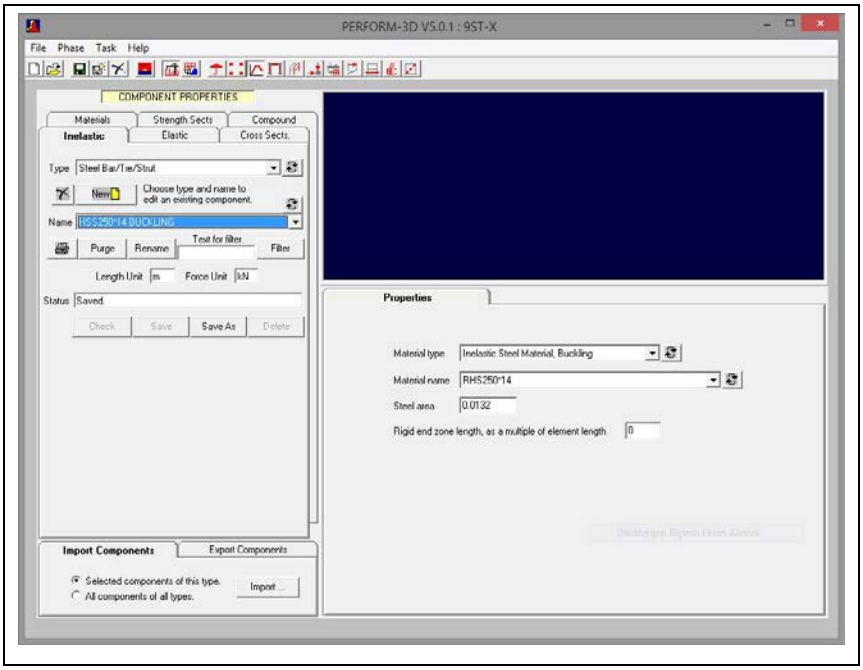

Figure 6.5: Inelastic Steel Bar menu in PERFORM 3D.

To define nonlinear properties in brace element, “Inelastic Steel Material, Buckling” type was used. With this material buckling properties of brace can be defined to the program. The Steel Material, Buckling Type has a hysteresis loop for axial stress vs. axial strain as shown in Figure 6.10.

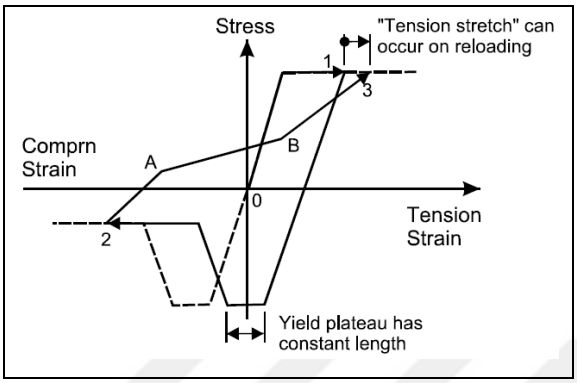

Figure 6.6: Buckling Hysteresis Loop.

The dashed lines in Figure 6.6 show the basic stress-strain relationship. The solid line 0-1-2-A-B-3 shows a hysteresis loop with (1) yield in tension, (2) buckling in compression and (3) reloading in tension. In PERFORM 3D “Inelastic Steel Material, Buckling” menu is given in Figure 6.7.

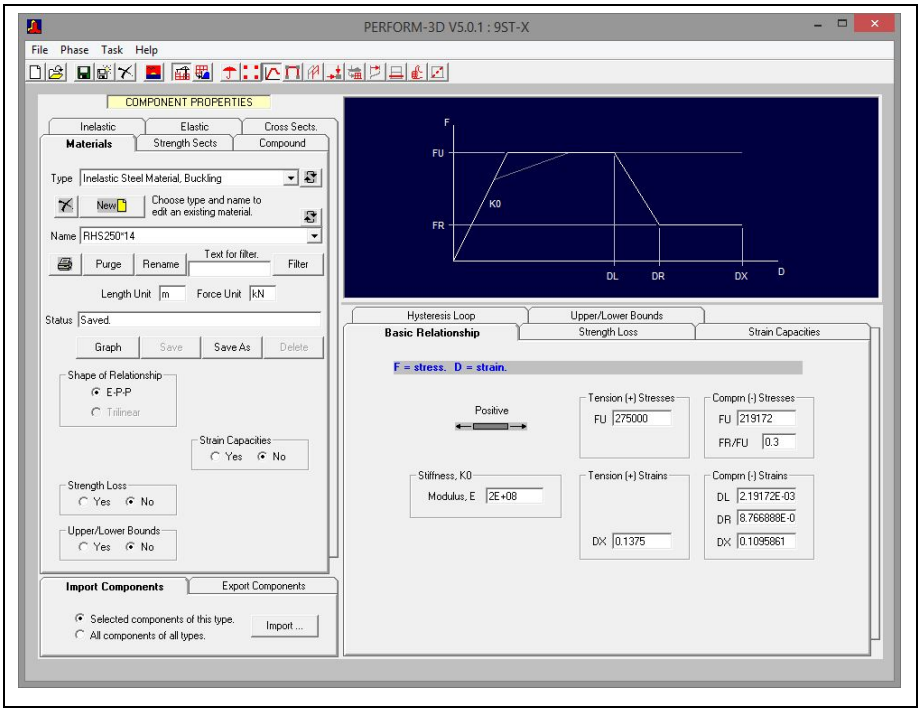

Figure 6.7: Inelastic Steel Material, Buckling menu.

Material properties such as young modulus, maximum tensile stress, and maximum compression stress, maximum strain in tension and minimum strain in compression are arranged in this menu. Deformation limits are as fallows;

- Maximum strain in tension is 100 times of yield strain (to avoid program termination).
- Maximum strain in compression is 100 times of yield strain in compression (to avoid program termination).
- DL is 2 times of yield strain in compression.
- DR is 8 times of yield strain in compression.

Columns and beams in non-braced bays were modeled as linear elastic. “Compound” menu for HE280A gravity column given as an example in Figure 6.8. As it’s seen in the compound menu, linear properties were assigned by XecColS-HE280A element given in Figure 6.9.

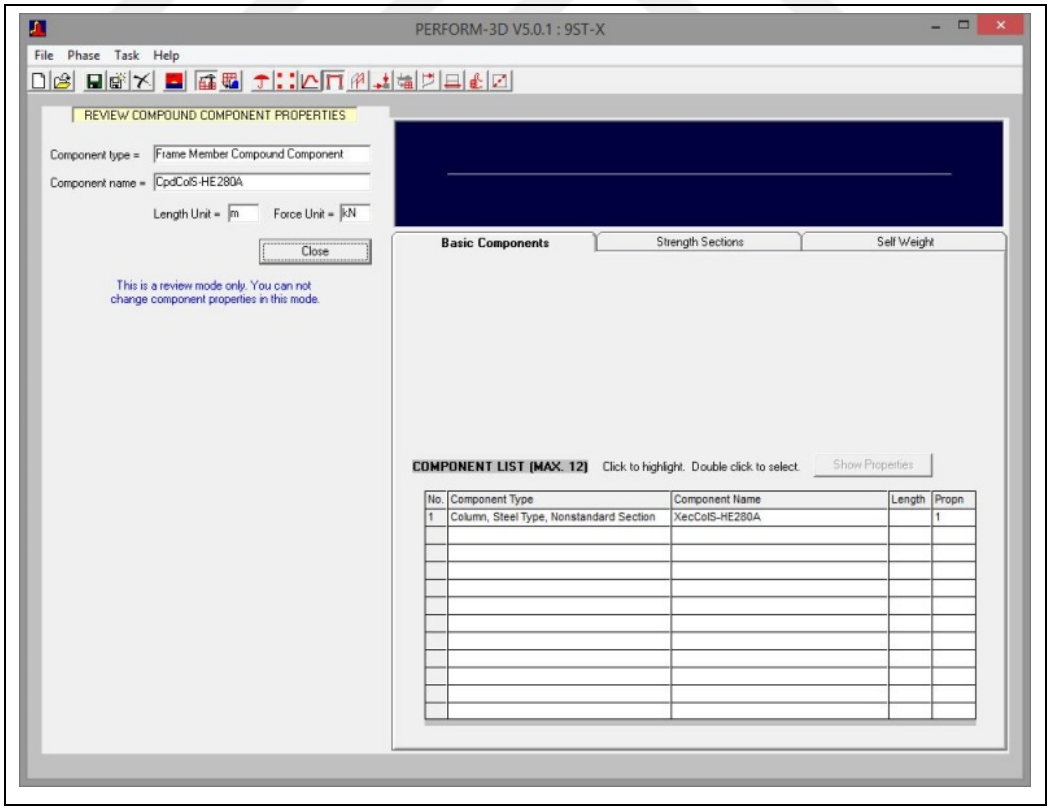

Figure 6.8: Compound menu for HE280A gravity column.

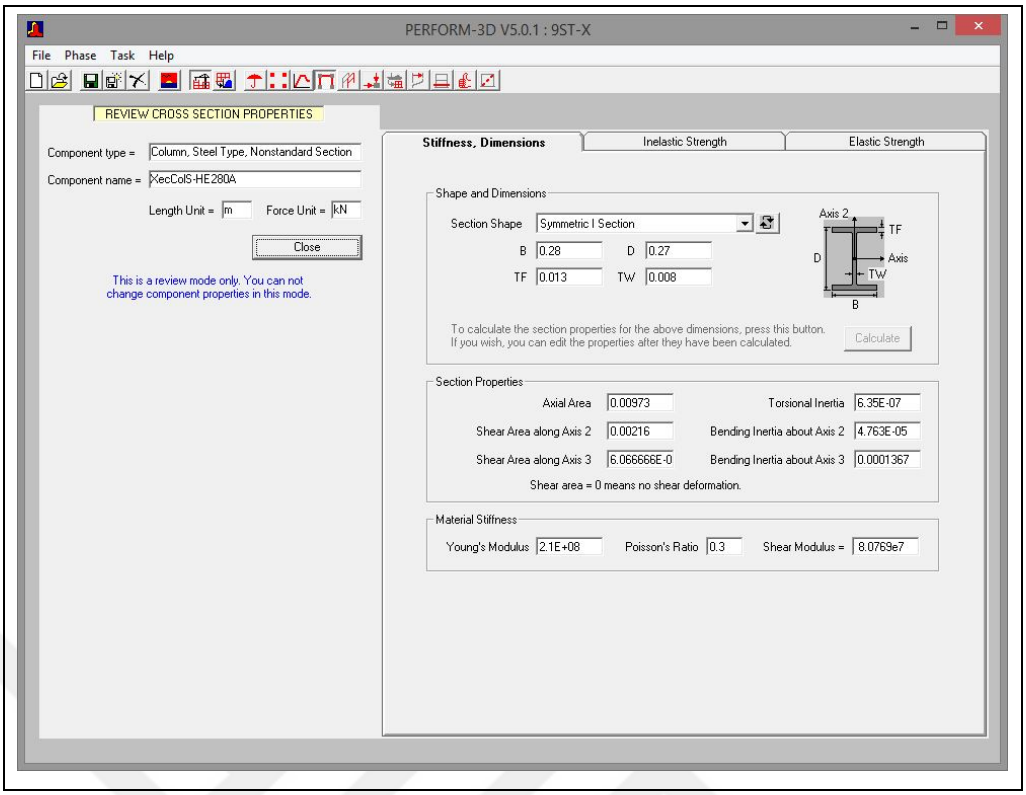

Figure 6.9: Section properties of linear XecColS-HE280A element.

Because of the unbalanced force caused by braces, beams in braced bays were modeled like column element. Compound menu for HE1000x584 beam on first story is given in Figure 6.10. All beams-column connections in braced by are pinned connections. To see nonlinear behavior due to unbalance force, P-M-M hinge was modeled in the middle of the beam, close to region where braces were connected. So ın PERFORM 3D, half-length beam were modeled in three part; moment release on column side, P-M-M hinge on the other end and linear section between each ends. P-M-M hinge defined as “Inelastic P-M2-M3 Hinge Steel Rotation Type” given in in Figure 6.11.

Section properties can be defined automatically by using programs own section database as “Column, Standard Steel Section” or by users as “Column, Non-Standard Steel Section”. As it’s seen in Figure 7.16, section properties such as young modulus, poisson ratio and yield stress are arranged in this menu. Users can also define inelastic properties in cross section tab (Figure 6.12) so all necessary data to form plastic hinge is given to the program.

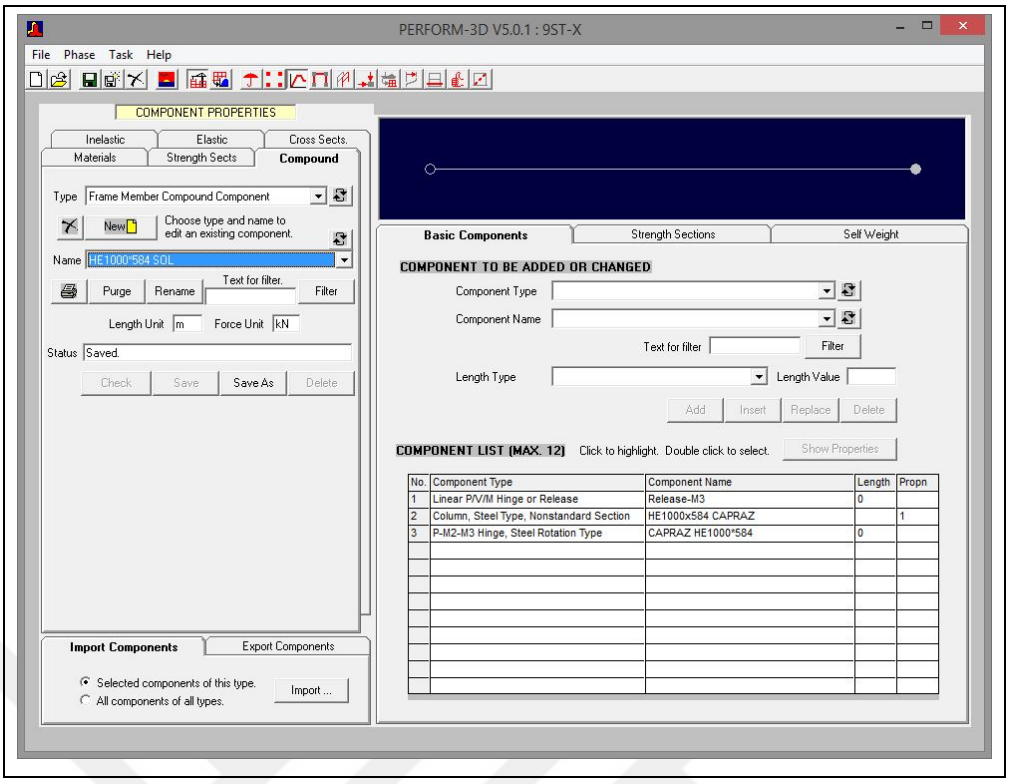

Figure 6.10: Compound menu for HE100x584 half-length beams.

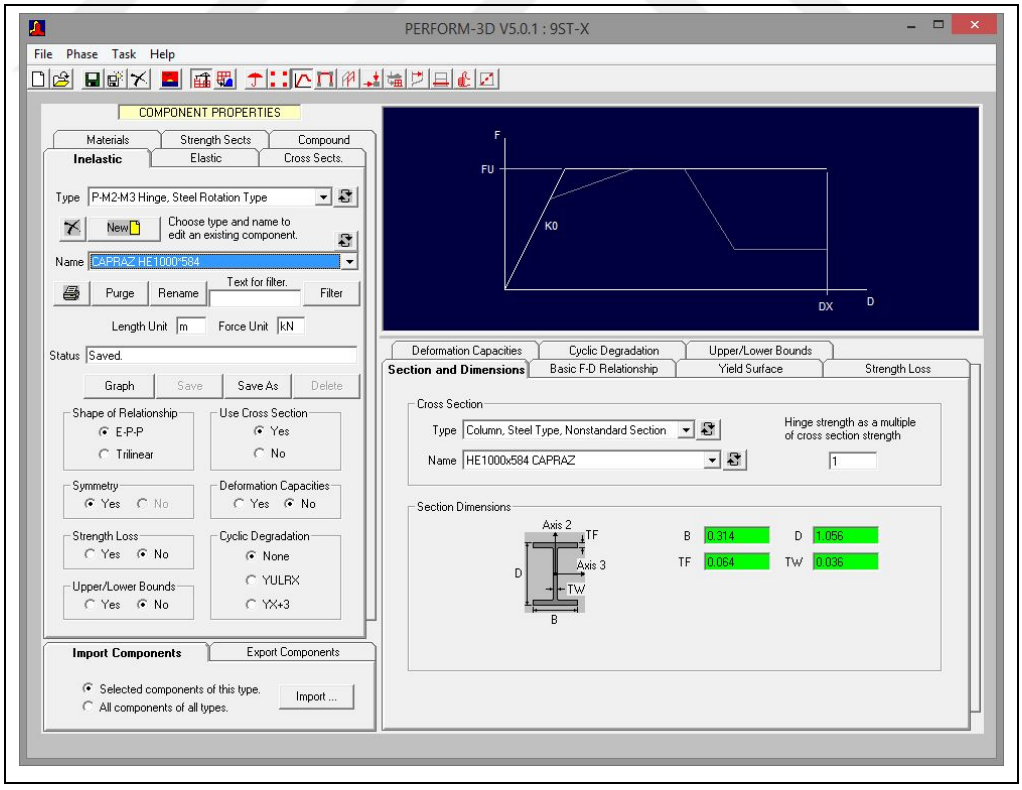

Figure 6.11: "*P-M2-M3* Hinge" menu for HE100x584.

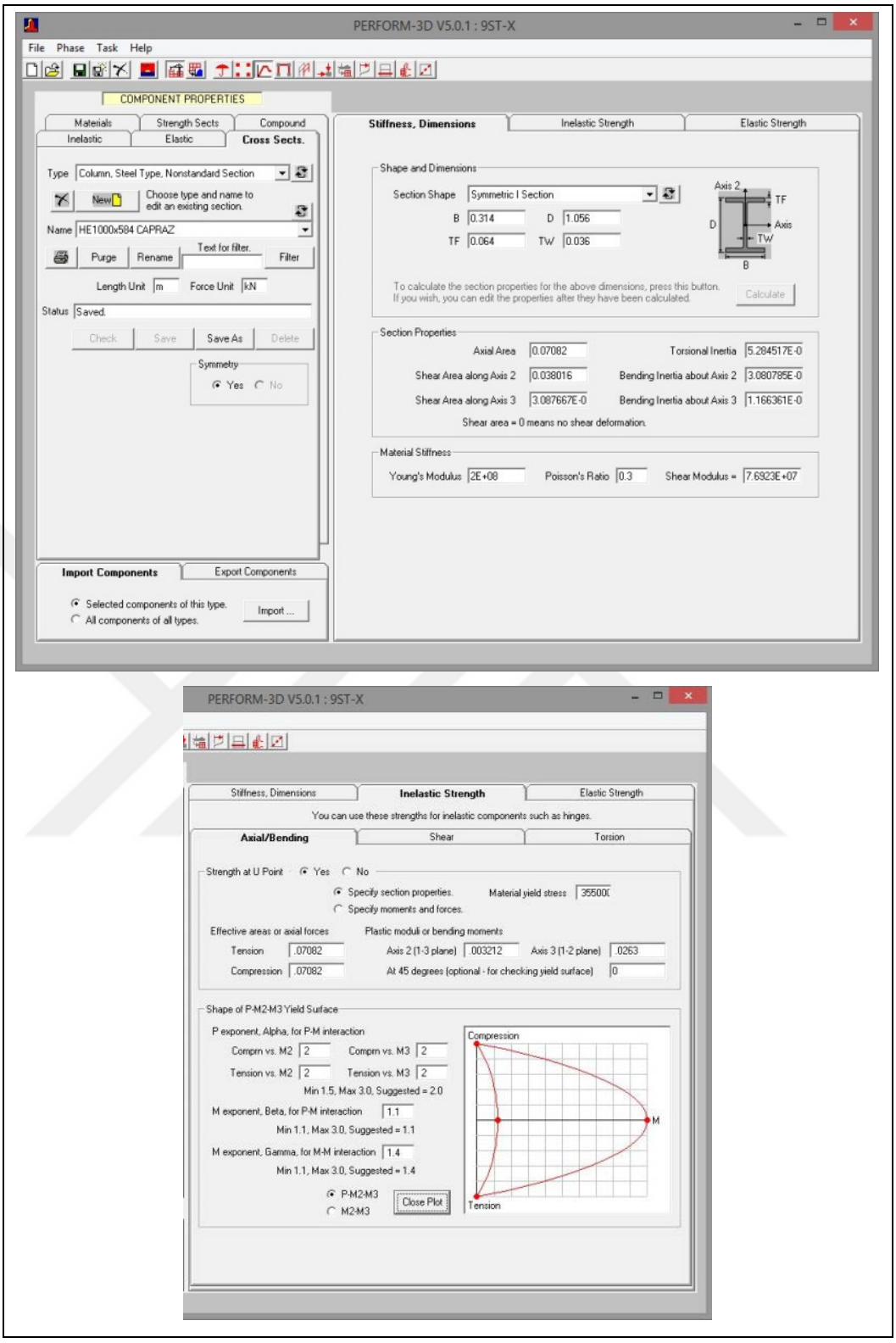

Figure 6.12: “Cross Section” menu for HE100x584.

4-, 8-, 12- and 20-story special braced frames with two different brace configurations (Case E and Case F) were modeled in PERFORM 3D V5 to conduct

nonlinear dynamic time history and pushover analyses. These frames are given is given in figure 6.13.

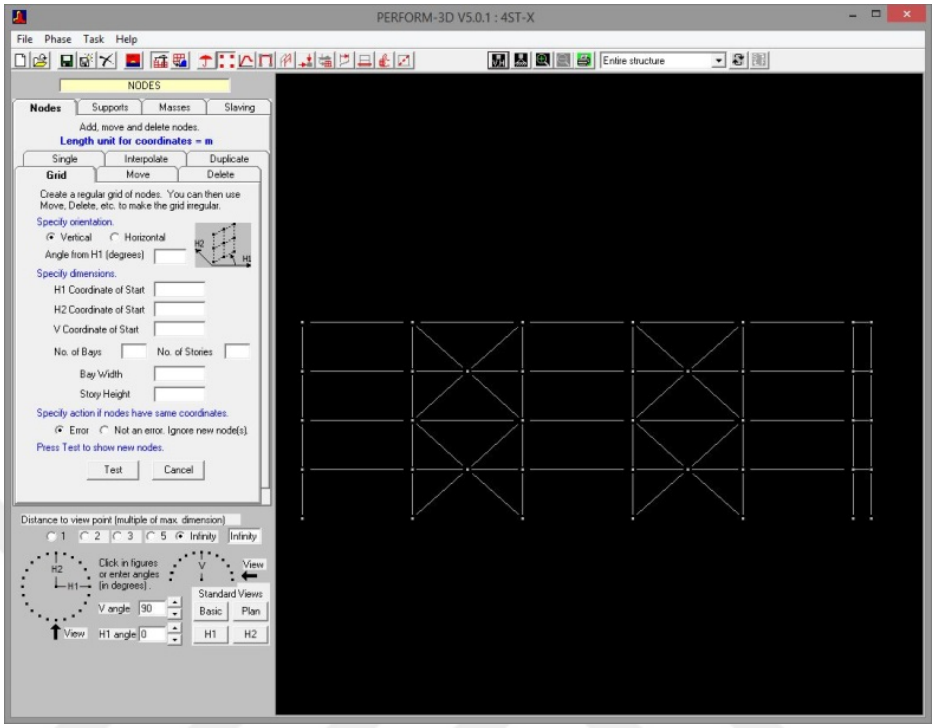

4 – Story Frame (two story X-Braced model)

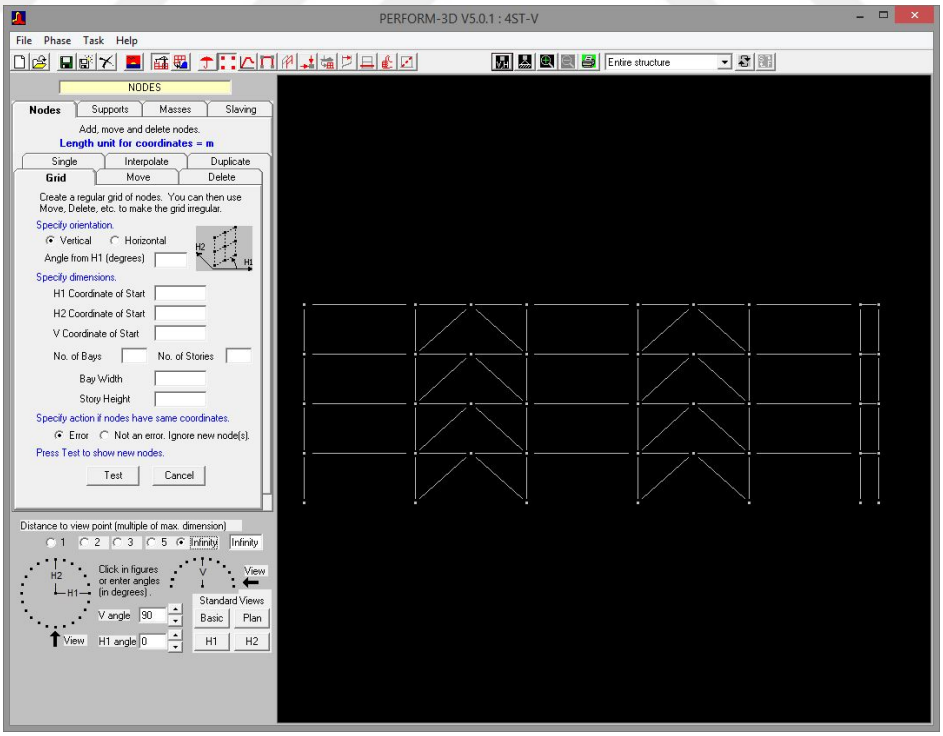

4 – Story Frame (two story Inverted-V Brace model)

Figure 6.13: Braced frame model in PERFORM 3D.

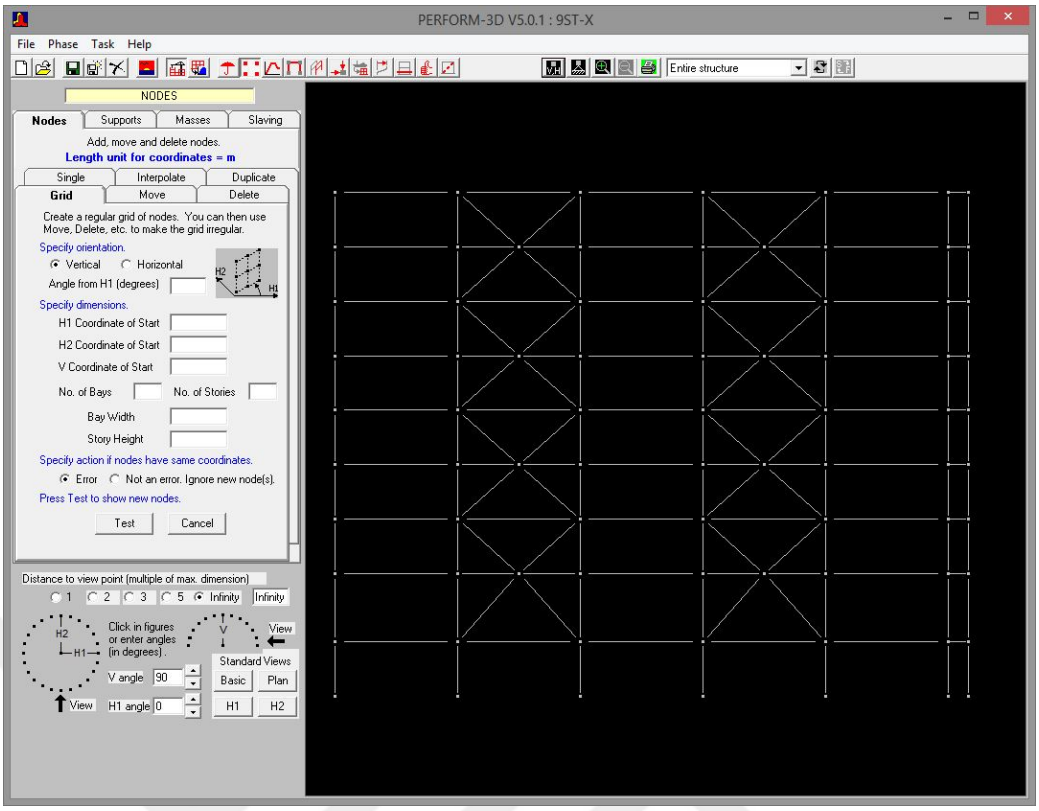

8 – Story Frame (two story X-Braced model)

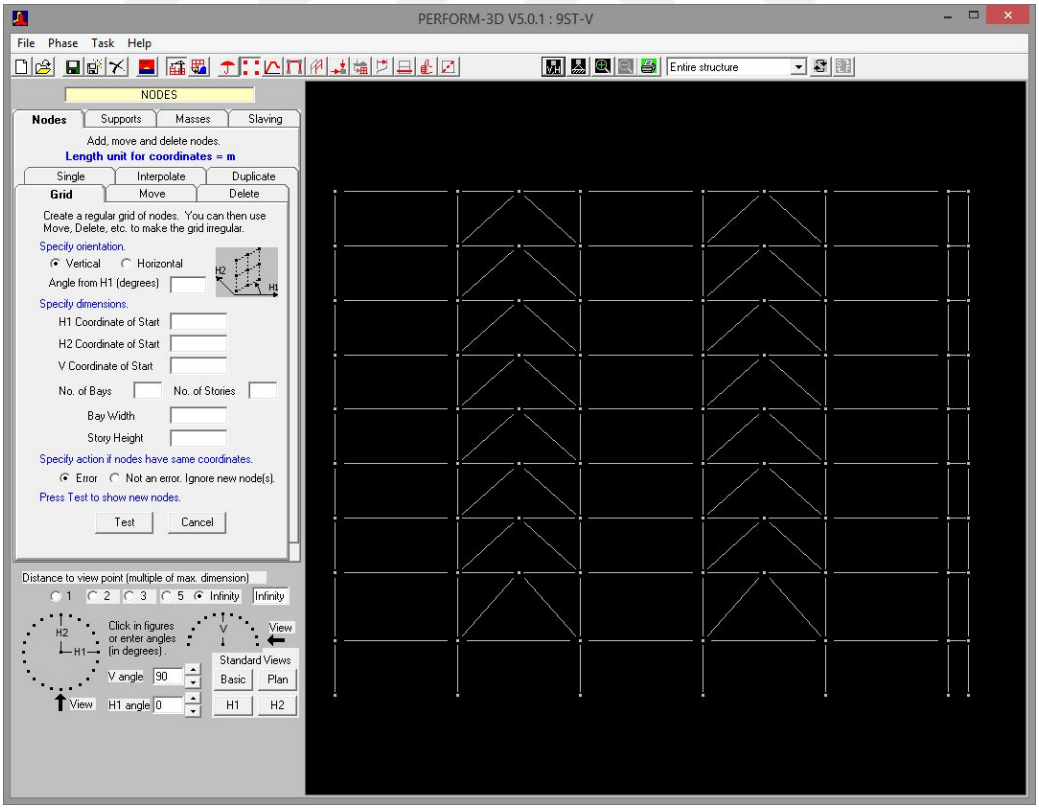

8 – Story Frame (two story Inverted-V Brace model)

Figure 6.13: Continuation of the figure.

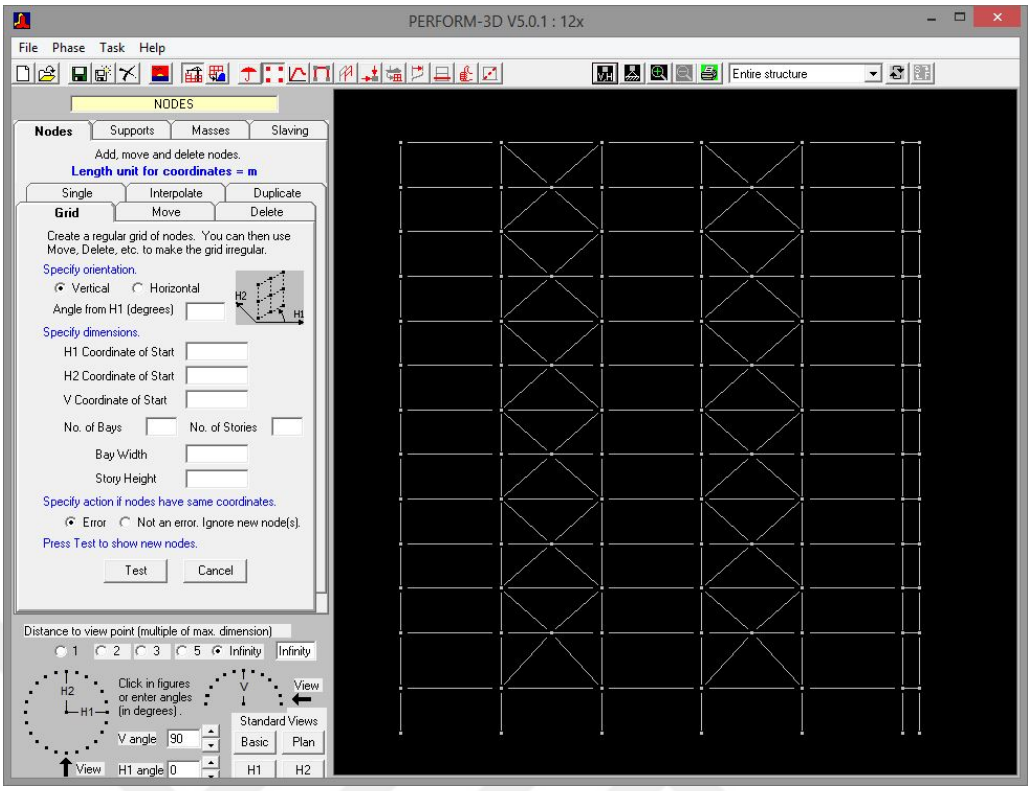

12 – Story Frame (two story X-Braced model)

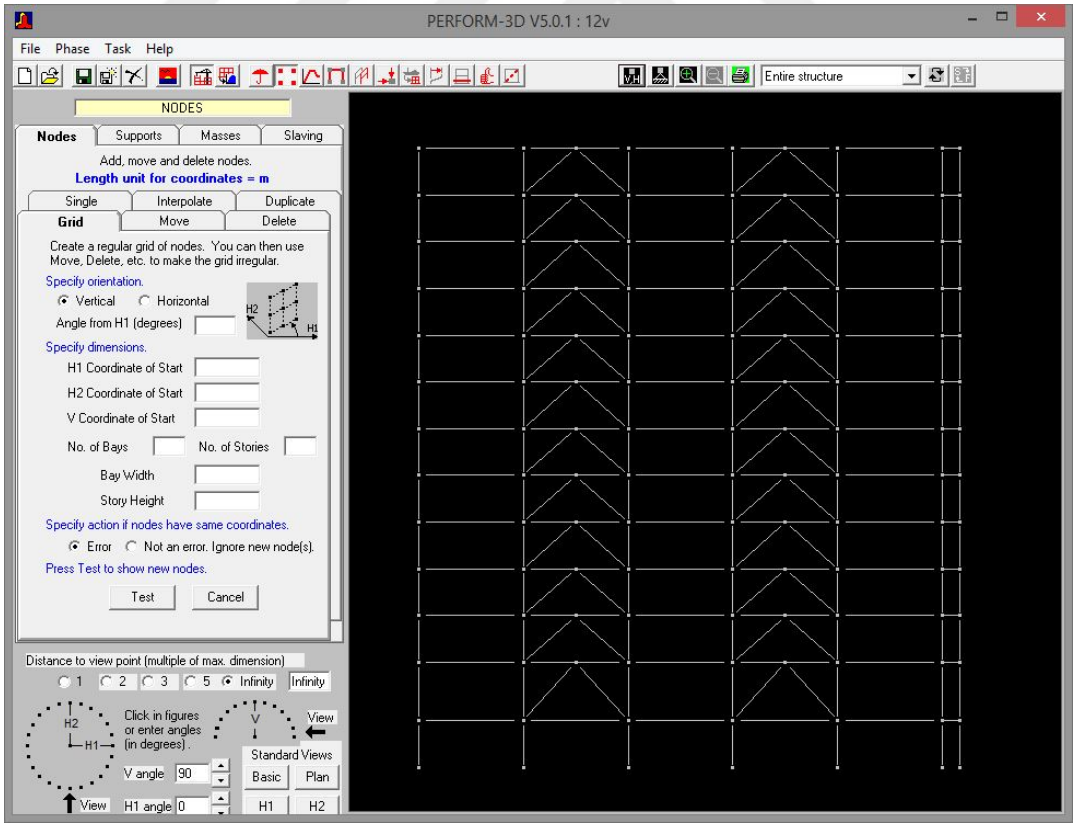

12 – Story Frame (two story Inverted-V Brace model)

Figure 6.13: Continuation of the figure.

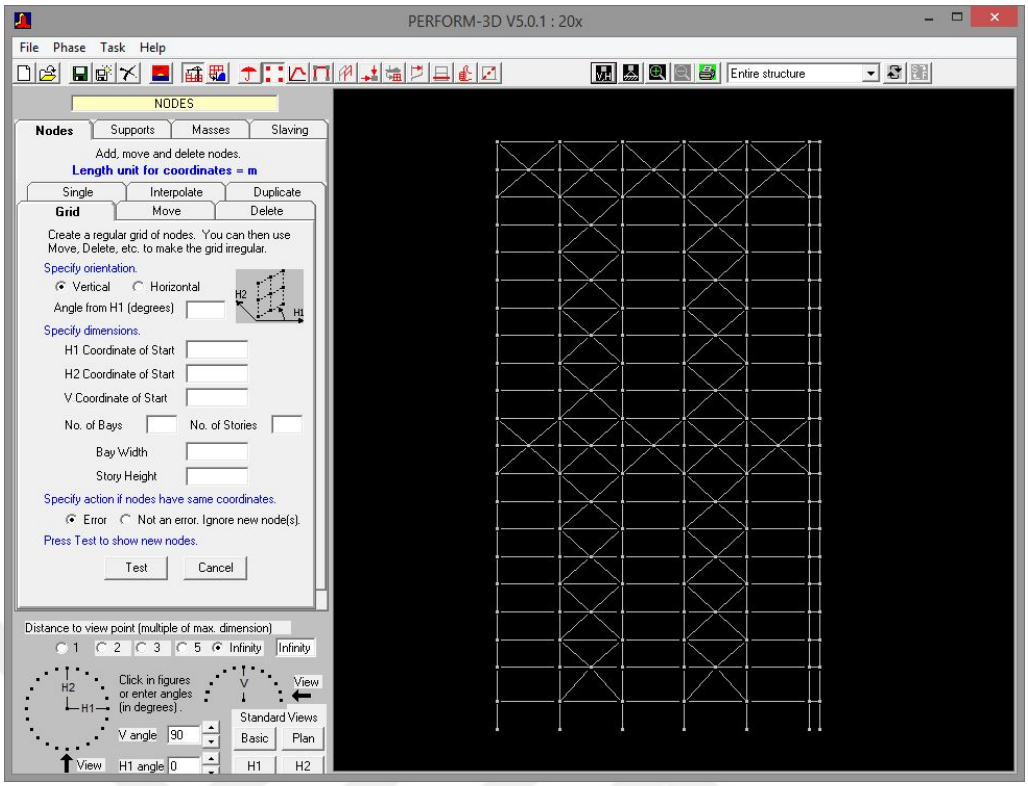

20 – Story Frame (two story X-Braced model)

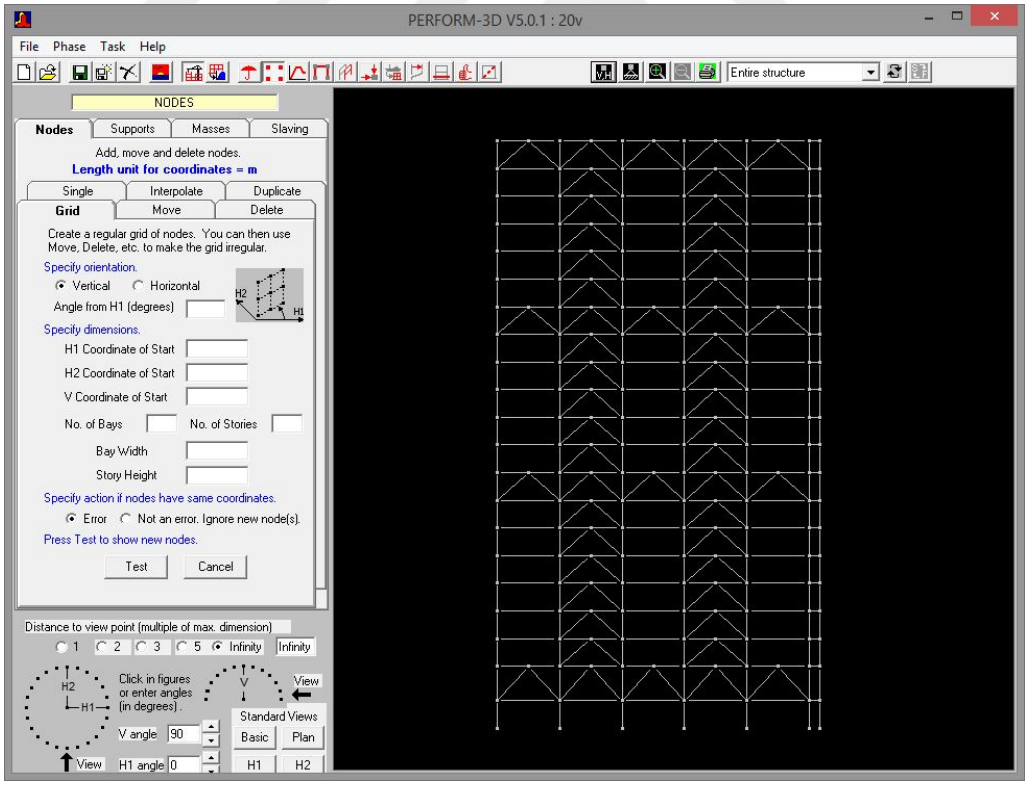

20 – Story Frame (two story Inverted-V Brace model)

Figure 6.13: Continuation of the figure.

6.3. Analytical Study on Braced Frames (SCBF)

Two sets of strong ground motion having a 2% and 10% probability of exceedance in 50 year were selected from Pacific Earthquake and Research Centre (PEER) strong ground motion data base for this study. Each set have seven ground motions. Site class selected for analyses have a shear wave velocity (V_s) between 300 m/s and 770 m/s. Response spectra curve was developed based on American regulations and all ground motions selected for this study were scaled with it. The spectrum parameters for the maximum-considered earthquake (MCE) level have a sort period spectral acceleration, S_S = 2.0g and one second spectral acceleration, S_1 = 1.0g. As for design spectrum the parameters are, S_{DS} =1.333 (g) S_{D1}= 0.666 (g). For both spectrums long-period transition period T_L is 12.0 seconds. The characteristic properties of selected strong ground motions are given in Table 6.3.

Table 6.3: Strong ground motion Characteristics selected from PEER database.

	NGA#	Record	Scale Factor	Duration (sec)	PGA (g)
GM 1 (%10)	265	Victoria	1.4530	24.54	0.9377
GM 2 (%10)	289	Irpinia	2.095	35.22	0.2649
GM 3 (%10)	587	New Zealand	1.5605	49.38	0.3757
GM 4 (%10)	881	Landers	1.8989	56.07	0.4235
GM 5 (%10)	1119	Kobe	0.6005	40.99	0.4187
GM 6 (%10)	4132	Park Field	2.0880	21.20	0.7667
GM 7 (%10)	8166	Düzce	1.7683	35.02	0.7007
GM 8 (%2)	265	Victoria	2.1795	24.54	1.4070
GM 9 (%2)	289	Irpinia	3.143	35.22	0.3974
GM 10 (%2)	587	New Zealand	2.3408	49.38	0.5636
GM 11 (%2)	881	Landers	2.8483	56.07	0.6353
GM 12 (%2)	1119	Kobe	3.1325	40.99	0.6281
GM 13 (%2)	4132	Park Field	2.6524	21.20	1.1500
GM 14 (%2)	8166	Düzce	0.9007	35.02	1.0510

Strong ground motions having a 10% probability of exceedance in 50 year were named from GM1 to GM7 that cause moderate structural damage and strong ground motions corresponding to 2% probability of exceedance in 50 year were named from GM 8 to GM14 that cause heavy structural damage. Acceleration time histories of the selected ground are given in Figure 6.14. and 6.15.

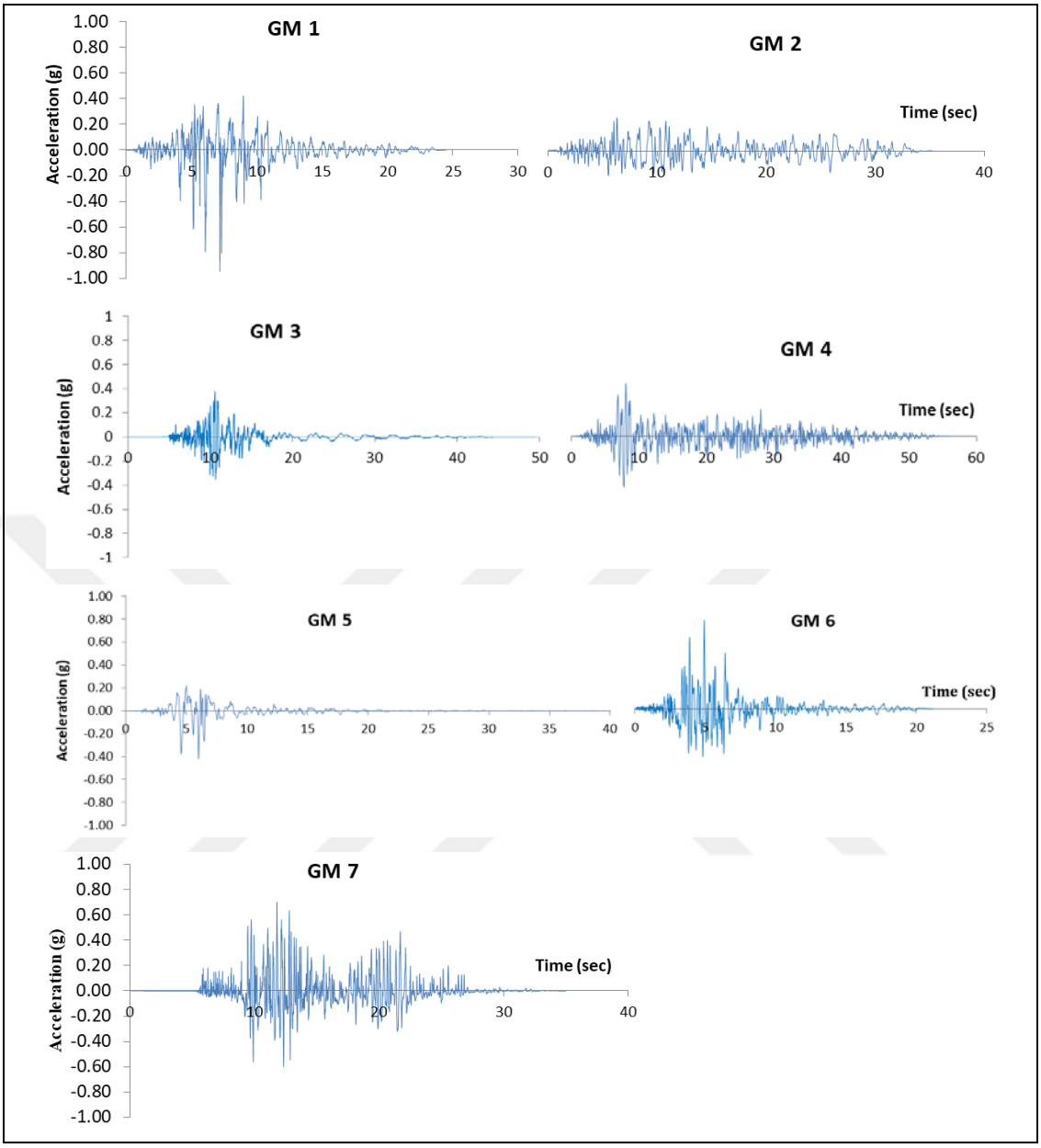

Figure 6.14: Acceleration time histories of the selected ground motions corresponding to 10% probability of exceedance in 50 year.

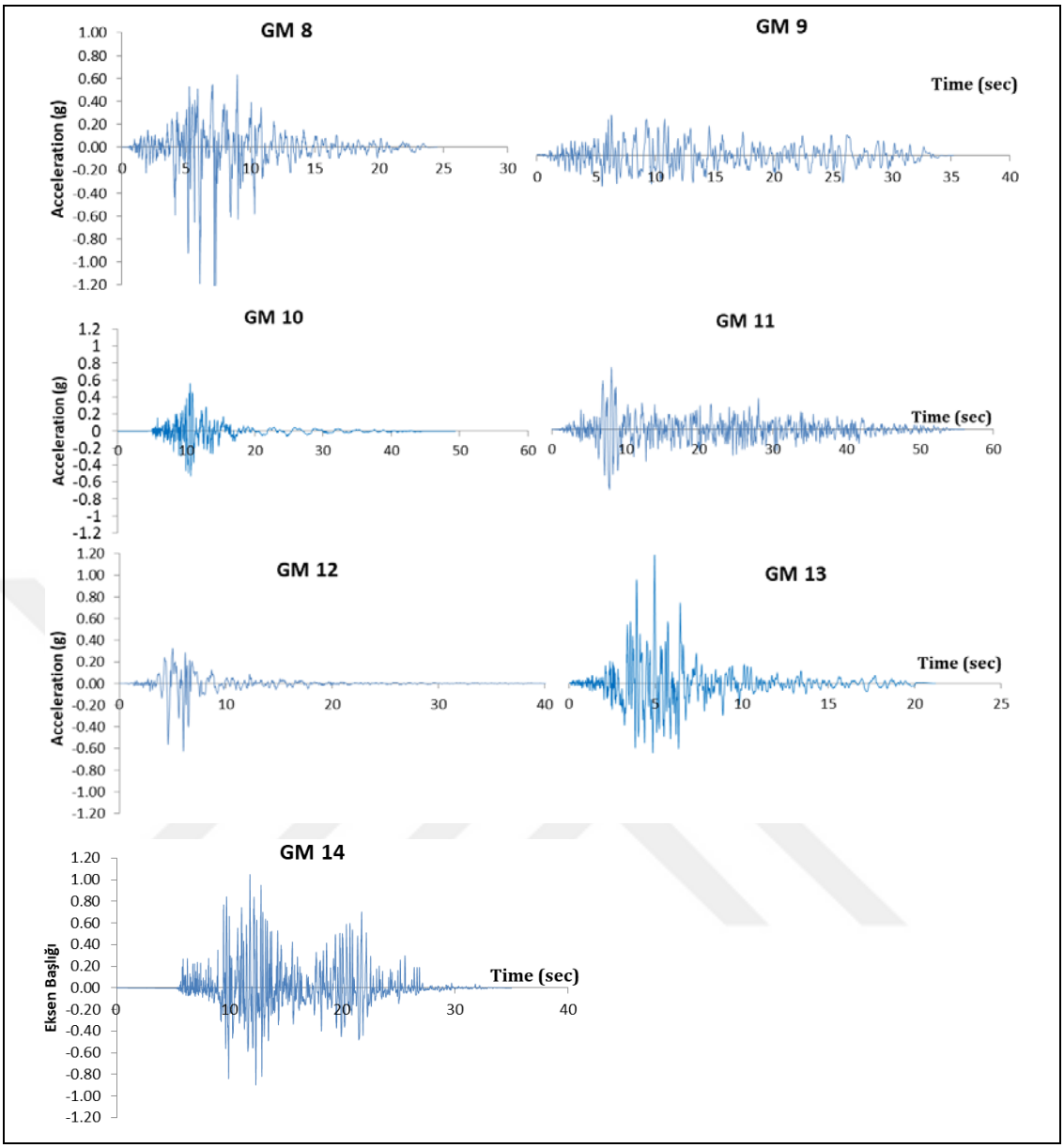

Figure 6.15: Acceleration time histories of the selected ground motions corresponding to 2% probability of exceedance in 50 year.

Response spectra of the selected strong ground motions having a 10% probability of exceedance in 50 year are given in Figure 6.16 and response spectra of the selected strong ground motions having a 2% probability of exceedance in 50 year are given in Figure 6.17.

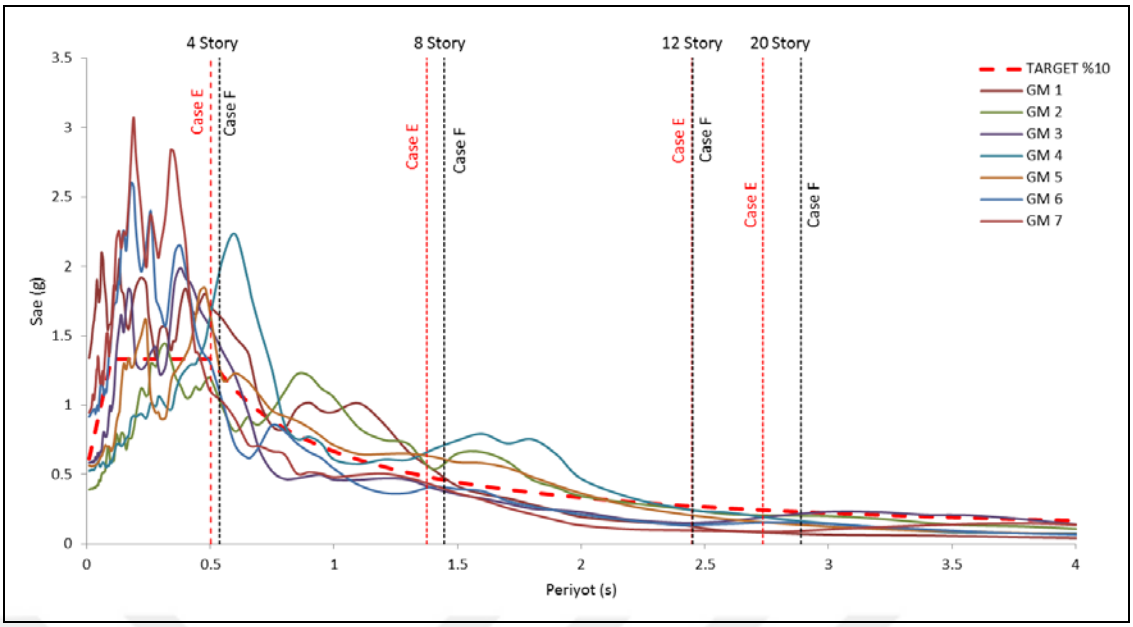

Figure 6.16: Response Spectra of the ground motions (GM1 to GM7) selected from PEER database for design earthquake level corresponding to 10% probability of exceedance in 50 year.

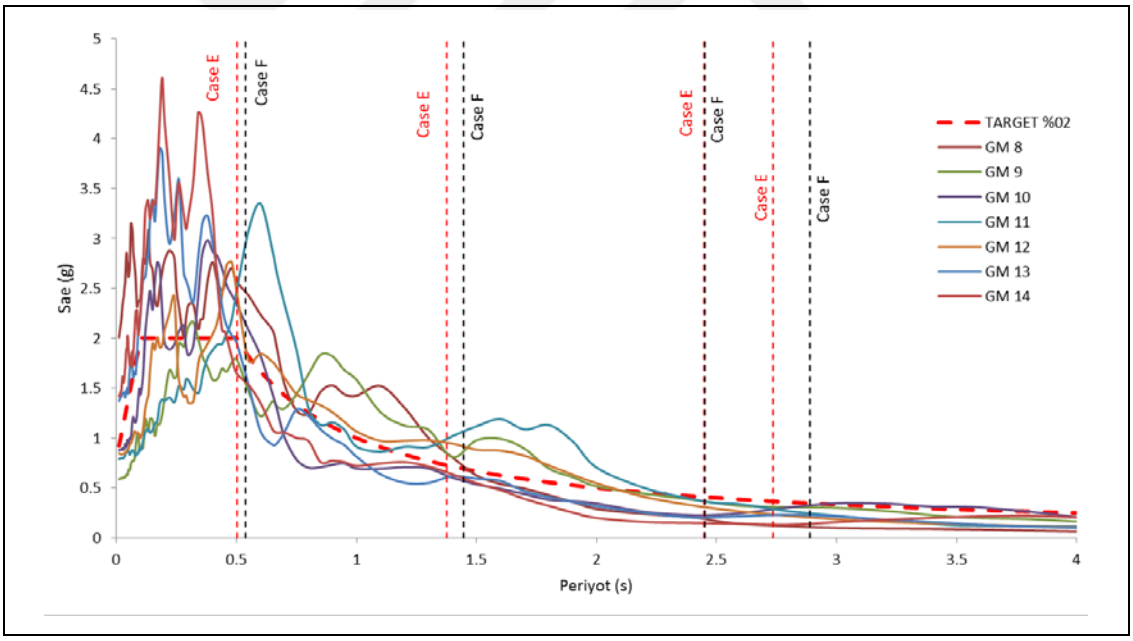

Figure 6.17: Response Spectra of the ground motions (GM8 to GM14) selected from PEER database for design earthquake level corresponding to 2% probability of exceedance in 50 year.

6.4. Analyses Result for Braced Frames (SCBF)

To investigate amplified seismic load effects on the 4-, 8-, 12- and 20-story frames, nonlinear dynamic time history analyses were conducted under two groups of ground motions (a total of 14 ground motions) corresponding to 10% and 2% probability of exceedance in 50 year.

The maximum drift ratios for each cases and story heights under strong ground motions correspond to 10% and 2% probability of exceedance in 50 year are given in Figure 6.18. to 6.21. Higher drift ratios occurs where cross section of brace element changes to smaller section. In 4-story frame, higher drift ratio obtained in Case F with 4.18% and like 4-story frame, maximum drift ratio occurs in Case F in 8-story frame with a value of 3.84%. Drift ratios for Case F and Case E are 3.47% and 3.26% respectively. Despite the other story level, maximum drift ratio occurs in Case E with a value of 3.04% in 20-Story frame.

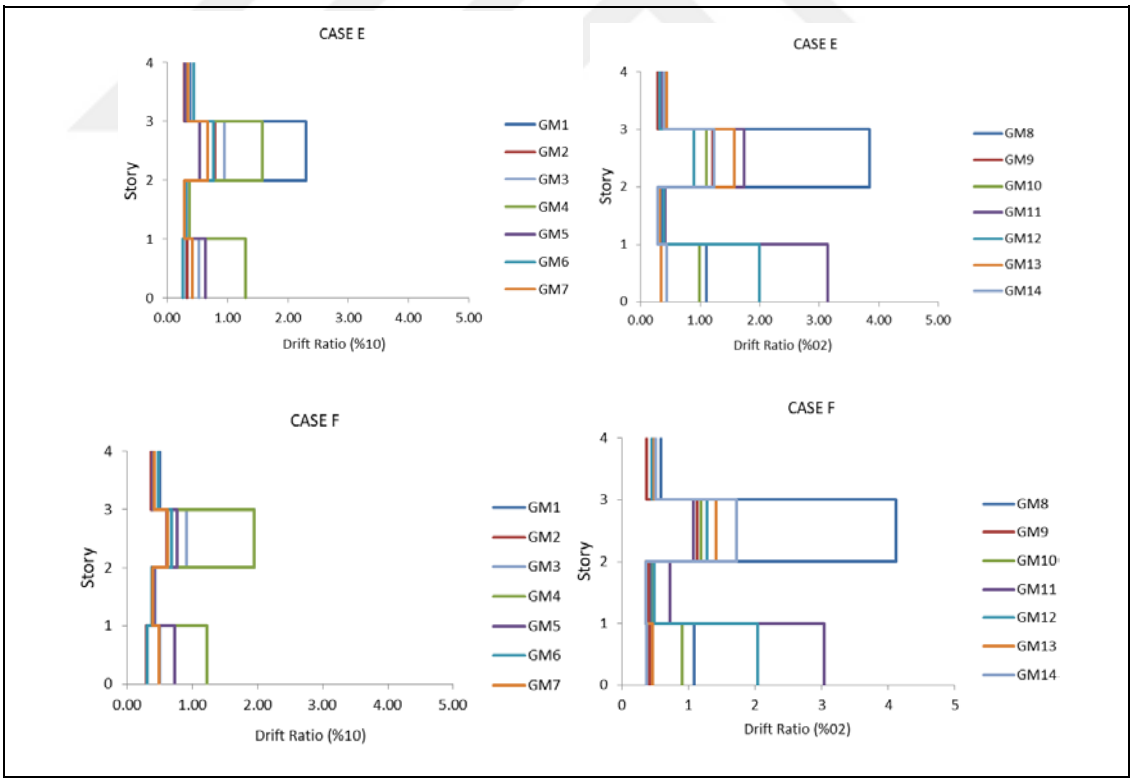

Figure 6.18: Drift ratios for 4- story frames corresponding to 2% and 10% probability of exceedance in 50 year.

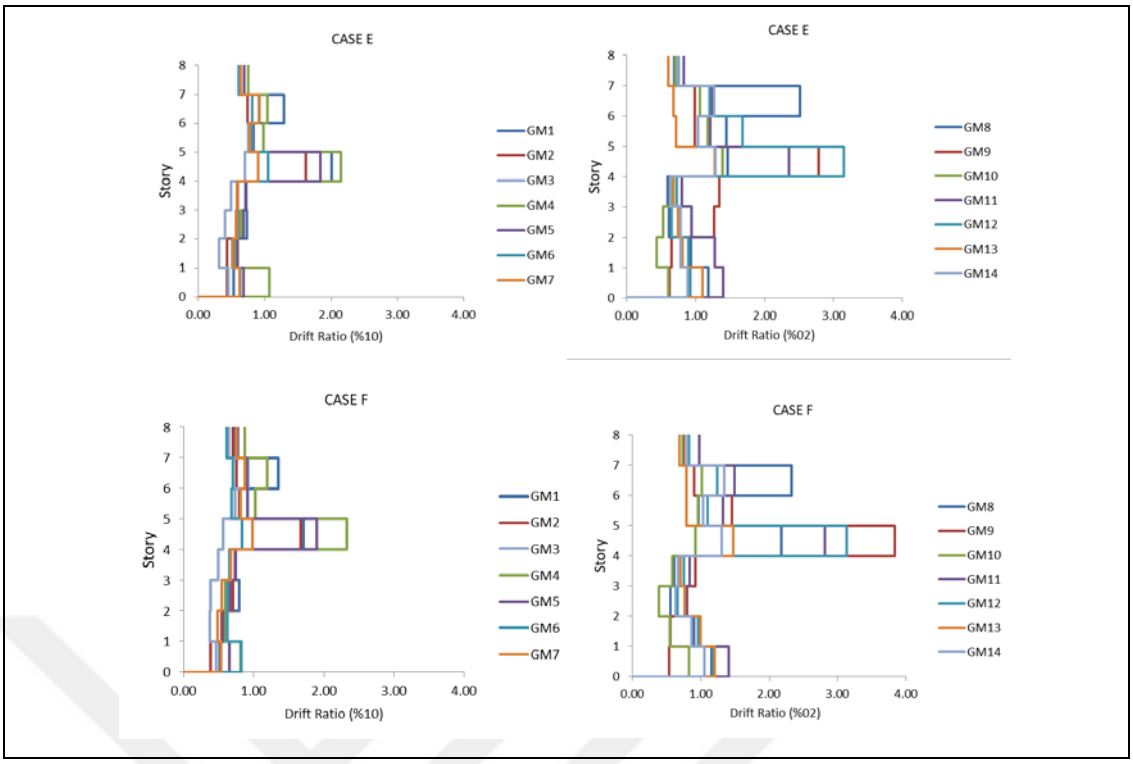

Figure 6.19: Drift ratios for 8- story frames corresponding to 2% and 10% probability of exceedance in 50 year.

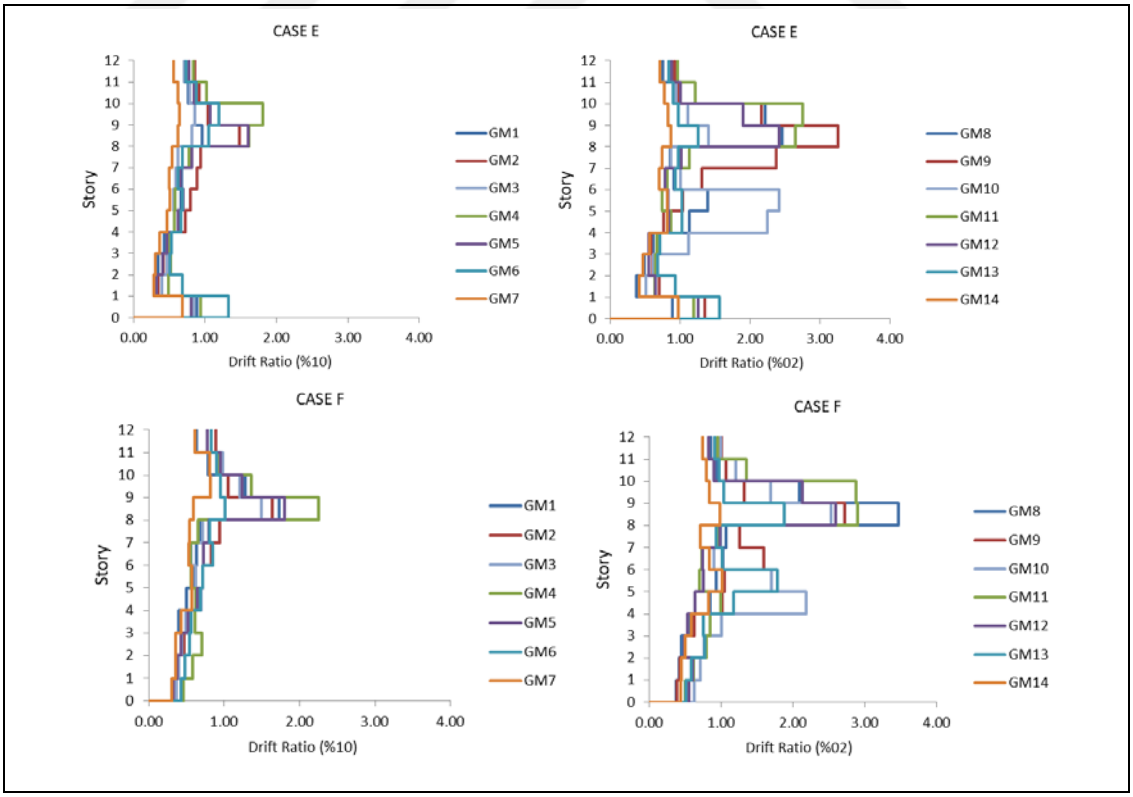

Figure 6.20: Drift ratios for 12- story frames corresponding to 2% and 10% probability of exceedance in 50 year.

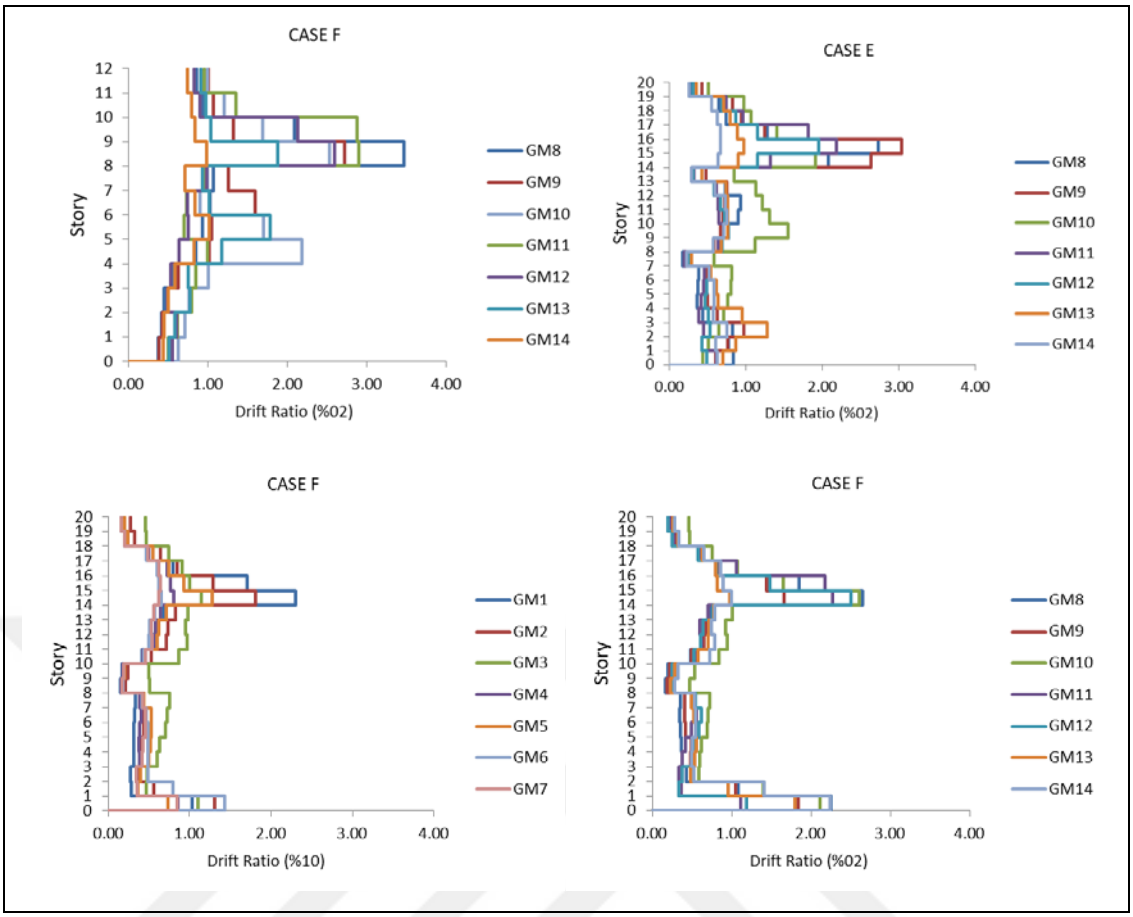

Figure 6.21: Drift ratios for 20- story frames corresponding to 2% and 10% probability of exceedance in 50 year.

Average of the maximum drift ratios for each frame under selected ground motion corresponding to 2% and 10% probability of exceedance in 50 year given in figure7.26. For 4-story frames, average maximum drift occurs in 3th story while for 8-, 12- and 20-story frames maximum drift occurs in 5th, 9th and 15th story respectively. Under strong ground motions corresponding to 10% probability of exceedance in 50 year, maximum average drift ratios do not exceed 2% for all frames and while it's up to 2.44% for strong ground motions corresponding to 2% probability of exceedance in 50 year.

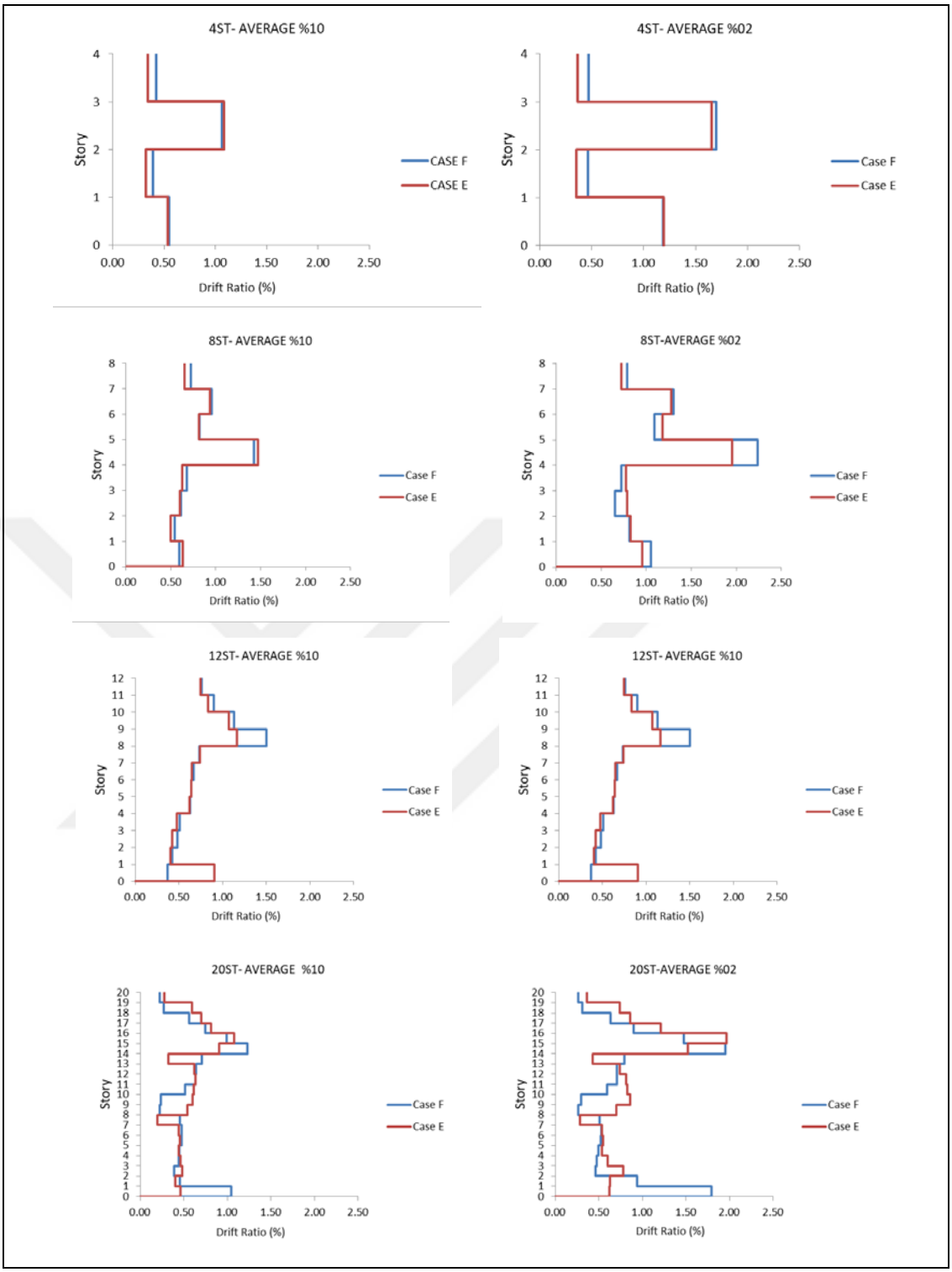

Figure 6.22: Average maximum drift ratio in frames corresponding to 2% and 10% probability of exceedance in 50 year.

The maximum drift ratio for each frame under selected ground motions are given in Fig 7.27. The maximum drift ratio varied between 0.61% and 4.12% for 4-story frames. For 8-story frames it varies between 0.83% and 3.84%, for 12-story

frames it varies from 0.69% to 3.47% and for 20-story frames drift ratio ranges from 0.48% to 3.04%.

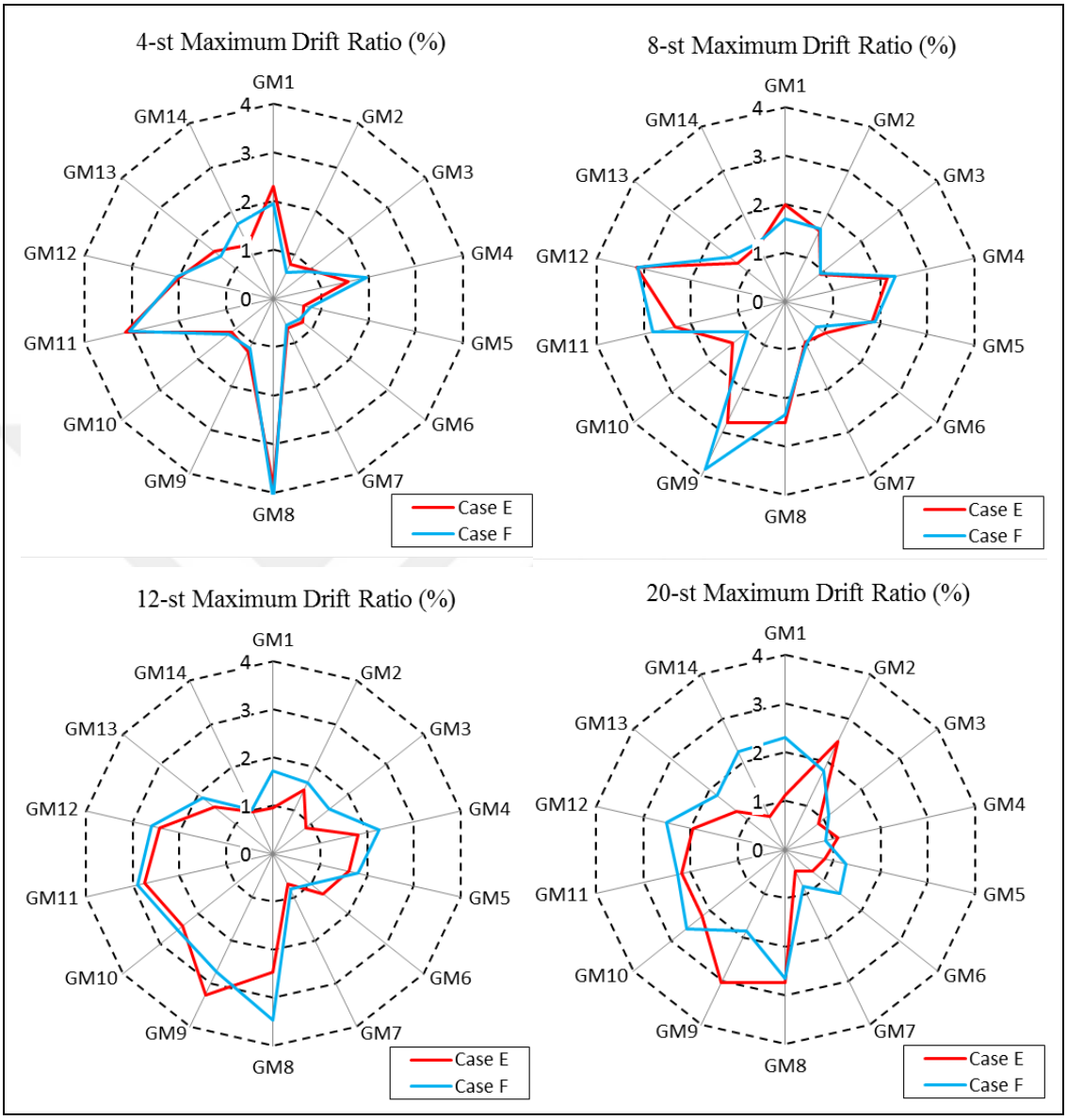

Figure 6.23: Drift Maximum drift ratio in each frame corresponding to 2% and 10% probability of exceedance in 50 year.

The amplification factors of axial compression in braced bay columns for 10% and 2% probability of exceedance in 50 year are given through Figure 6.24. to 6.27. Except 20-story frames, maximum increase in amplification factor occurs on the last story columns in Case F. Except 20-story frames, columns in Case F have higher amplification factors than columns in Case E. Columns on the last story have the lowest amplification factors in Case E.

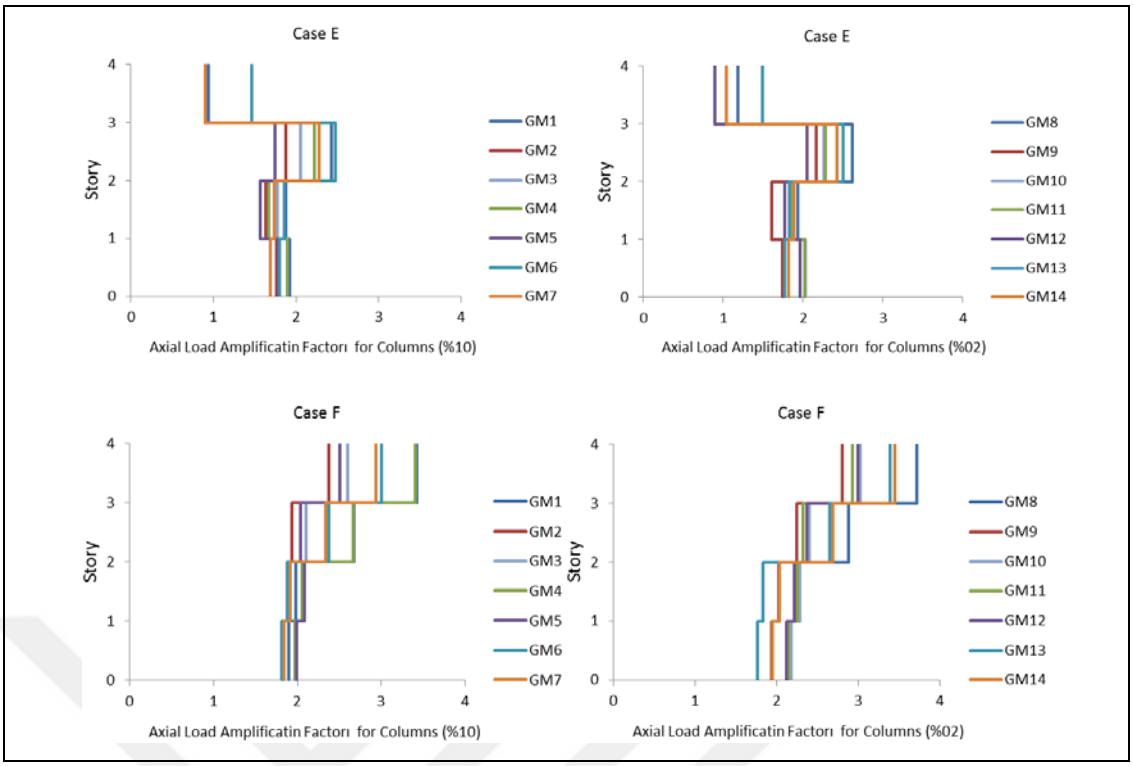

Figure 6.24: Maximum amplification factor for 4- story frames corresponding to 2% and 10% probability of exceedance in 50 year.

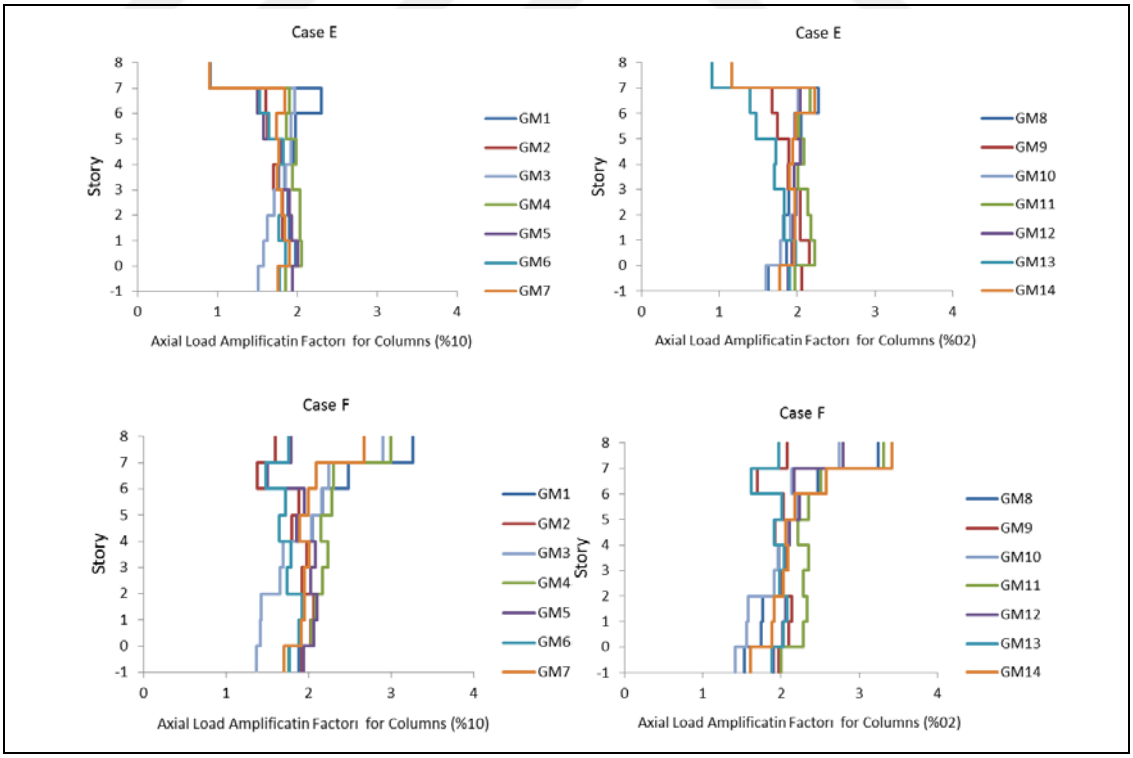

Figure 6.25: Maximum amplification factor for 8- story frames corresponding to 2% and 10% probability of exceedance in 50 year.

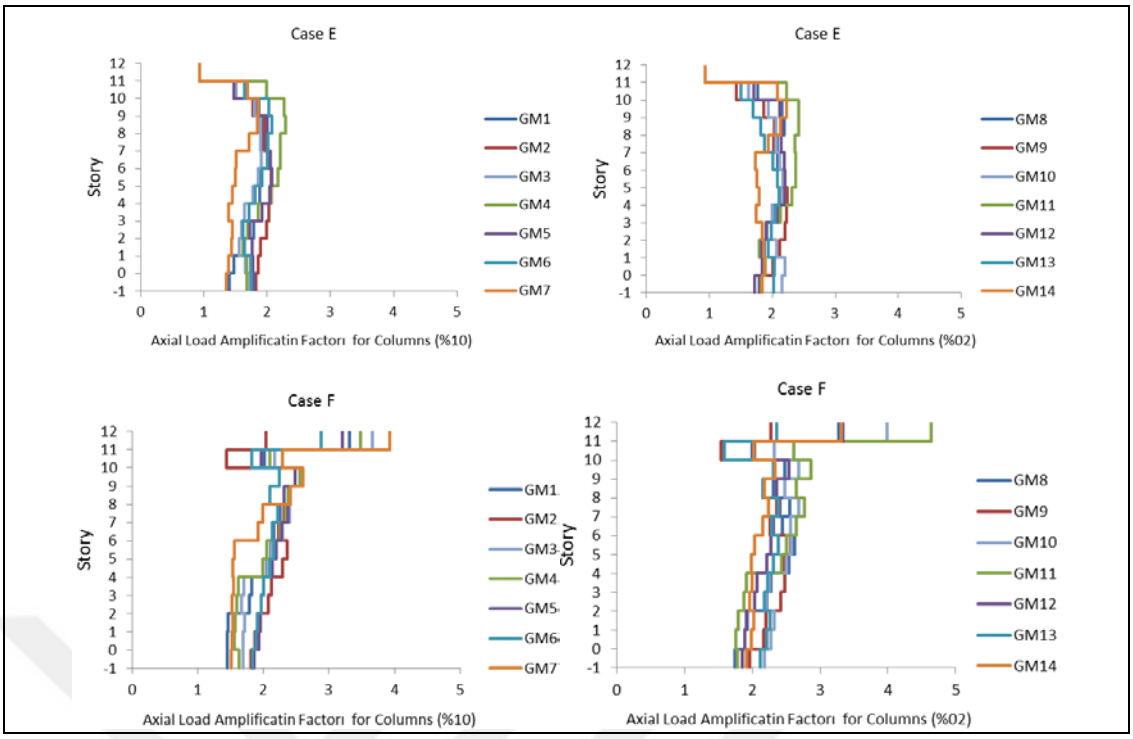

Figure 6.26: Maximum amplification factor for 12- story frames corresponding to 2% and 10% probability of exceedance in 50 year.

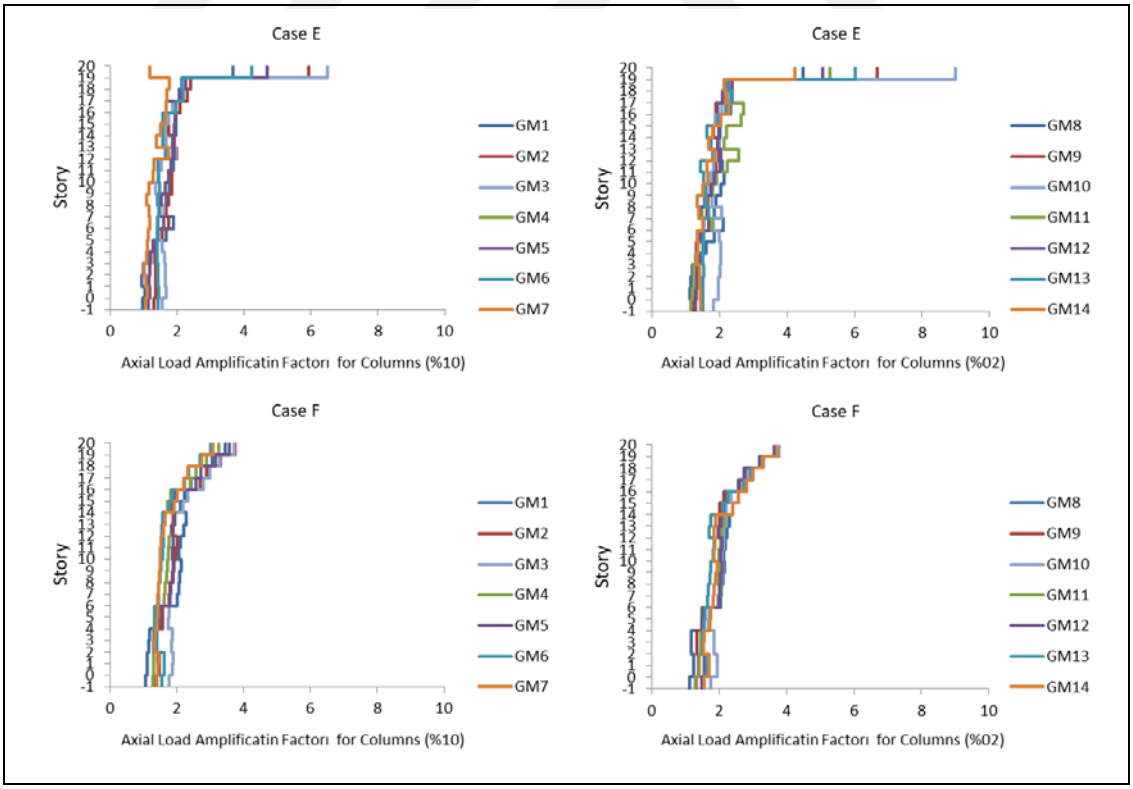

Figure 6.27: Maximum amplification factor for 20- story frames corresponding to 2% and 10% probability of exceedance in 50 year.

The amplification factors of axial compression in brace element for 10% and 2% probability of exceedance in 50 year are given through Figure 6.28. to 6.31. Except 20-story frames, maximum increase in amplification factor occurs on the last story brace members in both Cases.

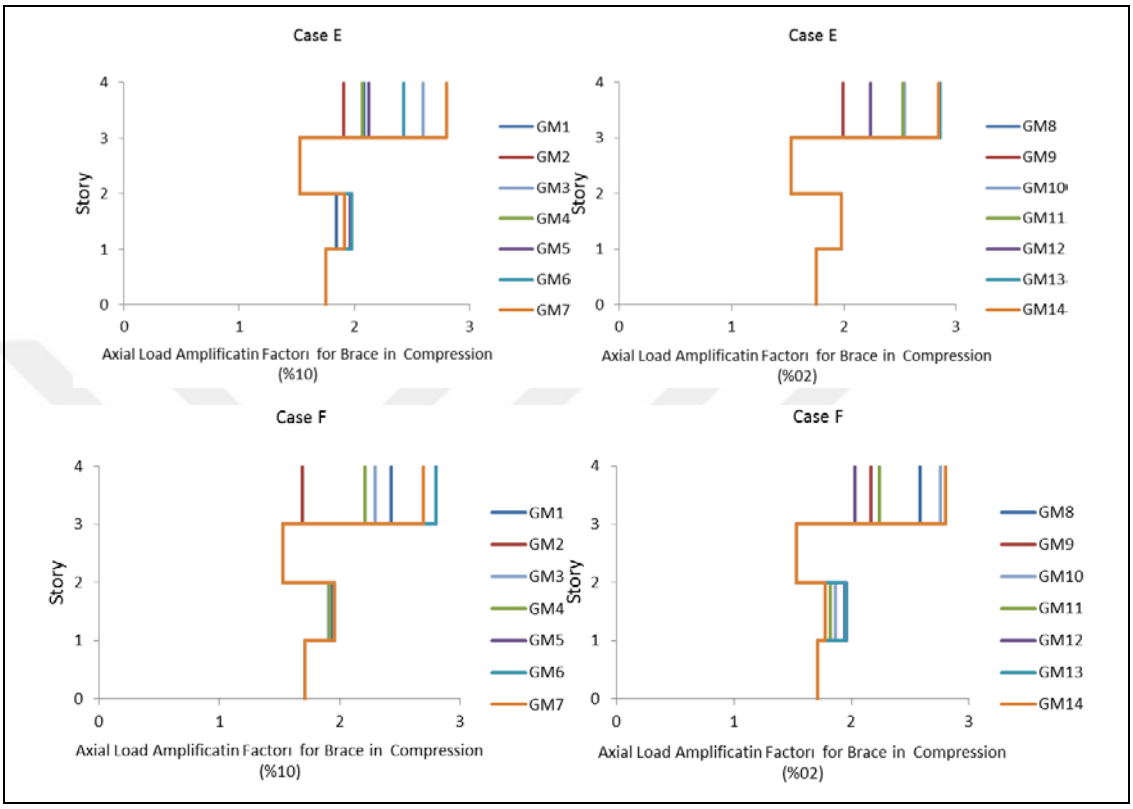

Figure 6.28: Maximum amplification factor for brace in compression in 4- story frames corresponding to 2% and 10% probability of exceedance in 50 year.

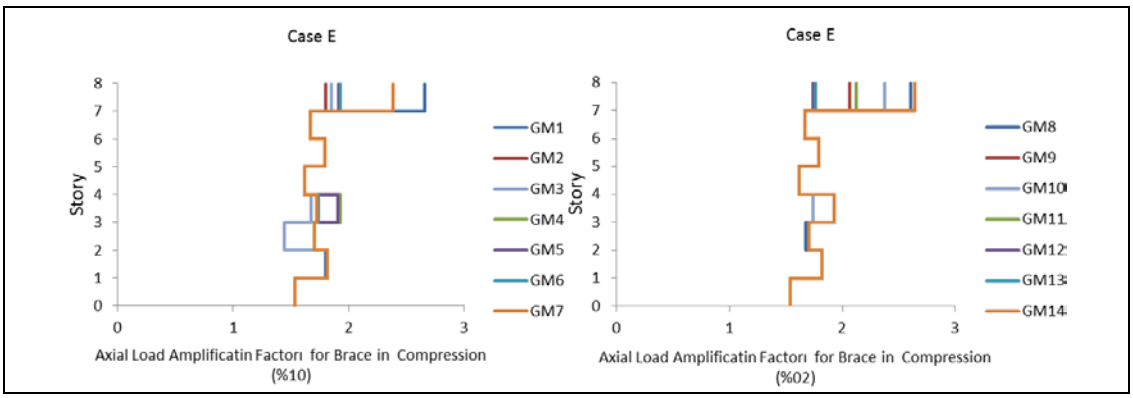

Figure 6.29: Maximum amplification factor for brace in compression in 8- story frames corresponding to 2% and 10% probability of exceedance in 50 year.

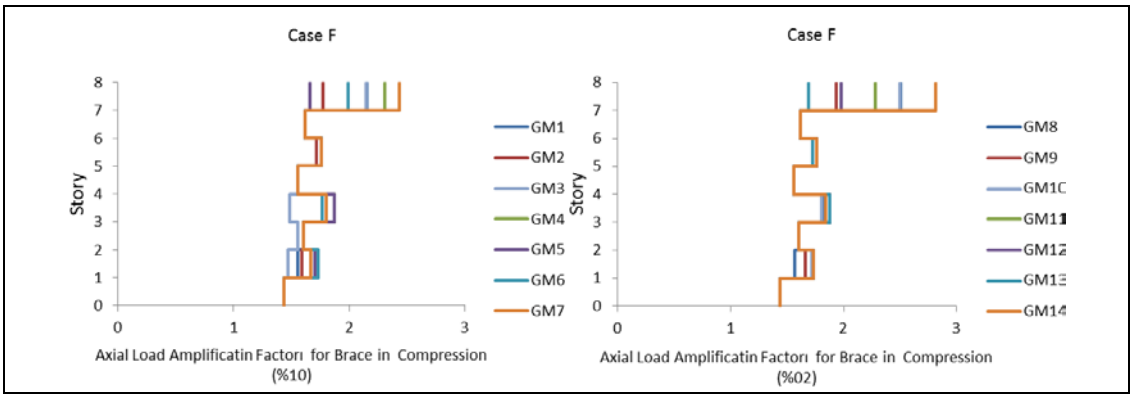

Figure 6.29: Continuation of the figure.

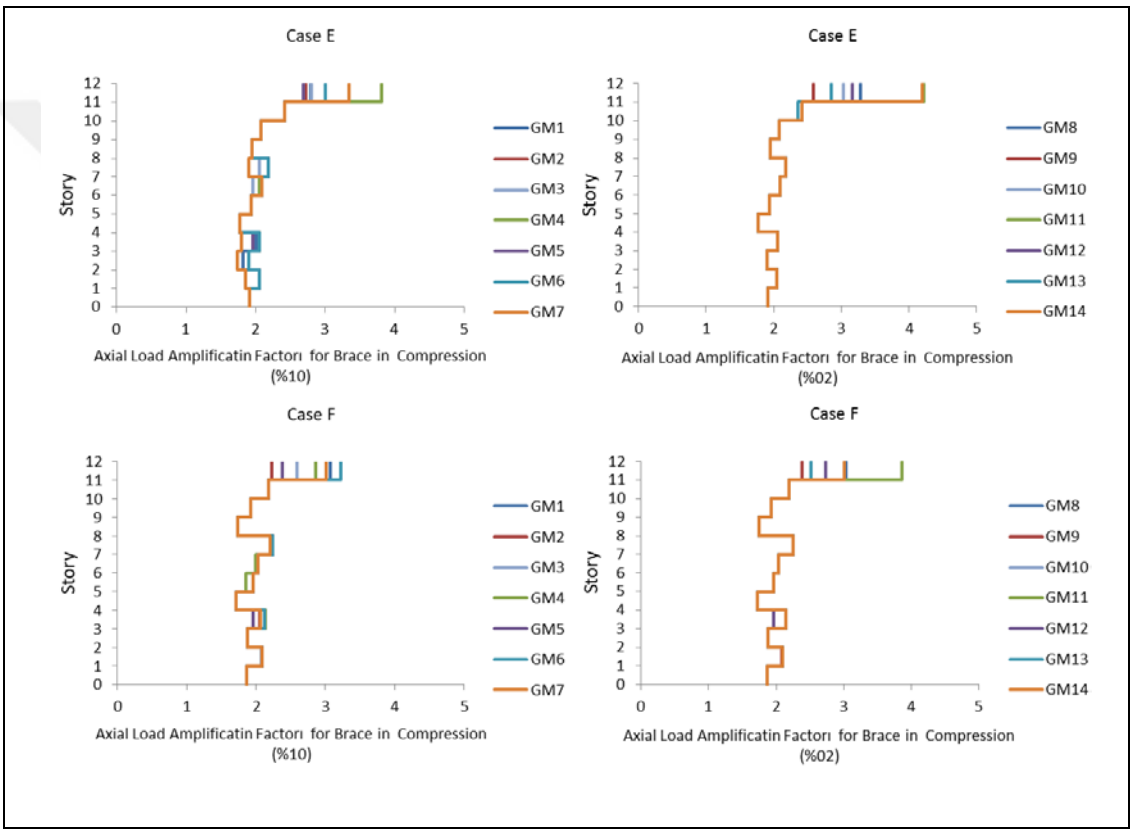

Figure 6.30: Maximum amplification factor for brace in compression in 12- story frames corresponding to 2% and 10% probability of exceedance in 50 year.

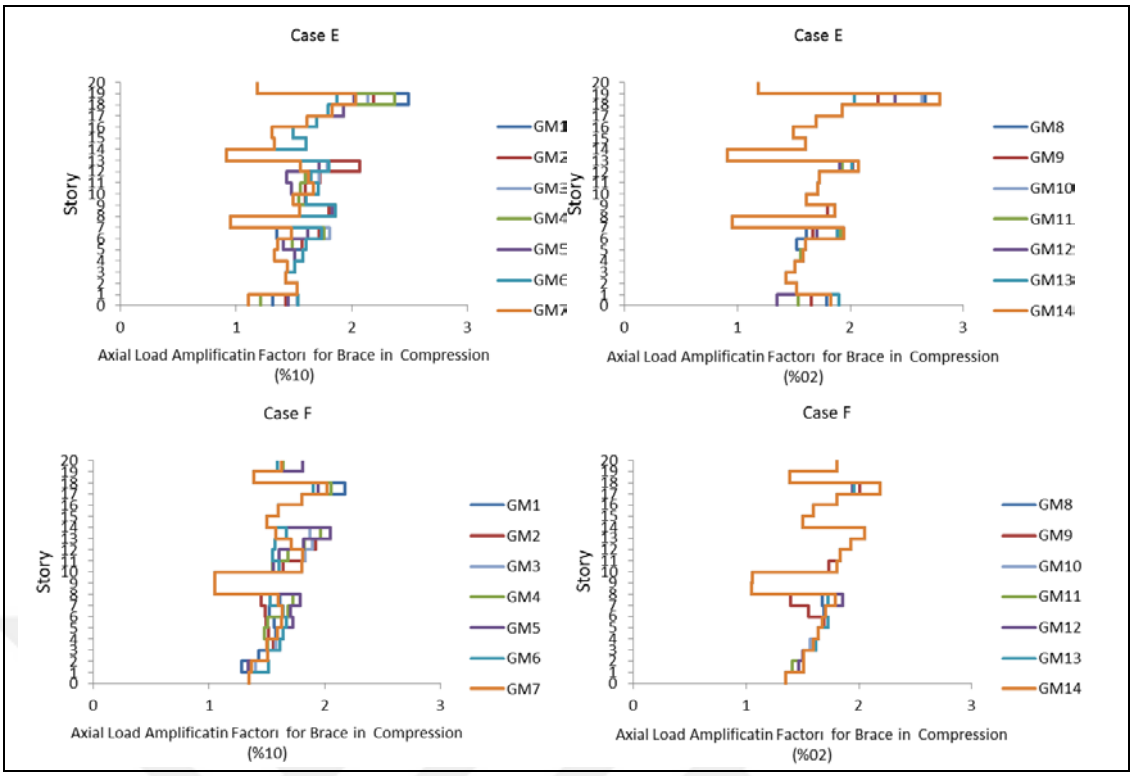

Figure 6.31: Maximum amplification factor for brace in compression in 20- story frames corresponding to 2% and 10% probability of exceedance in 50 year.

The amplification factors of brace in tension under 10% and 2% probability of exceedance in 50 year are given through Figure 6.32. to 6.35.

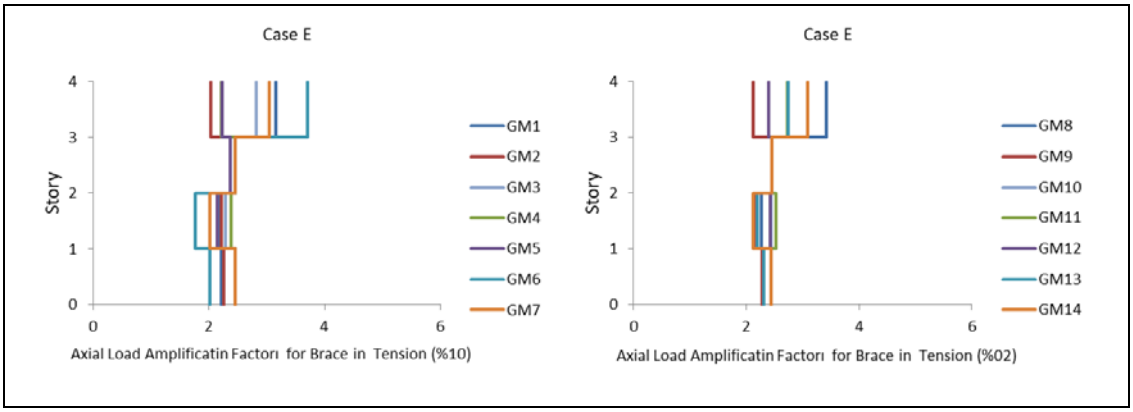

Figure 6.32: Maximum amplification factor for brace in tension in 4- story frames corresponding to 2% and 10% probability of exceedance in 50 year.

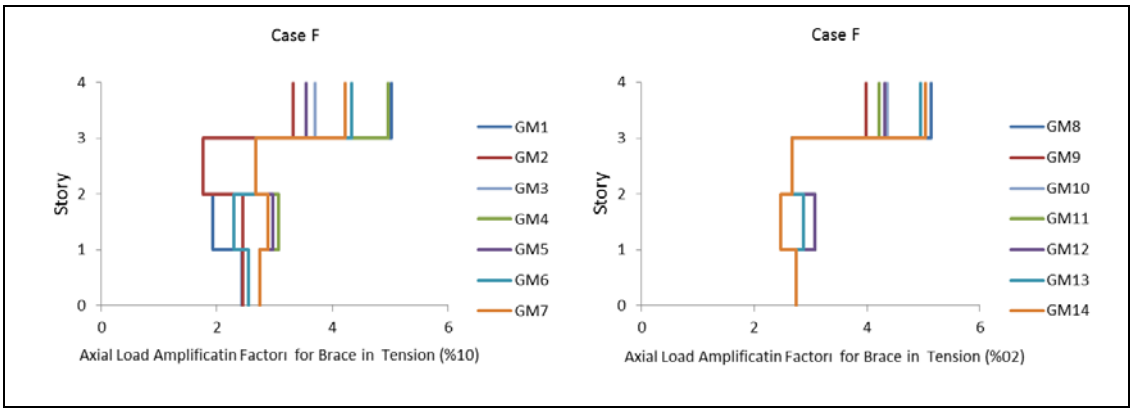

Figure 6.32: Continuation of the figure.

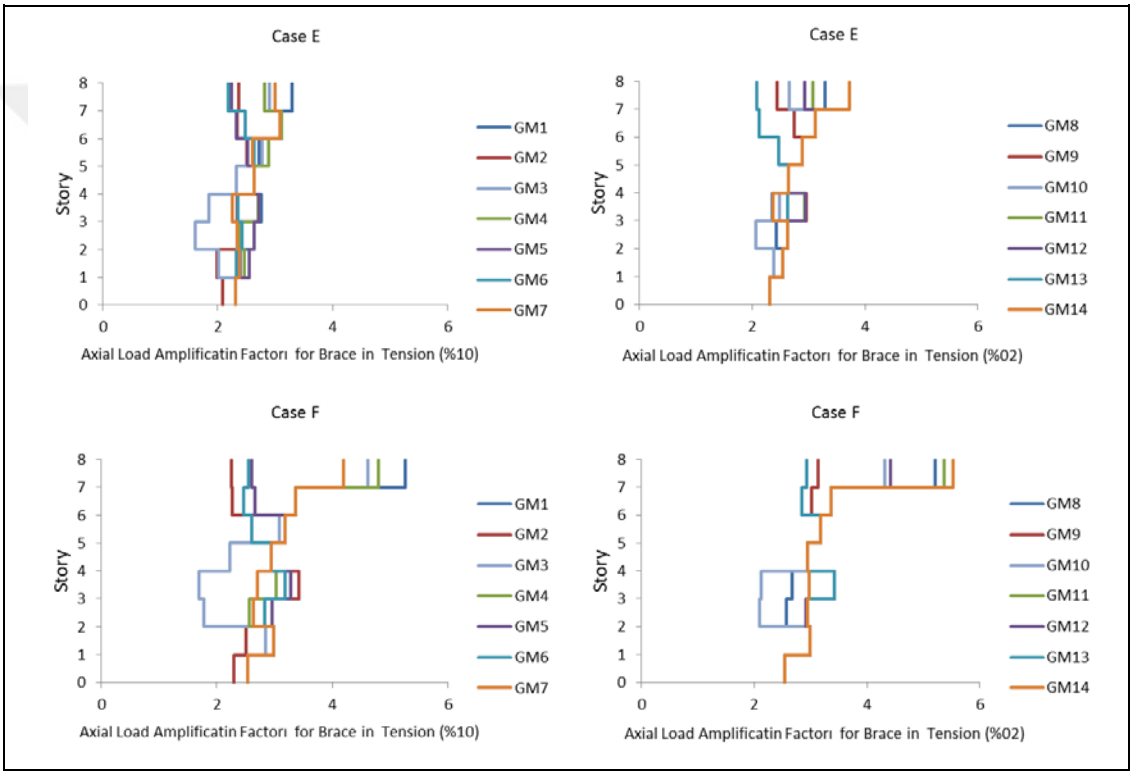

Figure 6.33: Maximum amplification factor for brace in tension in 8- story frames corresponding to 2% and 10% probability of exceedance in 50 year.

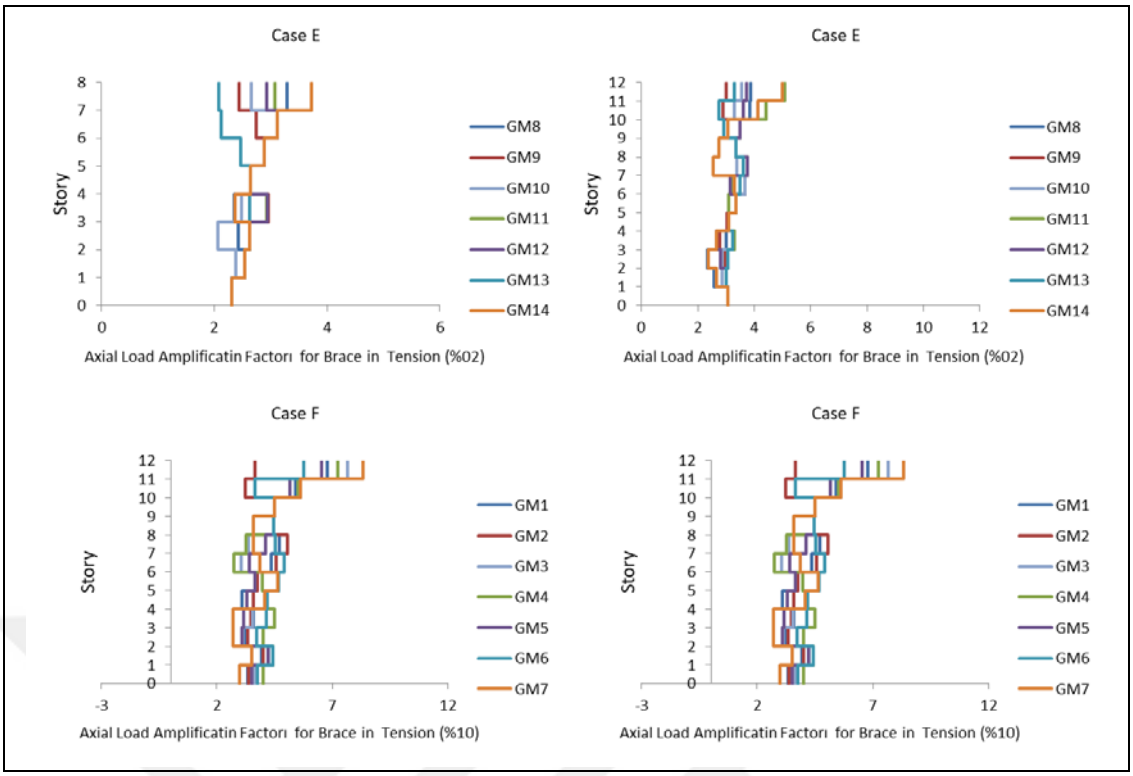

Figure 6.34: Maximum amplification factor for brace in tension in 12- story frames corresponding to 2% and 10% probability of exceedance in 50 year.

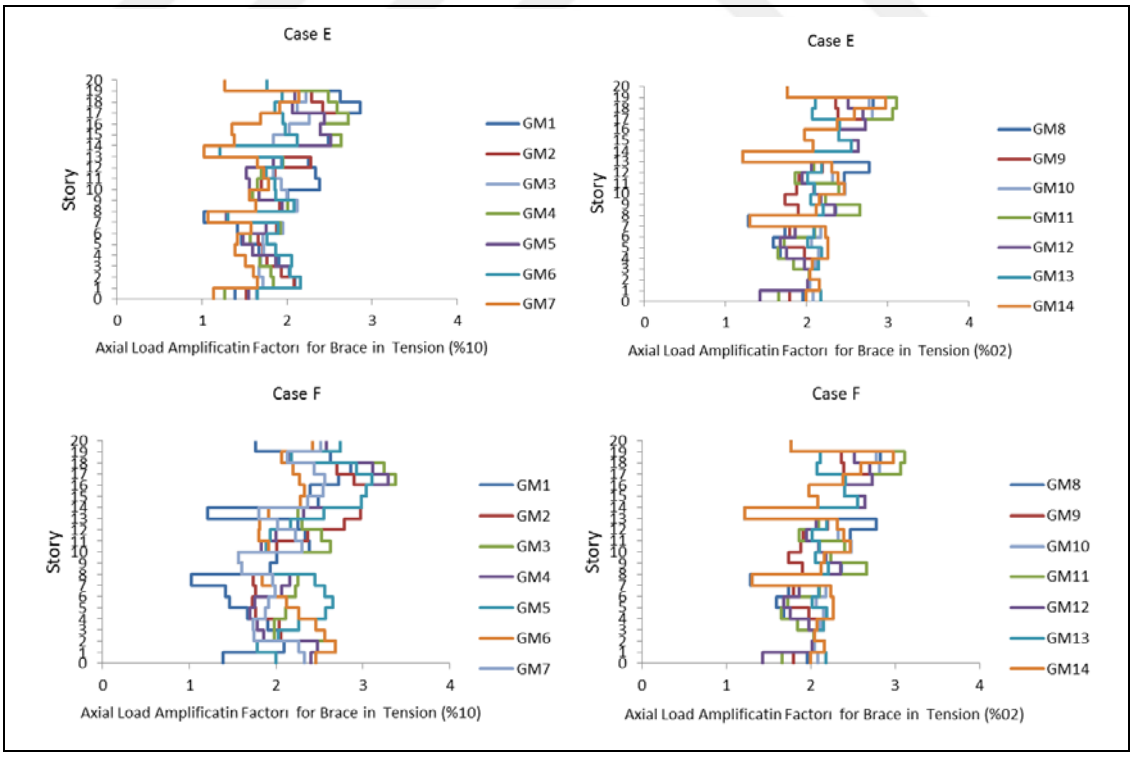

Figure 6.35: Maximum amplification factor for brace in tension in 20- story frames corresponding to 2% and 10% probability of exceedance in 50 year.

The average of the maximum amplification factors for axial compression in each story columns, axial compression in braces and axial tension in braces under 10% and 2% probability of exceedance in 50 year are given in Figure 6.36. – 6.41. For 4-, 8- and 12- Story frames, amplification factor for columns in axial compression gets higher values in Case F while amplification factor for braces in axial compression have similar values. But for axial tension, braces in Case F have higher amplification factor values than Case E.

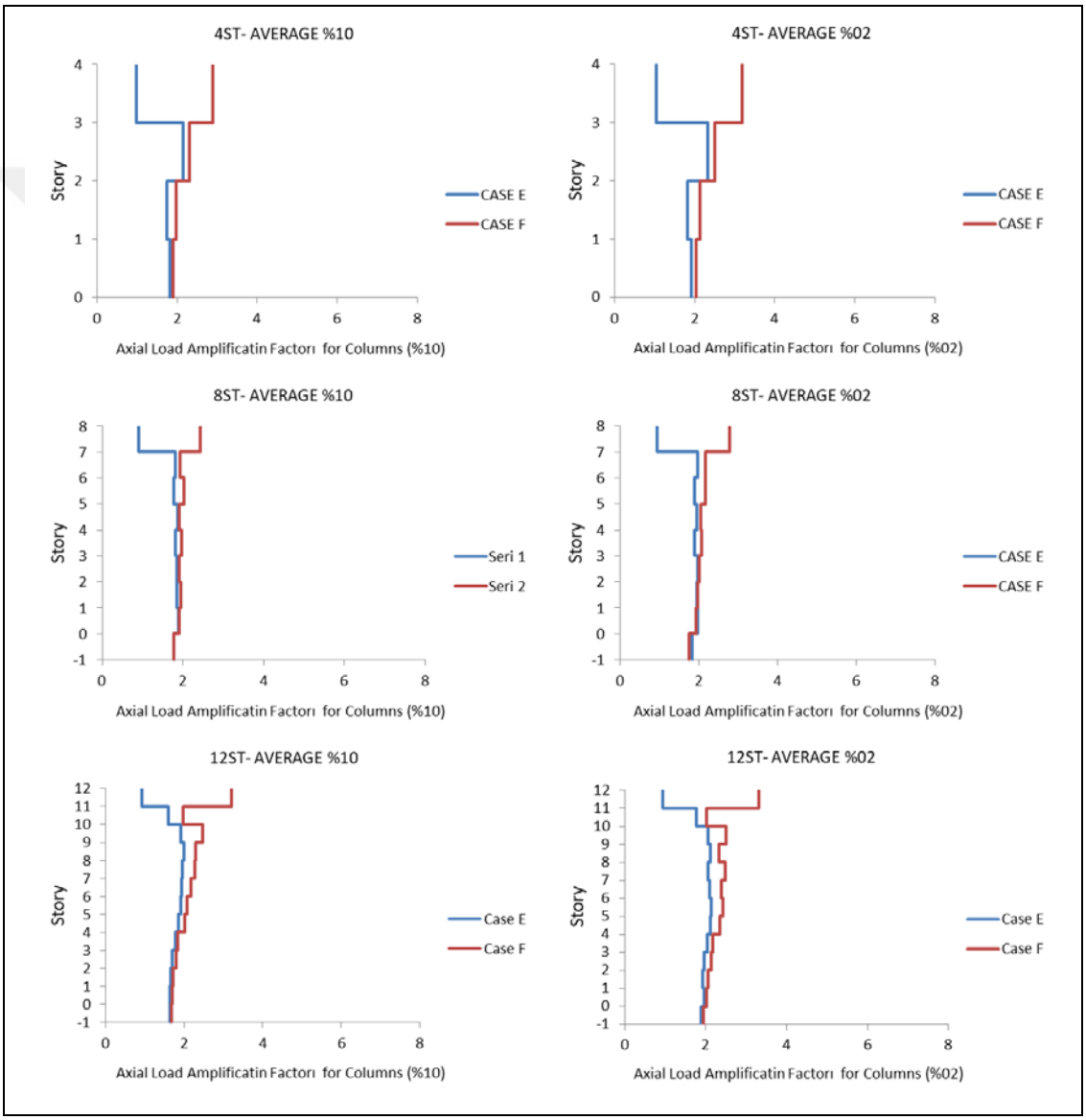

Figure 6.36: Maximum average axial compression amplification factor for column corresponding to 2% and 10% probability of exceedance in 50 year.

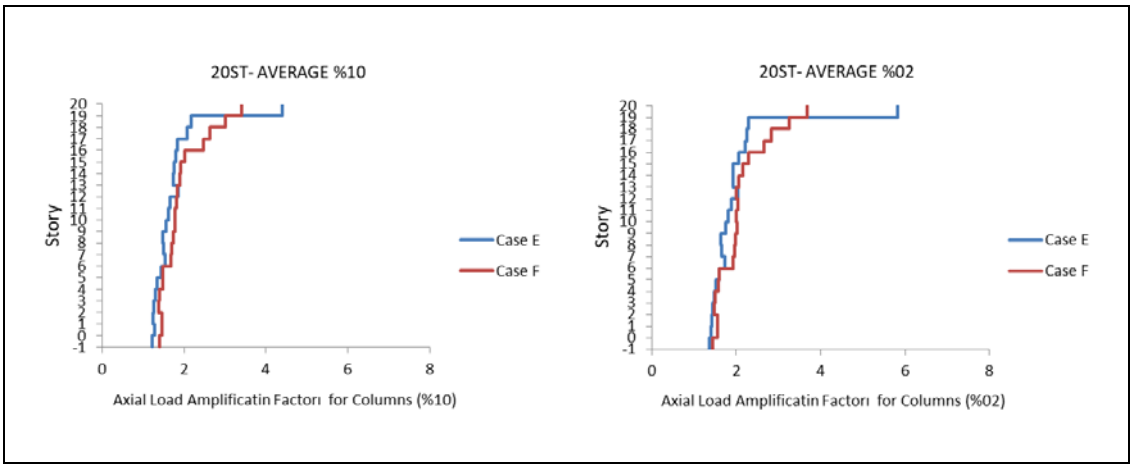

Figure 6.36: Continuation of the figure.

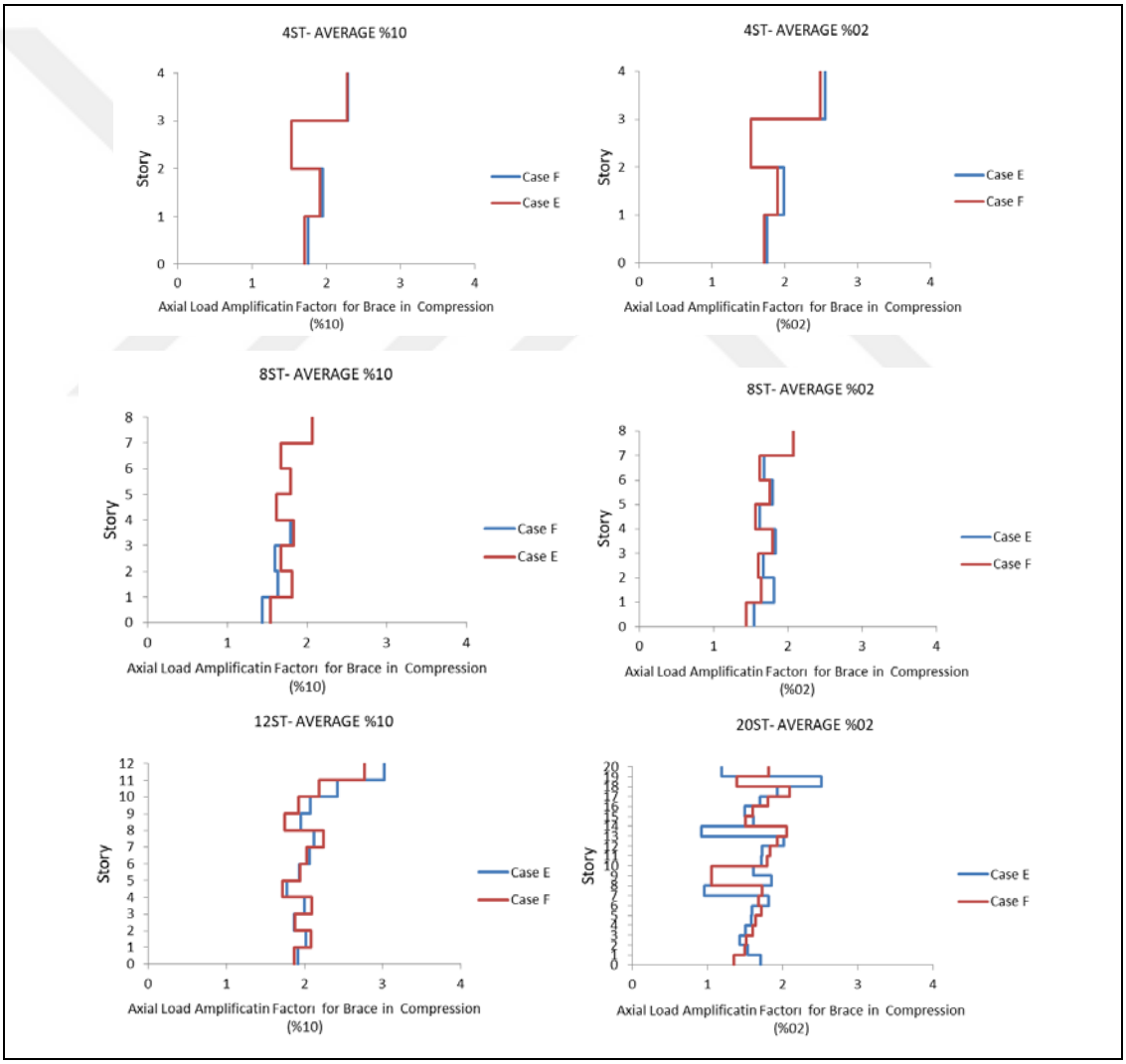

Figure 6.37: Maximum average axial compression amplification factor for brace corresponding to 2% and 10% probability of exceedance in 50 year.

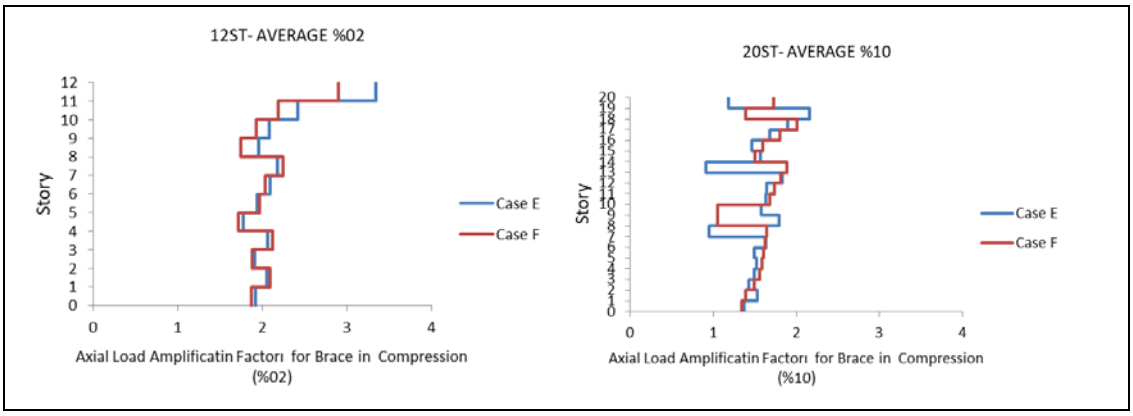

Figure 6.37: Continuation of the figure.

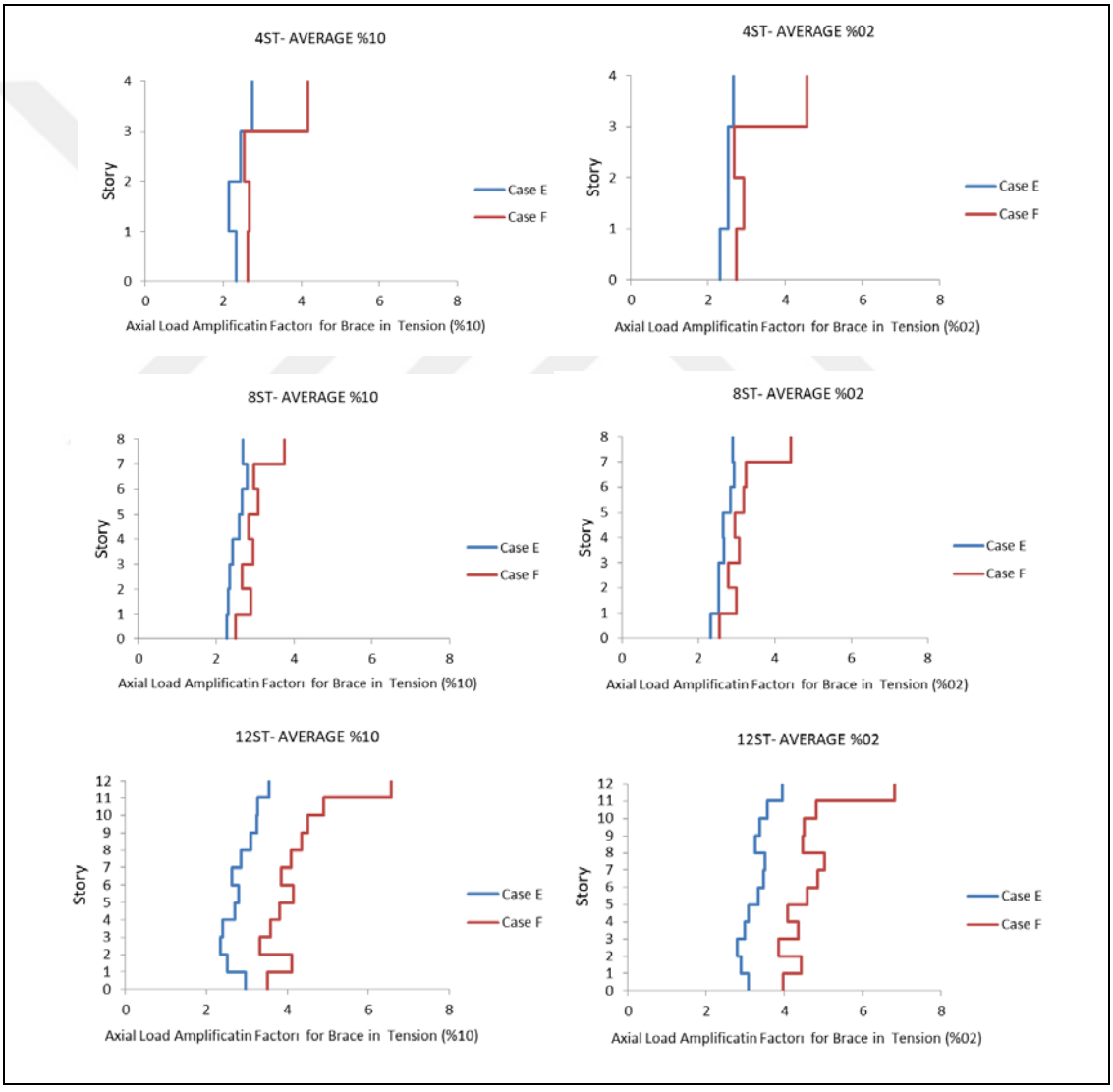

Figure 6.38: Maximum average axial tension amplification factor for brace corresponding to 2% and 10% probability of exceedance in 50 year.

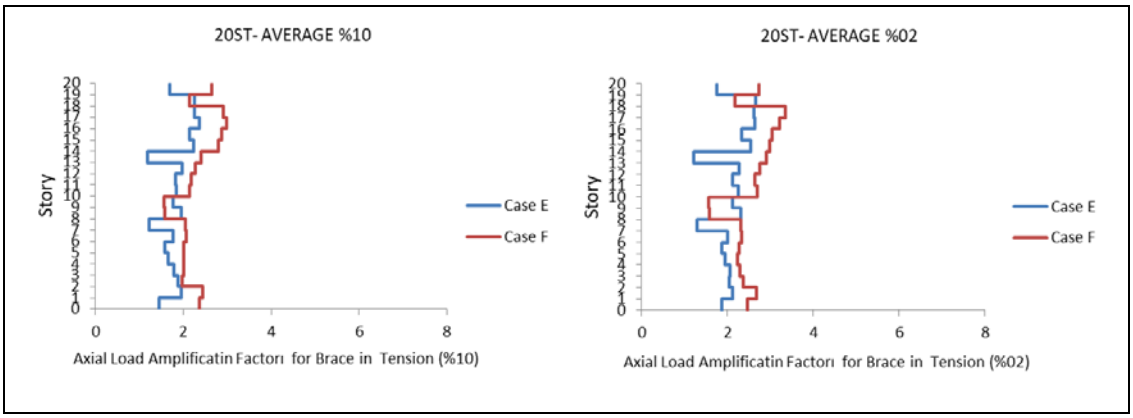

Figure 6.38: Continuation of the figure.

Overstrength factors Ω_0 are calculated under GM1 to Gm14 for 4-, 8-, 12- and 20- story frames for all case are given in Figure 6.39. For 4- story frames over strength factors are between 1.89- 2.19. Values vary from 1.70 to 2.22 for 8- story frames while in 12- and 20- story frames, over strength values ranged from 1.69 to 2.83 and 1.40 to 2.43 respectively. System overstrength factor degreases with the increase in story height.

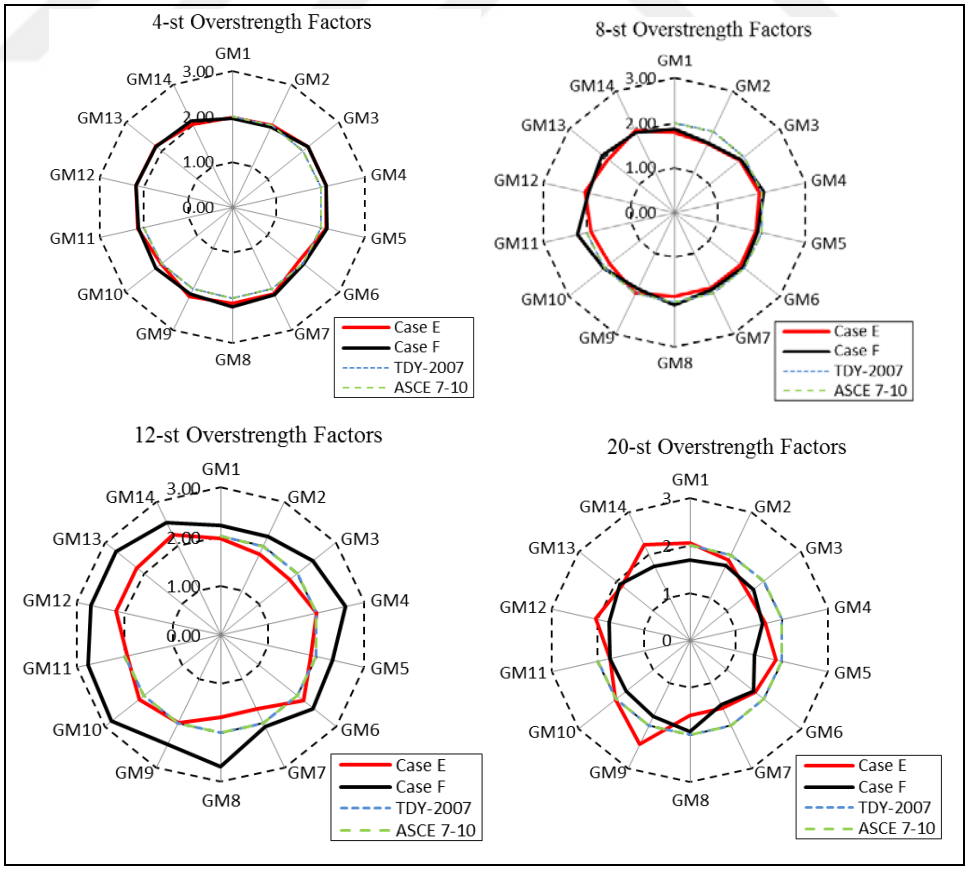

Figure 6.39: Overstrength factors for SCBF's under selected ground motions.

System overstrength factor are given with their average, minimum and maximum values are given in Table 6.4. For comparison, overstrength factor given in Turkish and American regulations also be in Table 6.4.

Table 6.4: Overstrength factors values for SCBF's under selected ground motions.

	4 Story		8 Story		12 Story		20 Story	
	Case E	Case F	Case E	Case F	Case E	Case F	Case E	Case F
GM1	1.97	1.95	1.80	1.86	1.96	2.23	2.06	1.69
GM2	2.00	1.96	1.70	1.73	1.83	2.22	1.87	1.76
GM3	2.13	2.14	1.86	1.90	1.79	2.40	1.58	1.72
GM4	2.12	2.13	1.94	2.04	2.00	2.60	1.63	1.57
GM5	2.12	2.15	1.87	1.91	1.89	2.33	1.87	1.40
GM6	1.89	2.01	1.89	1.96	2.15	2.41	1.76	1.72
GM7	2.11	2.14	1.87	1.90	1.69	2.08	1.59	1.51
AVG	2.05	2.07	1.85	1.90	1.90	2.33	1.77	1.63
MAX	2.13	2.15	1.94	2.04	2.15	2.60	2.06	1.76
MİN	1.89	1.95	1.70	1.73	1.69	2.08	1.58	1.40
GM8	2.11	2.19	1.87	2.05	1.69	2.68	1.59	1.94
GM9	2.17	2.13	1.99	1.89	1.99	2.49	2.43	1.78
GM10	2.01	2.16	1.84	2.01	2.11	2.83	2.01	1.73
GM11	2.14	2.13	1.90	2.22	1.95	2.77	1.74	1.73
GM12	2.18	2.17	2.04	1.96	2.17	2.70	2.05	1.76
GM13	2.16	2.15	1.91	2.06	2.18	2.72	1.85	1.90
GM14	2.04	2.11	2.02	1.98	2.25	2.53	2.23	1.74
AVG	2.12	2.15	1.94	2.02	2.05	2.68	1.98	1.80
MAX	2.18	2.19	2.04	2.22	2.25	2.83	2.43	1.94
MİN	2.01	2.11	1.84	1.89	1.69	2.49	1.59	1.73
TDY-2007	2.00	2.00	2.00	2.00	2.00	2.00	2.00	2.00
ASCE 7-10	2.00	2.00	2.00	2.00	2.00	2.00	2.00	2.00

7. RESULT & RECOMENDATION

In this thesis, amplified seismic load are investigated for low-, medium- and high-rise steel special moment frames (SMF) and steel special concentrically braced frames (SCBF) designed based on requirements of American provisions. Four special cases are used for SMF and two special cases are used for SCBF in nonlinear dynamic time history analyses. Two groups of ground motions (a total of 14 ground motions) corresponding to 10% and 2% probability of exceedance in 50 year were used in the analyses. The main outcomes of this study can be summarized as follows:

For SMF;

- Higher increase in axial compression load level occurs in non-uniform span length condition for all story level.
- Higher axial compression load values obtained in upper stores for 4-, 8- and 12- story frames.
- For 4-, 8-, 12- and 20 story frames Case A, Case C has similar axial load amplification factor values. Case D has the lowest increase in axial load level.
- For all frames and cases, the plastic hinge distribution is uniform and plastic hinge rotations do not exceed 4% under selected ground motions. For 8- and 12- story frames highest plastic hinge rotation occurs in upper stories.
- Axial load level in first story side columns increase with the story level and higher value obtained in 20-story frames with a value of %75.
- For all cases, system overstrength factor value degreases with the increase in story level.
- For 4- story frames, calculated overstrength factors under design and MCE levels ground motions exceed the value given in the both Turkish and American regulations for moment frames.
- For 8-, 12- and 20- story frames, calculated overstrength factors under design level ground motions do not exceed the value given in the American regulations for moment frames. However, calculated overstrength factors under design level ground motions for Case A and Case D in 8-story frames exceed the value given in Turkish regulations.

- In 8- story frames, calculated overstrength factors under MCE level ground motions exceed the value given in both regulations for moment frames.
- For 12- story frames, calculated overstrength factors under MCE level ground motions do not exceed the value given in the American regulations, but overstrength factors exceed the value given in the Turkish regulations for moment frames.
- For 20- story frames, calculated overstrength factors under MCE level ground motions do not exceed the value given in both Turkish and American regulations,

For SCBF;

- In all frames, maximum drift ratios occur where cross section of brace element changes to smaller section.
- Case F has slightly higher drift ratio values than Case E for 4-, 8- and 12- story frames
- Due to the brace configuration, columns in Case F have higher axial compression amplification factors than columns in Case E.
- Axial compression amplification factor in braces have similar values in 4-, 8- and 12 story frames.
- Case F gives higher axial tension amplification factors for braces in all cases and story height. And maximum values occur in upper stories.
- In some cases and ground motions calculated overstrength factors slightly exceed values given in both American and Turkish regulations. But generally, values given in design codes are compatible with calculated values for braced frames in this study.

This study show that, the overstrength factors for moment frames given in Turkish and American regulations are not compatible with the analyses result and given values needed to be re-evaluated. For more comprehensive analytical investigation frame configurations and strong ground motion number should be increased. However, the views expressed in this study belong to the author alone and do not necessarily represent the position of any other organization or person.

REFERENCES

Abdollahzadeh G. R., Banihashemi M., (2013), "Response modification factor of dual momentresistant frame with buckling restrained brace (BRB)", Steel and Composite Structures, 14 (6), 621-636.

Annan C. D., Youssef M. A., El Naggar H., (2008), "Seismic Overstrength in Braced Frames of Modular Steel Buildings", Journal of Earthquake Engineering, 13(1), 1-21.

Arslan H., Topkaya C., (2010), "A numerical study on response factors for steel wall–frame systems", Earthquake Engineering And Structural Dynamics, 39, 1611-1630.

ASCE 7-10, (2010), Minimum Design Loads for Buildings and Other Structures, American Society of Civil Engineers, Reston,VA, USA.

AISC 341-10, (2010), Seismic Provisions for Steel Structural Buildings, American Institute of Steel Construction, Chicago,IL, USA.

AISC 360-10, (2010), Specification for Structural Steel Buildings, American Institute of Steel Construction, Chicago, IL, USA.

ASCE/SEI 41-13, (2010), Seismic Evaluation And Retrofit Of Existing Buildings, American Society of Civil Engineers, Reston,VA, USA.

Astaneh-Asl A., Modjtahedi D., McMullin K., Shen J., D'Amore E., (1998), "Stability of damaged steel moment frames in Los Angeles", Engineering Structures, 20 (4-6), 433-446.

Balendra T., Huang X., (2003), "Overstrength and Ductility Factors for Steel Frames Designed According to BS 5950", Journal of Structural Engineering, ASCE, 129 (8).

Chopra A. K., (2010), "Dynamics of Structures: Theory and Applications to Earthquake Engineering", Prentice-Hall, Inc., NJ, USA.

Denavit M. D., Hajjar J. F., Perea T., Leon R. T., (2016), " Seismic performance factors for moment frames with steel-concrete composite columns and steel beams", Earthquake Engineering & Structural Dynamics, 45, 1685-1703.

Dickof C., Stiemer S. F., Bezabeh M. A., Tesfamariam S., (2014), " CLT–Steel Hybrid System: Ductility and Overstrength Values Based on Static Pushover Analysis", American Society of Civil Engineers.

Dogru S., Aksar B., Akbas B., Shen J., (2017), "Parametric study on energy demands for special steel concentrically braced frames", Steel and Composite Structures, 24 (2).

Elkady A., Lignos D. G., (2014), ” Effect of gravity framing on the overstrength and collapse capacity of steel frame buildings with perimeter special moment frames”, Earthquake Engineering & Structural Dynamics, 44, 1289-1307.

Fanaie N., Ezzatshoar S., (2014), “Studying the seismic behavior of gate braced frames by incremental dynamic analysis (IDA)”, Journal of Constructional Steel Research, 99, 111-120.

Fanaie N., Shamlou S. O., (2015), “Response modification factor of mixed structures”, Steel and Composite Structures, 19 (6), 1449-1466.

Farokhi1 B., Bazvand A., (2014), “Seismic performance evaluation of steel knee-braced moment frames”, Academia Arena, 6 (1), 1-8.

Gencturk B., Kaymaz I., Hosseini F., (2016), “Derivation of Seismic Design Parameters for ECC and Multi Material Special Moment Resisting Frames”, Journal of Earthquake Engineering, 20 (7), 1054-1076.

Ghassemieh M., Kargarmoakhar R., (2013), “Response modification factor of steel frames utilizing shape memory alloys”, Journal of Intelligent Material Systems and Structures, 24 (10), 1213-1225.

Jin J., El-Tawil S., (2005), “Seismic performance of steel frames with reduced beam section connections”, Journal of Constructional Steel Research, 61, 453–471.

Kappos A. J., (1999), “Evaluation of Behavior Factors on the Basis of Ductility and Overstrength Studies”, Engineering Structures, 21, 823–835.

Kim J., Choi H., (2005), “Response Modification Factors of Chevron-Braced Frames”, Engineering Structures, 27.

Kim J., Park J., (2009), “Seismic behavior factors of buckling-restrained braced frames”, Structural Engineering and Mechanics, 33 (3), 261-284.

Kim J., Jun Y., Kang H., (2016), ” Seismic Behavior Factors of RC Staggered Wall Buildings”, International Journal of Concrete Structures and Materials, 10 (3), 355–371.

Kuşyılmaz A., Topkaya C., (2013), “Design Overstrength of Steel Eccentrically Braced Frames”, International Journal of Steel Structures, 13 (3), 529-545.

Lee D. G., Cho S. H., Ko H., (2005), “Response Modification Factors for Seismic Design of Building Structures in Low Seismicity Regions”, Korea Earthquake Engineering Research Center.

Mahmoudi M., Zaree M., (2009), “Evaluating the overstrength of concentrically braced steel frame systems considering members post-buckling strength”, International Journal of Civil Engineering, 9 (1).

Massumia A., Mohammadi R., (2016), “Structural redundancy of 3D RC frames under seismic excitations”, Structural Engineering and Mechanics, 59 (1), 15-36.

Mellati A., Tehrani M. H., Zeinali Y. H., Banazadeh M., (2013), “Evaluation of Overstrength Factor of Steel Moment Resisting Frames”, Advances in Structural, Civil and Environmental Engineering.

Osteraas, J. D., Krawinkler H., (1990), “Strength and Ductility Considerations in Seismic Design”, Rep.No. 90, John A. Blume Earthquake Engineering Center, Stanford University, California,

PEER Database, (2014), Pacific Earthquake Engineering Research Center, 325 Davis Hall, University of California, Berkeley, CA, USA.

PERFORM-3D, (2011), Nonlinear Analysis and Performance Assessment for 3D Structures Software, Version 5.

Rahgozar M. A., Humar J. L., (1998), “Accounting for Overstrength In Seismic Design of Steel Structures”, Canadian Journal of Civil Engineering, 25, 1–5.

Shen J., Sabol T. A., Akbas B., Sutchiewcharn N., (2010), “Seismic demand on column splices in steel moment frames” , Engineering Journal, AISC, 47, 4th quarter, 223-240.

Shen J., Akbas B., Seker O., Doran B., Wen R., Uckan E., (2015), “Seismic Axial Loads in Steel Moment Resisting Frames”, International Journal of Steel Structures, 15 (2), 375-387.

Tabeshpoura M. R., Golafshanib A. A., Shalmanib A. M., (2011), “Response Modification Factors of Steel Moment Frames Equipped with Completely Closed Ribbed Bracing System (CC-RBS)”, Advances in Structural Engineering, 15 (7).

BIOGRAPHY

Bora AKŞAR was born in Istanbul, Turkey, in 1984. He received his bachelor of science degree (B.Sc) in Department of Civil Engineering from Yıldız Technical University in 2006. He earned his Master of Science degree (M.Sc) in Earthquake Engineering from Istanbul Technical University in 2009. He has been a PhD student in Department of Civil Engineering at Gebze Technical University since 2010. He joined the research project funded by the Scientific and Technological Research Council of Turkey (TUBITAK) in 2014 and completed in 2016. He presented the research project at national and international conferences. He worked as a research assistant at Gebze Technical University from 2013 to 2017. He is interested in earthquake engineering, performance-based design, seismic performance of steel and rc structures, industrial structures and structural health monitoring.

APPENDICES

Appendix A: Publications Based on the Thesis

Aksar B., Dogru S., Akbas B., (2017), "Çelik Moment Çerçevelerde Kuvvetli Deprem Yer Hareketi Altında Arttırılmış Deprem Etkileri,"Journal of the Faculty of Engineering and Architecture of Gazi University (in print).

Aksar B., Dogru S., Akbas B., Shen J., Seker O., Wen R., (2016), "Amplified Seismic Loads in Steel Moment Frames," Applied Mechanics and Materials, 847, 222-232.

Appendix B: The Member Sizes of The Moment Frames

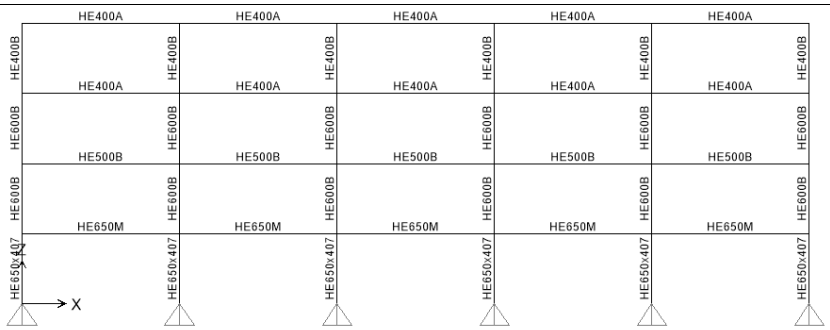

Case A

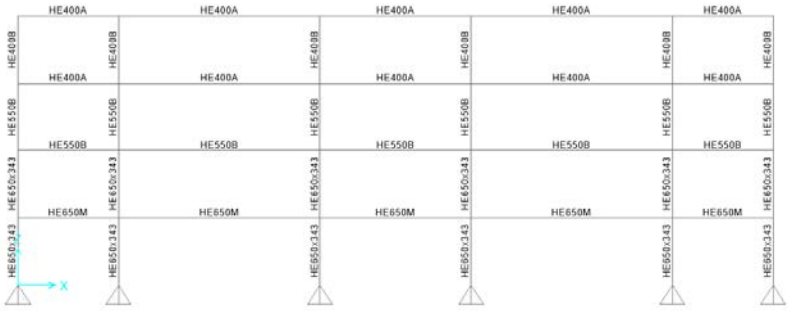

Case B

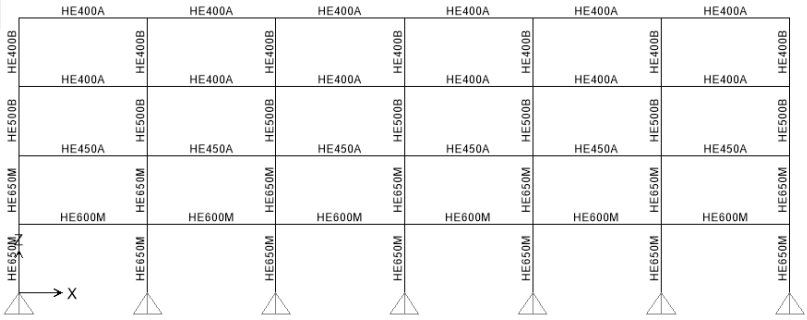

Case C

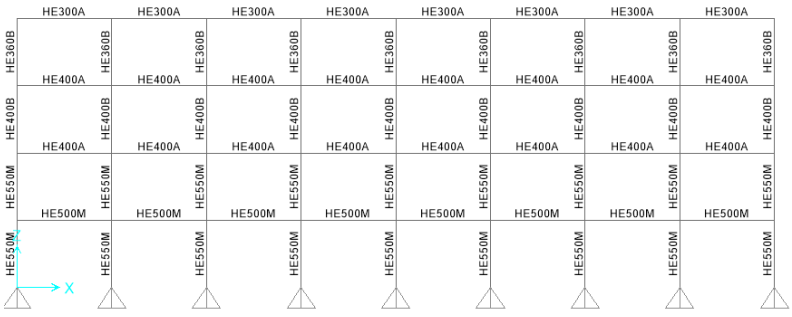

Case D

Figure B1.1: Elevations and member sizes for the 4- story SMF.

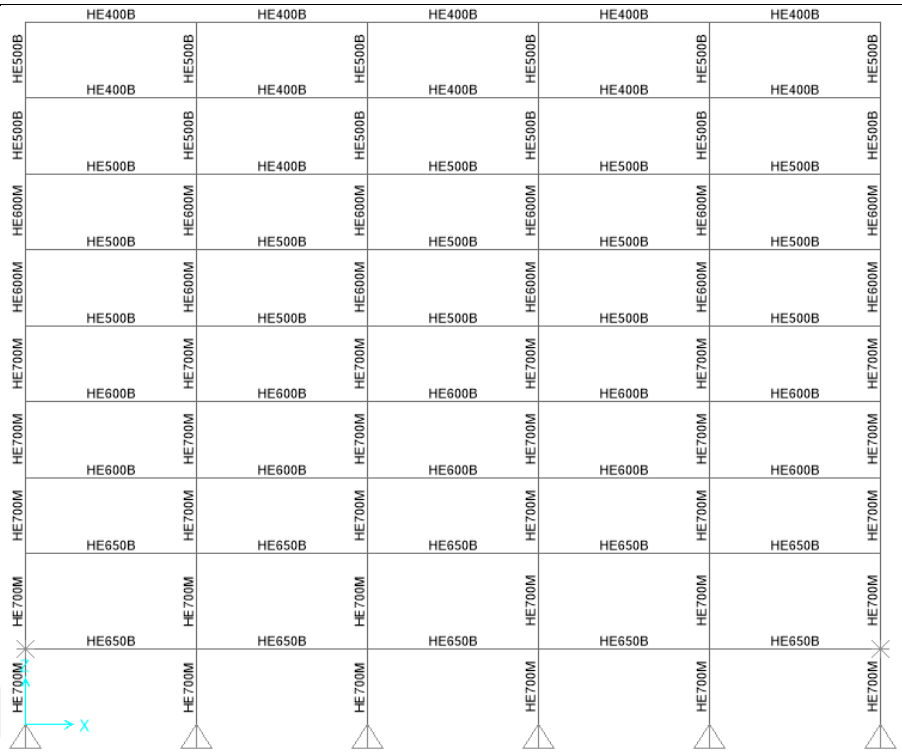

Case A

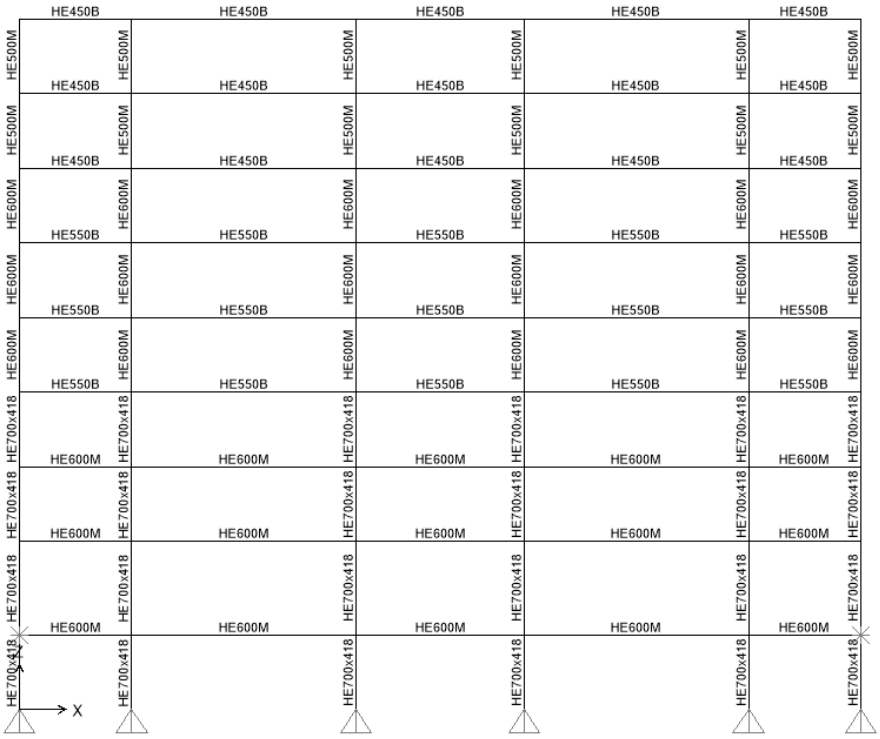

Case B

Figure B1.2: Elevations and member sizes for the 8- story SMF.

Case C

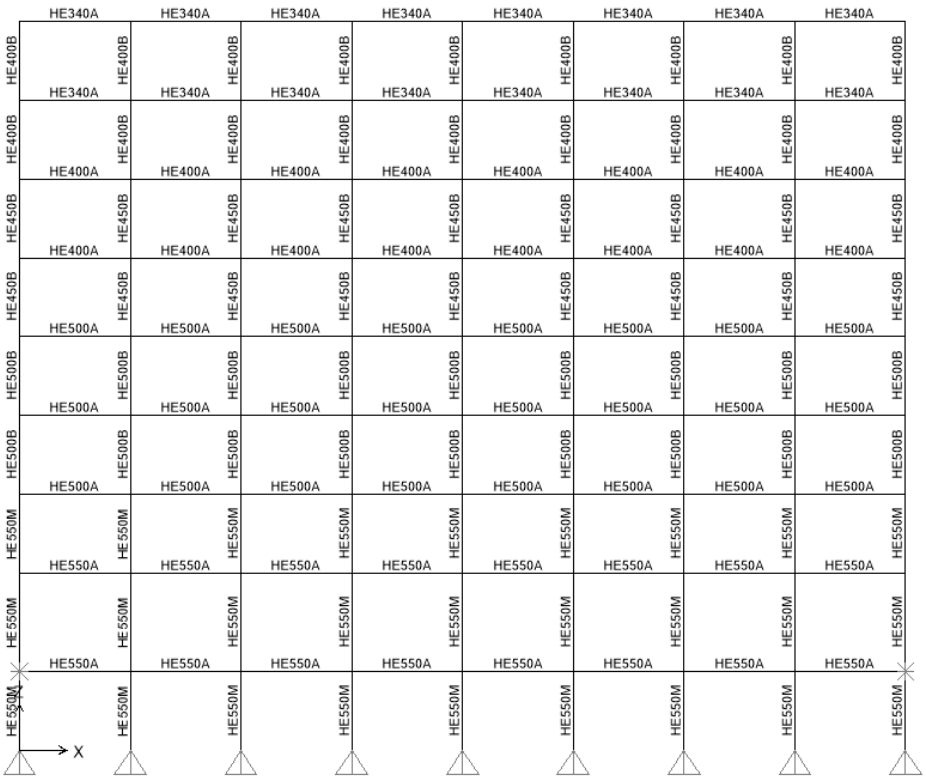

Case D

Figure B1.2: Continuation of the figure.

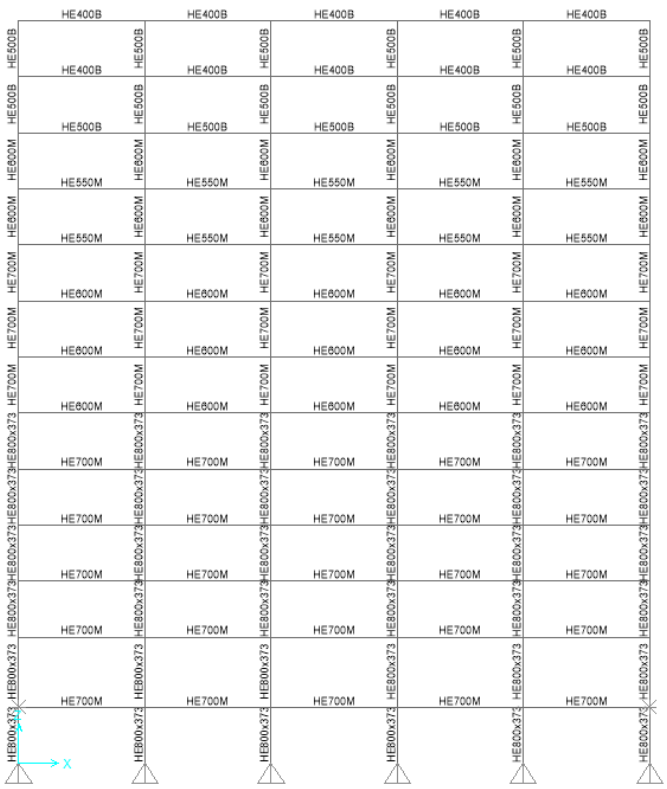

Case A

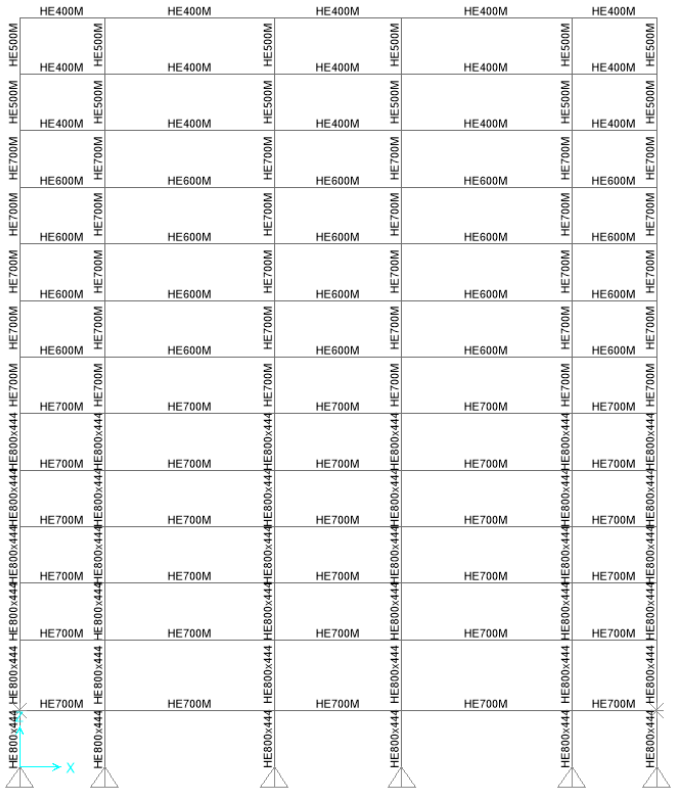

Case B

Figure B1.3: Elevations and member sizes for the 12- story SMF.

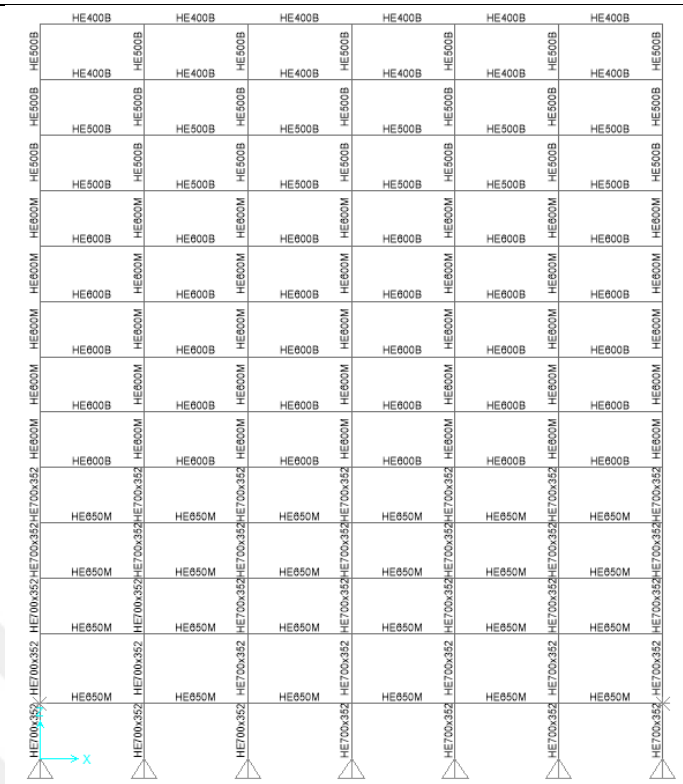

Case C

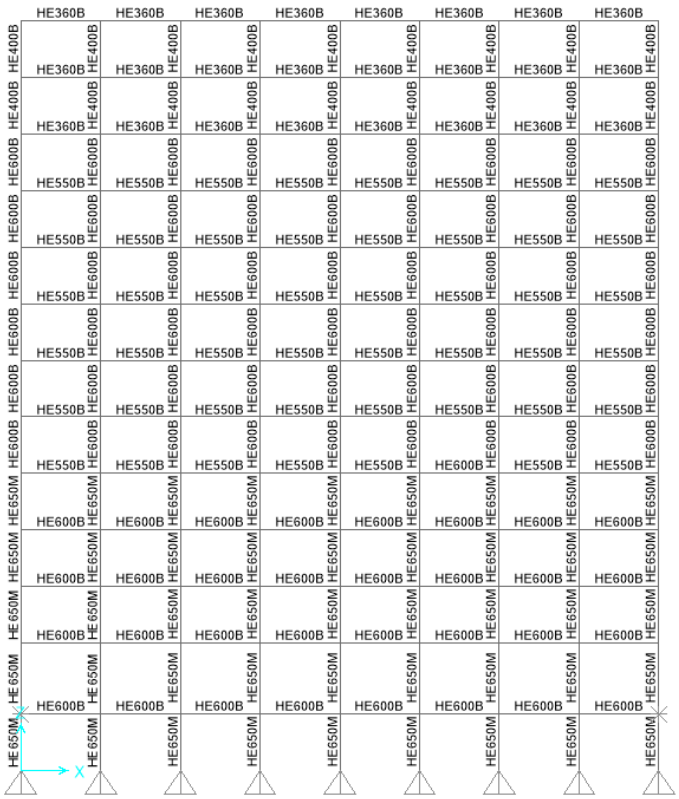

Case D

Figure B1.3: Continuation of the figure.

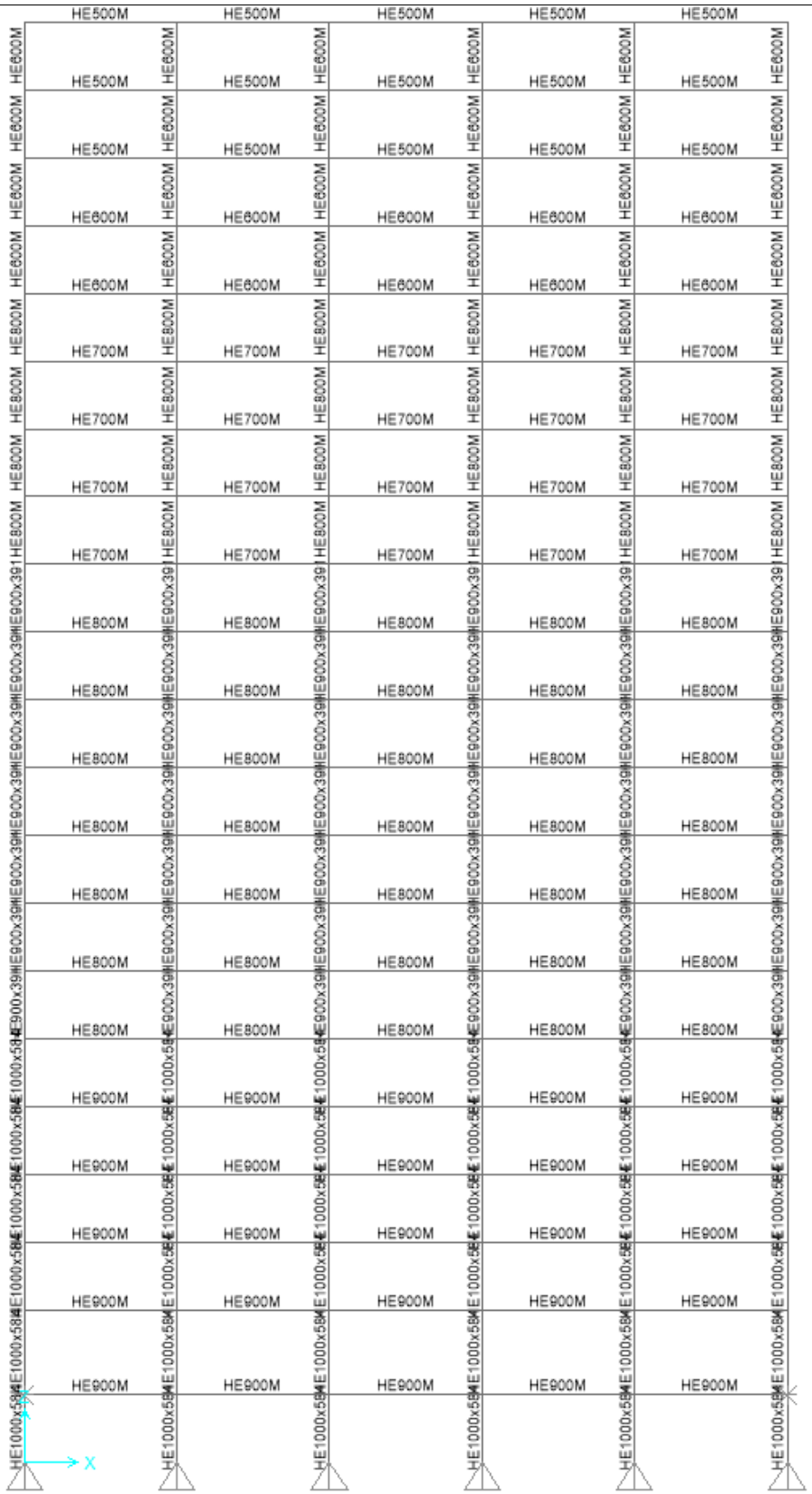

Case A

Figure B1.4: Elevations and member sizes for the 20- story SMF.

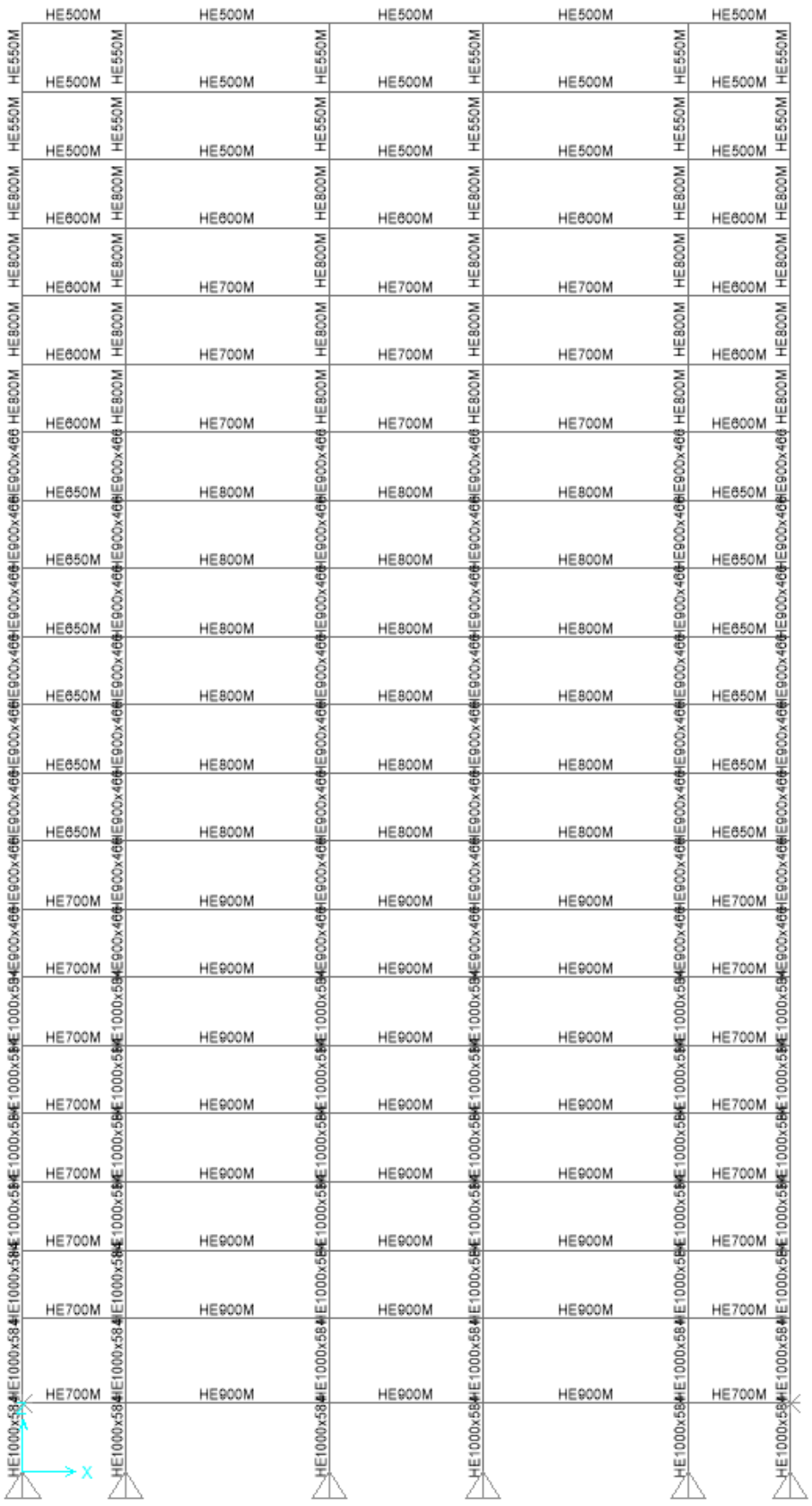

Case B

Figure B1.4: Continuation of the figure.

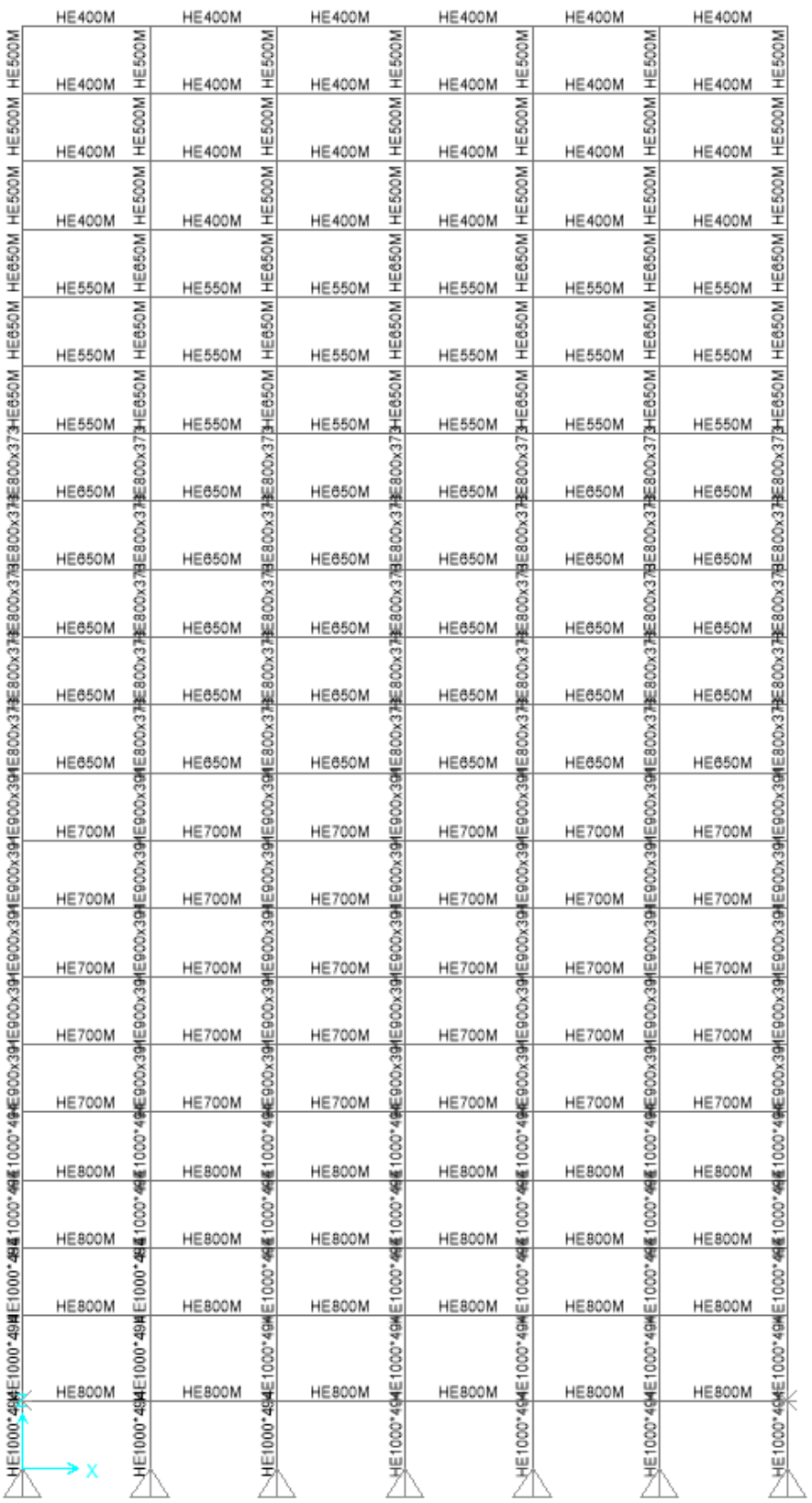

Case C

Figure B1.4: Continuation of the figure.

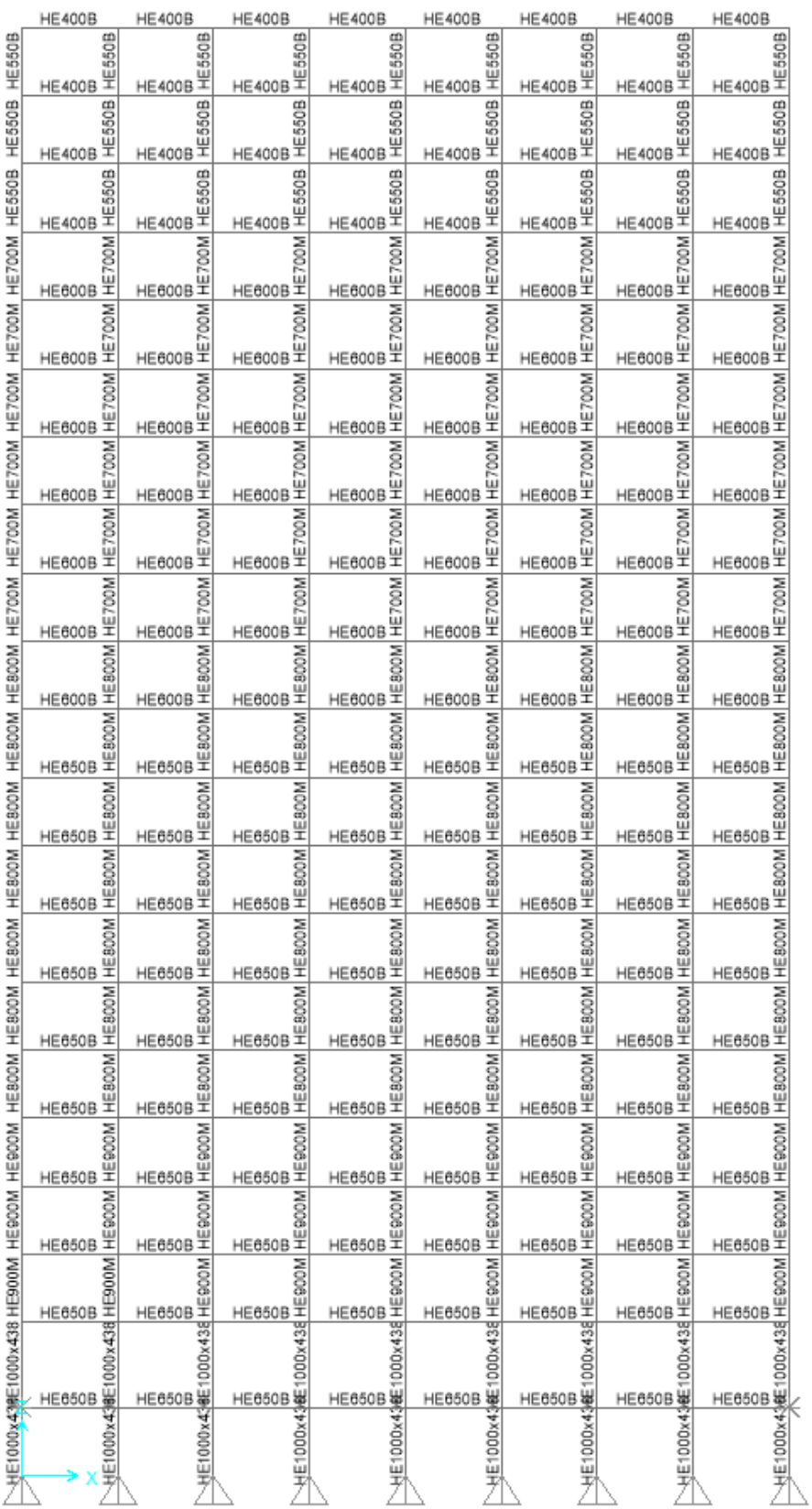

Case D

Figure B1.4: Continuation of the figure.

Appendix C: The Member Sizes of The Braced Frames

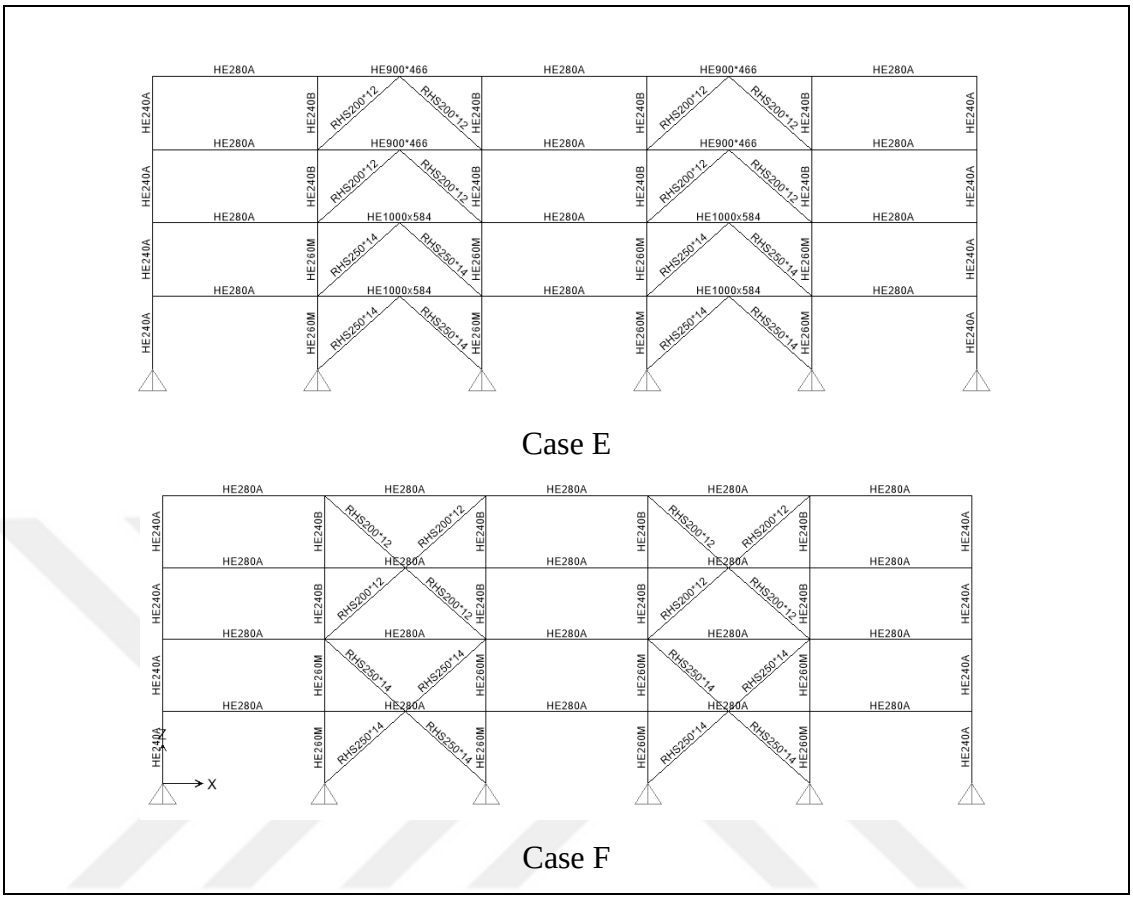

Figure C1.1: Elevations and member sizes for the 4- story SCBF.

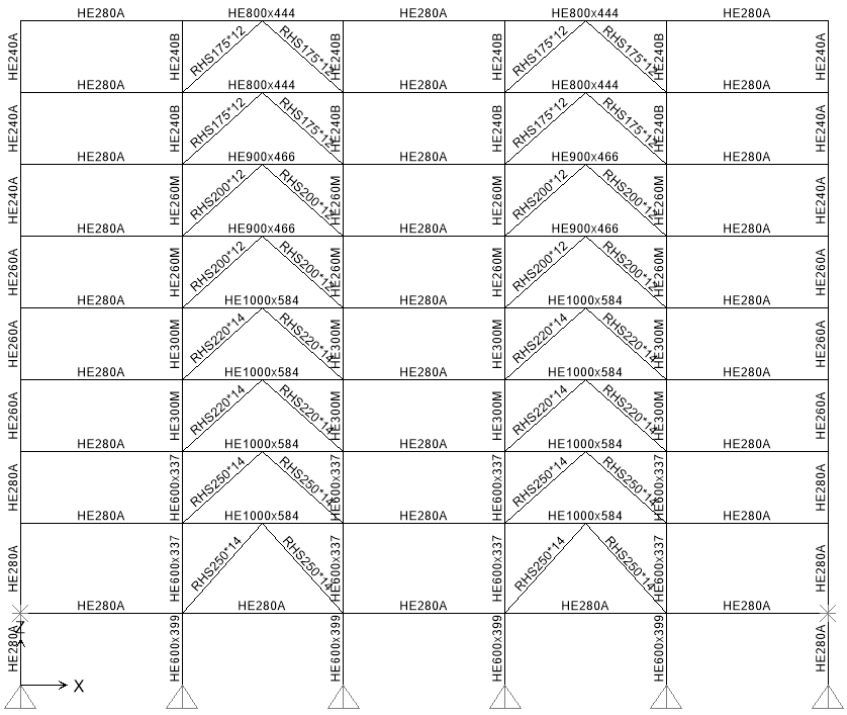

Case E

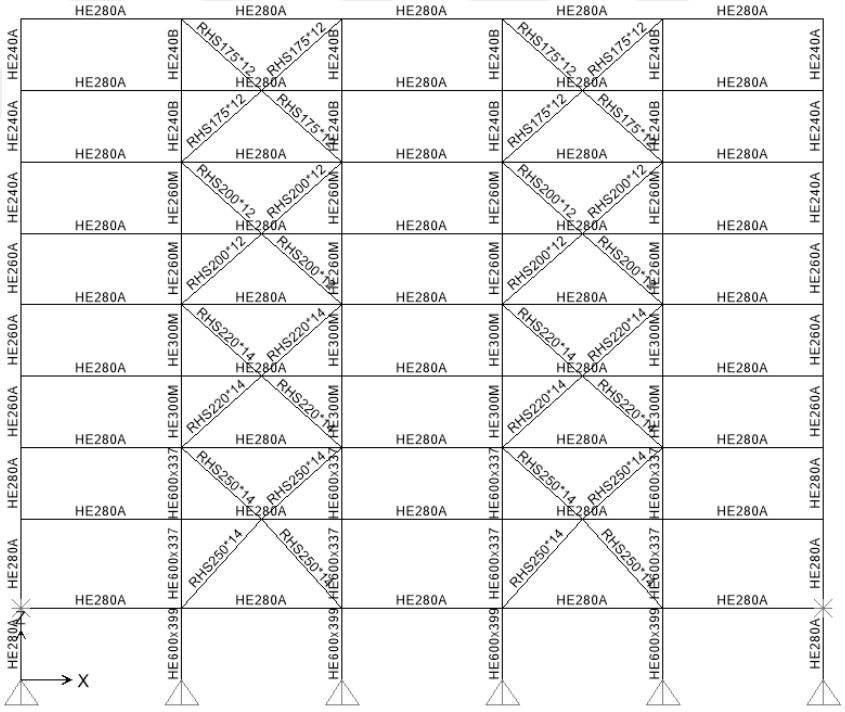

Case F

Figure C1.2: Elevations and member sizes for the 8- story SCBF.

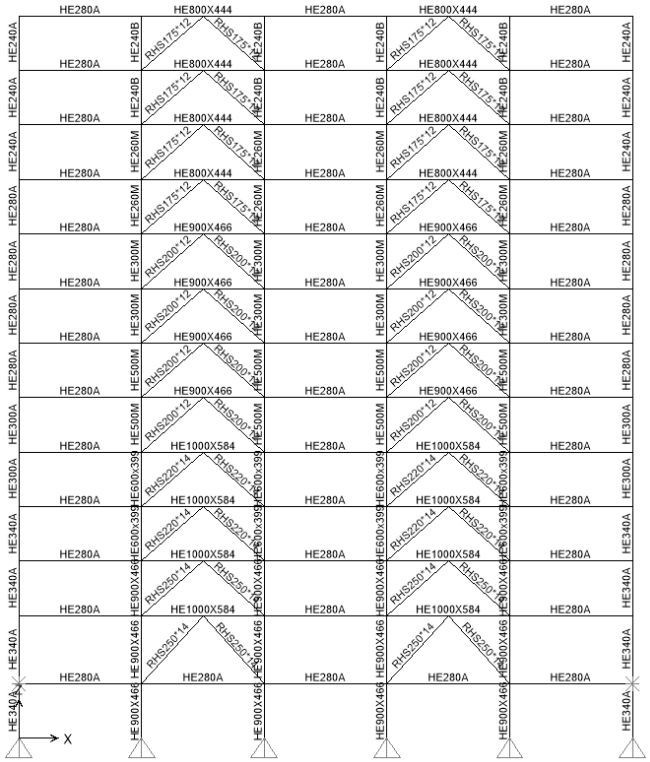

Case E

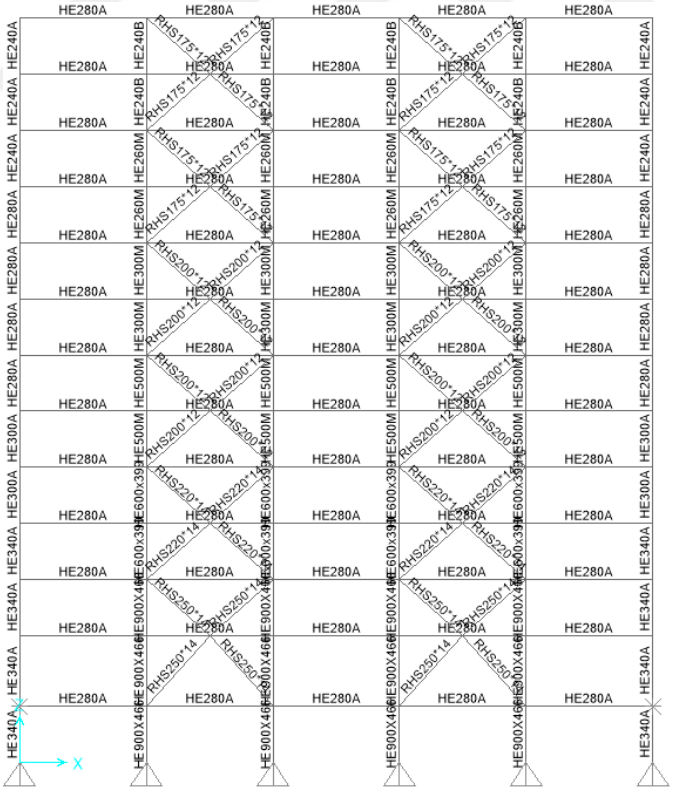

Case F

Figure C1.3: Elevations and member sizes for the 12- story SCBF.

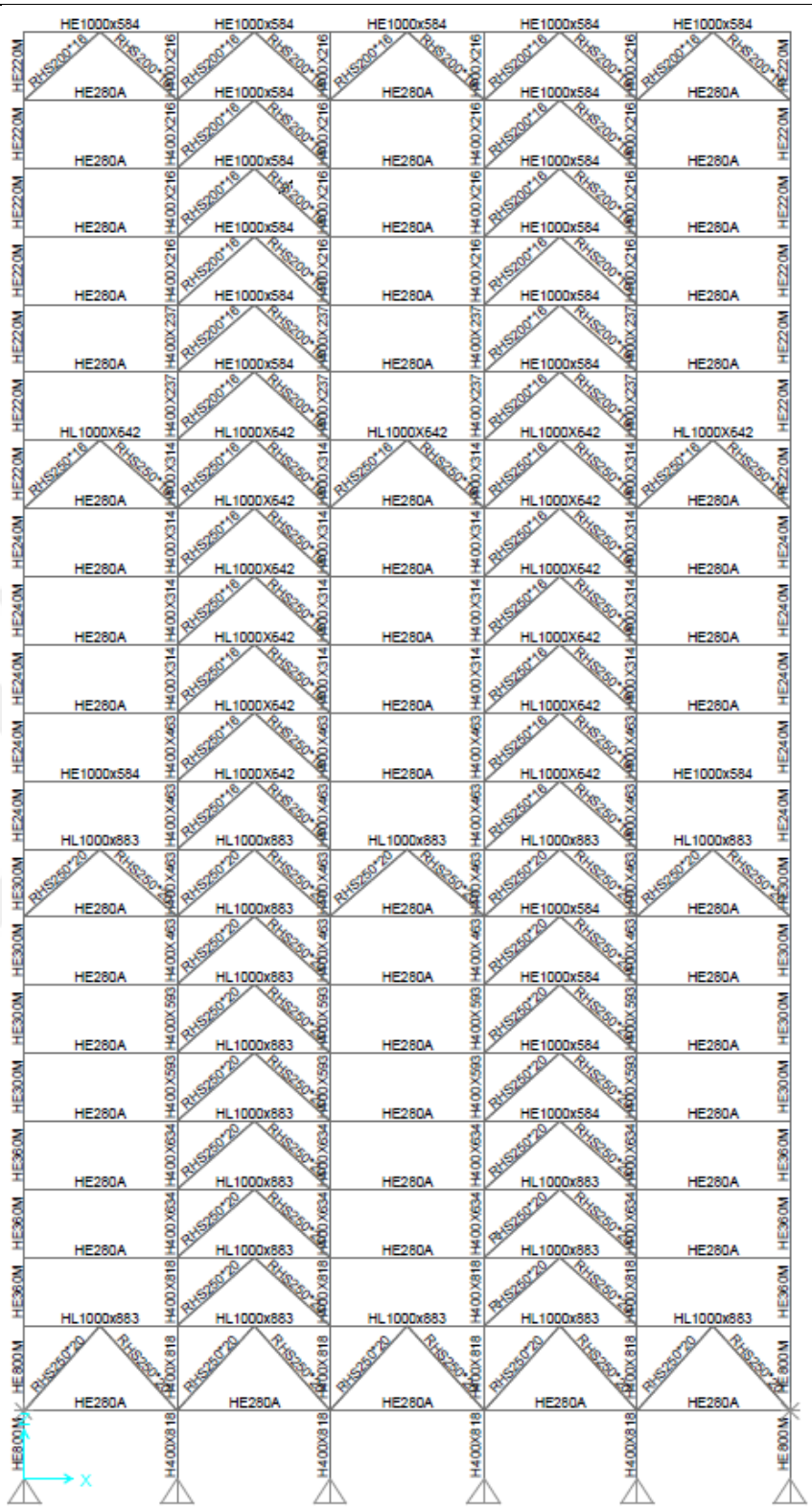

Case E

Figure C1.4: Elevations and member sizes for the 20- story SCBF.

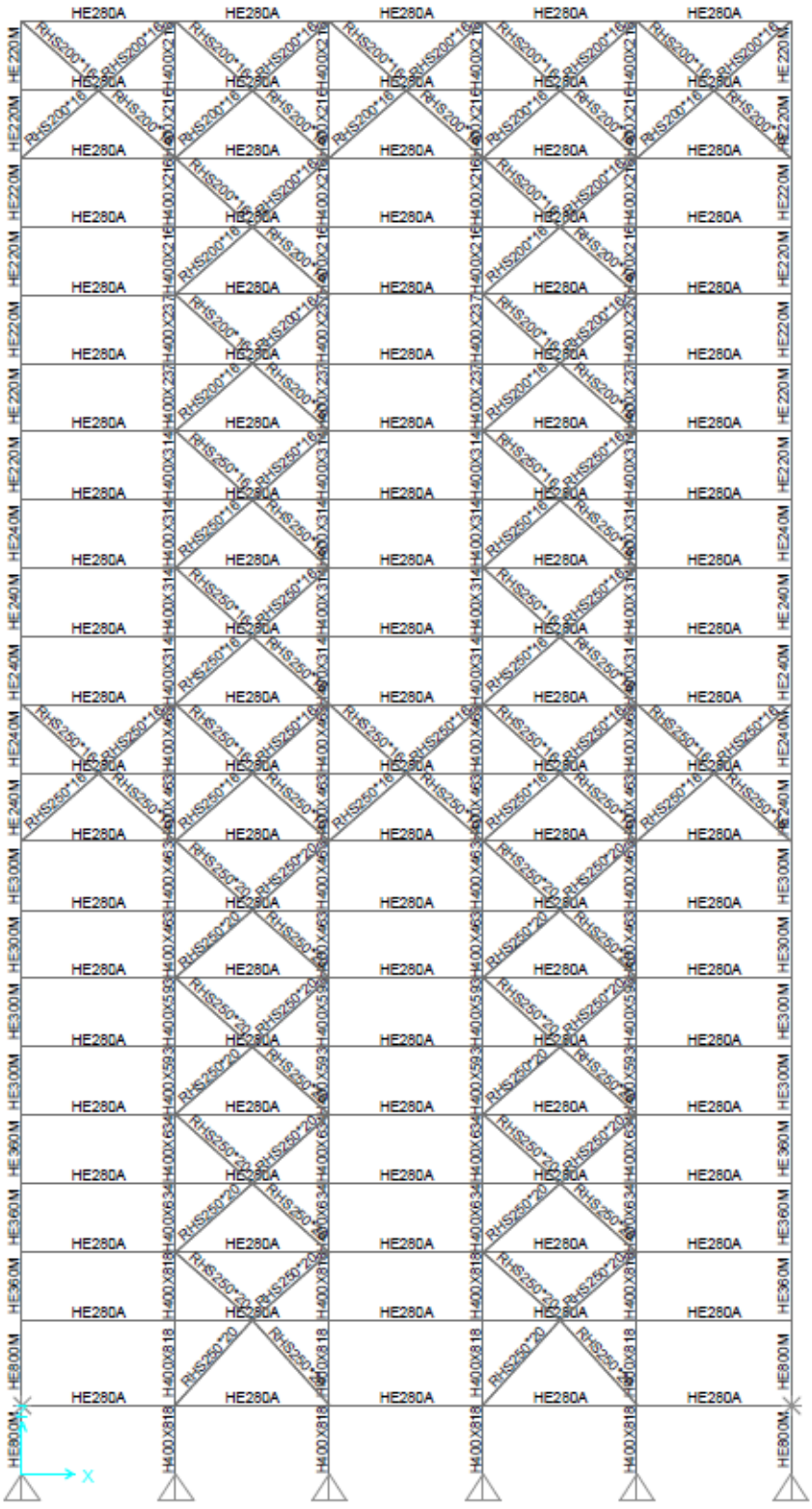

Case F

Figure C1.4: Continuation of the figure.